

**FACULTY OF SCIENCE,
ENGINEERING AND COMPUTING**

**School of Life Science, Pharmacy and
Chemistry**

MScR DEGREE

IN

***Anatomy, Physiology and
Pathology***

Name: Elisabeth Spiritosanto

ID Number: k1843108

Project title: Understanding bladder smooth
muscle repair capacity in healthy and overactive
bladders.

Date: 14th February 2020

Supervisors: Dr Natasha Hill

Dr Francesca Mackenzie

Mr Eduardo Cortes

Kingston University London

WARRANTY STATEMENT

This is a student project. Therefore, neither the student nor Kingston University makes any warranty, express or implied, as to the accuracy of the data or conclusion of the work performed in the project and will not be held responsible for any consequences arising out of any inaccuracies or omissions therein.

Abstract

Overactive bladder (OAB) is a urological condition characterised by frequency, urgency, nocturia and sometimes incontinence. The prevalence of OAB in the USA and Europe is estimated to be 10-17% (Coyne *et al.*, 2008), and it has a major impact on the patient's quality of life, particularly in the elderly. Since the aetiology of the pathology is poorly understood, therapeutic efforts to date are aimed primarily at symptom resolution rather than targeting underlying causes or mechanisms that could improve tissue function.

Insulin-like growth factor 1 (IGF-I) stimulates proliferation and differentiation in muscle growth and repair. Alternative splicing generates three distinct variants in human tissues: IGF-1Ea, which is the predominant variant in muscle and liver, IGF-1Eb, and IGF-1Ec. The translated product of IGF-1Ec is also known as "mechano growth factor" (MGF) due to its transcriptional upregulation following injury and mechanical stress. MGF role and mechanism of action have been studied mainly in skeletal muscle, where IGF-1Ec has been shown to be upregulated after muscle damage, correlating with repair and regeneration. On the other hand, very little is known about its function in smooth muscle.

The hypothesis that drove this study is that MGF may be produced in normal bladder to promote detrusor cell proliferation and tissue repair. In the OAB, MGF production may be decreased, leading to a reduction in smooth muscle cell proliferation and loss of function. Our aim was to test this hypothesis, investigating MGF function in the bladder.

We determined MGF protein expression in bladder tissue by immunohistochemistry, and quantified expression in normal and pathological human bladder biopsies by Western blot and immunohistochemistry techniques. We further assessed the tissue composition of each biopsy sample using RT-qPCR and examined the statistical correlation between clinical parameters, MGF expression and biopsy composition. Finally, we examined the effect of MGF peptide on bladder smooth muscle proliferation *in vitro*.

Our data shows for the first time that MGF is detectable in normal and overactive bladders, and expression is around two-fold higher in pathological (mean relative expression=0.48 \pm 0.09, n=28) compared to control samples (mean=0.27 \pm 0.07, n=12), though the difference does not reach statistical significance (p=0.11). The biopsy samples showed different composition patterns in terms of presence/absence of the different layers of the bladder. The increase in MGF expression was particularly striking in the subset of the samples expressing markers of smooth muscle tissue (mean=0.49 \pm 0.11 in pathological samples and 0.23 \pm 0.09 in control samples; p=0.06; n=17 and n=8, respectively). This suggests that smooth-muscle derived MGF increased in patients with OAB, perhaps reflecting activation of tissue regeneration in an attempt to compensate for muscle degeneration associated with the pathology of OAB. While a trend towards a positive correlation between maximum cystometric capacity (MCC) of the bladder and MGF expression was observed, statistical significance was not reached (p=0.15). Finally, the preliminary treatment of primary bladder

cells with different concentrations of MGF peptide showed a significant increase in cellular proliferation following treatment with 100 ng/ml MGF compared to the control after 72 hours, as determined by EdU assay ($p=0.008$).

The results of this study suggest that increased MGF is associated with OAB pathology, and its application may represent a new avenue of research for OAB patients. However, further research is required.

Acknowledgements

I would like to thank all the people who helped me and supported me during this journey, and all the institutions that made my research project possible.

- First of all, Kingston Hospital Charity for covering the tuition fees and bench fees of my Masters.
- Secondly, my academic supervisors: Dr Natasha Hill for her guidance, patience, support, time and kindness; Dr Francesca Mackenzie for her help and sweet words of encouragement.
- A special thanks to Mr Eduardo Cortes for his fundamental role in conceiving, carrying out and guiding this project: from recruiting the patients involved in the study and providing the biopsy samples to gaining funding for the implementation of the MSc by Research, from introducing me clinically and scientifically to the world of overactive bladder to supporting me along the way.
- Kingston Hospital urogynaecology patients who participated in this study, and the staff who helped for this purpose.
- Dr Amanda Munasinghe for her help and constant presence both in my academic and private life.
- Almas Mahmood for the academic collaboration we shared at the beginning of our projects and for her loving attitude.
- King's College London for supplying the mice for my experiments.
- Dr Rosemary McNiece for introducing me to the use of SPSS and statistics.
- My research group for their guidance and support.
- Kingston University staff who has assisted me along the way.
- All my "English" and Italian friends for making my Masters more enjoyable.
- Dr Mark Turner for telling me of this MSc by Research opportunity.
- Last but not least, my family for their moral and economical support during these years.

Table of Contents

Abstract	II
Acknowledgements	IV
1. Introduction.....	1
1.1 Overactive Bladder	1
1.1.1 What is overactive bladder.....	1
1.1.2 Diagnosis of OAB	2
1.1.3 Treatments currently available	3
1.1.4 Aetiology of OAB	5
1.2 IGF-1 splice variants in OAB.....	5
1.2.1 Insulin-like growth factors.....	5
1.2.2 Alternative splicing and translational products	7
1.2.3 MGF	9
1.3 Hypothesis and aims of the project.....	15
2. Materials and Methods	16
2.1 Processing of murine and human bladder biopsy samples using ThermoFisher PARIS Kit	16
2.2 Cell culture	16
2.3 Isolation of RNA from cell lines	16
2.4 Reverse transcription of RNA into cDNA	17
2.5 RT-PCR	17
2.6 Agarose gel electrophoresis	17
2.7 RT-qPCR	18
2.8 BCA protein quantification	18
2.9 Western blot	19
2.9.1 SDS-PAGE.....	19
2.9.2 Transfer and blocking of the membrane.....	19
2.9.3 Incubation in primary and secondary antibodies	19
2.9.4 Membrane viewing and image analysis	20
2.10 Immunohistochemistry	20
2.10.1 Fixation, preparation and embedding in paraffin of the tissue	20
2.10.2 Slides preparation, antigen retrieval and permeabilization	20

2.10.3 Incubation in primary and secondary antibodies	20
2.10.4 Development of the staining and counterstaining	21
2.10.5 Mounting of slides and imaging	21
2.11 Establishment of primary cell culture	22
2.12 Treatment of primary cells with MGF protein	22
2.13 Proliferation assay and immunocytochemistry	23
2.14 Bioinformatics	23
2.15 Statistics	24
3. Results	25
3.1 Validation and optimization of ThermoFisher PARIS Kit for RNA and protein extraction from murine samples	25
3.2 Optimization of protein and RNA yield extracted from biopsy samples	26
3.3 Primer design strategy and optimization in cell lines	28
3.4 Inconsistent detection of IGF-1Ec transcripts in bladder biopsy samples	30
3.5 Optimization of MGF and IGF-1 protein detection by western blot.....	34
3.6 Quantification of MGF protein in bladder biopsies	38
3.7 Optimization and validation of MGF detection by IHC in mouse samples and analysis of human biopsies	39
3.8 Analysis of association between MGF expression and clinical symptoms	42
3.9 Composition analysis by RT-qPCR	46
3.9.1 Design and amplification efficiency of the primers	46
3.9.2 Composition analysis	47
3.10 Analysis of association between MGF expression and tissue composition	50
3.11 Validation and optimization of primary smooth muscle cell culture from murine sample	51
3.12 Effect of MGF on murine bladder primary cells <i>in vitro</i>	54
4. Discussion	60
5. Conclusions	63
6. Appendix.....	64
6.1 Materials	64
6.2 Ethics	66
7. References.....	67

1. INTRODUCTION

1.1 Overactive Bladder

1.1.1 What is Overactive Bladder (OAB)?

“I stopped running, I stopped taking walks. Basically, I stopped doing things that didn't allow me immediate access to a bathroom. I was so embarrassed that I didn't talk to anyone about it for a long time. That was a mistake.” This is what one of the 33 million Americans affected by Overactive Bladder (OAB) said about the pathology (*Urology Care Foundation*, 2019). As stated in 2010 by the IUGA (International Urogynecological Society) and the ICS (International Continence Society) (Haylen *et al.*, 2010), three main symptoms characterise this condition: urgency (the sudden feeling to urgently urinate), increased daytime and night-time (nocturia) voiding frequency, and occasional urinary incontinence (the leakage of small amount of urine) (Fig. 1.1.1).

Although it is not a mortal disease, OAB can have serious social and psychological implications for the people affected as it affects many aspects of their everyday life, from work to social and sexual activities (Stewart *et al.*, 2003). In fact, they stop doing normal activities outdoors that would prevent easy access to the toilet, as stated by the witness above, therefore leading them to isolation and depression (Mcghan, 2001). The subsequent lack of movement causes an increased risk of fractures and domestic incidents, due to increased bone fragility and muscular disuse (Brocklehurst, 1993).

The elderly are the most affected community, as their decreased mobility and independence leads to increased risk of fractures because of trying to rush for the bathroom to avoid leakage (Truzzi *et al.*, 2016a).

Fig. 1.1.1: Normal vs. overactive bladder. Physiologically, the detrusor muscle contracts when the bladder is full with urine. In the OAB pathology, the smooth muscle contracts when the bladder is not completely full, leading to the frequent need to urinate.

Image adapted from: taoofherbs.com/articles/132/BladderControl – Natural Alternative For Overactive Bladder

1.1.2 Diagnosis of OAB

Although OAB is a widespread pathology, current diagnostic methods are still mainly unreliable/based on expert opinion. Self-completion questionnaires are the first step to assess this condition, ranging over questions about symptoms and their impact on the patients' daily life. Among these, commonly used by urologists are: OAB-SF (Coyne *et al.*, 2015), OAB-V-8 (Peterson *et al.*, 2018) and B-SAQ (Basra *et al.*, 2006) (Fig. 1.1.2).

BLADDER CONTROL SELF-ASSESSMENT QUESTIONNAIRE

ARE YOU: MALE ☐ FEMALE ☐

Please put the **NUMBER** that applies to you in the boxes shown by the arrows based on the following:

NOT AT ALL = 0 A LITTLE = 1 MODERATELY = 2 A GREAT DEAL = 3

SYMPTOMS	BOTHER
<input type="checkbox"/> ← Is it difficult to hold urine when you get the urge to go?	How much does it bother you? → <input type="checkbox"/>
+	+
<input type="checkbox"/> ← Do you have a problem with going to the toilet too often during the day?	How much does it bother you? → <input type="checkbox"/>
+	+
<input type="checkbox"/> ← Do you have to wake from sleep at night to pass urine?	How much does it bother you? → <input type="checkbox"/>
+	+
<input type="checkbox"/> ← Do you leak urine?	How much does it bother you? → <input type="checkbox"/>
+	+
=	=
<input type="text"/> NOW ADD THE TWO COLUMNS DOWNWARDS AND PUT THE SCORES IN THESE BOXES	<input type="text"/>
My symptom score	My 'bother' score

SYMPTOM SCORE	THIS SYMPTOM SCORE MEANS:	THIS 'BOTHER' SCORE MEANS:	'BOTHER' SCORE
0	You are fortunate and don't have a urinary problem	You aren't bothered by a urinary problem	0
1-3	Your symptoms are mild	You are bothered slightly by your symptoms	1-3
4-6	You have moderate symptoms	You are moderately bothered by your symptoms	4-6
7-9	You have significant symptoms	Your symptoms are of significant bother for you	7-9
10-12	You have very significant problems	Your symptoms are a major problem for you	10-12

If your symptom score (above) is 4 or over you should seek help. If your bother score (above) is 1 or over you may benefit by seeking help

Fig. 1.1.2: Bladder control Self-Assessment Questionnaire (BSAQ). The BSAQ is a self-completion questionnaire, taking into account the patient's symptoms and sensations. If the symptom score is above 4 and the bother score is above 1 the patient may have OAB.

However, these questionnaires are not used diagnostically due to their subjective nature.

Voiding diaries are the objective record of the voiding frequency and volume throughout the day and, therefore, are useful to distinguish between overactive and normal bladders.

Physical examination is also usually required to identify medical conditions contributing to symptoms. The **urinalysis** is the first analysis due to its low-cost and non-invasiveness. It helps excluding other conditions such as urinary tract infection, kidney problems and diabetes (Rovner *et al.*, 2002). **Postvoid residual urine volume tests** help to check if the bladder empties fully after urinating. This can be done either through a catheter (invasive) or ultrasound (non-invasive), the latter also used to visualize inside the urethra and the bladder (Reviewed by Melinda Ratini, 2018). The **pressure-flow urodynamic** testing is usually reserved for patients refractory to other treatments for OAB, due to the invasiveness and risk of urinary tract infections (Caruso *et al.*, 2010). Briefly, the bladder is filled with a saline solution through a catheter, which also allows the measurement of the pressure within the bladder, and the patient is asked to tell the intensity of his/her desire to urinate. The patient is also asked to cough and stand to check any leakage of urine. This urodynamic test distinguishes between people with detrusor overactivity and people with just pelvic floor dysfunction. The **cystoscopy** test is reserved to those patients that suffer the symptoms of overactive bladder with the suspicion of bladder cancer (Truzzi *et al.*, 2016a).

1.1.3 Treatments currently available

Currently available treatments primarily address symptom resolution rather than the causes underlying the pathology. The first attempt to improve the symptoms is through **pelvic floor muscle retraining**, which consists of exercises to strengthen the above-mentioned muscle and, therefore, avoiding sudden episodes of leakage (Wooldridge, 2016). The outcomes, though, are difficult to maintain for long periods (Lucas *et al.*, 2013).

The first pharmacological treatment tried in patients with OAB is **anticholinergic agents**, which act by binding and therefore blocking the muscarinic receptors of the urinary tract, M2 and M3 (Hegde, 2006), which are indirectly or directly responsible for detrusor contraction. The antimuscarinic drugs used to treat overactive bladder are: *Darifenacin*, *Fesoterodine*, *Oxybutynin*, *Propiverine*, *Solifenacin*, *Tolterodine*, *Trospium* (Robinson and Cardozo, 2012). Despite their efficacy, antimuscarinic agents have a rate of discontinuation up to 80% among the patients, due to their side effects (Saks and Arya, 2009) which include dry mouth, blurred vision, constipation, erythema and fatigue (Truzzi *et al.*, 2016b). The second-line treatment in patients who do not respond to or tolerate the anticholinergic agents is represented by **β-3-adrenoreceptor agonists**; Mirabegron is the only one currently approved (Chapple, 2012). These agents, by binding to the β-3-adrenoreceptor on the bladder wall, stimulate the accumulation of cyclic adenosine monophosphate (cAMP) by stimulation the adenylyl cyclase enzyme, leading to relaxation of the detrusor muscle and, therefore, improvement of bladder filling (Truzzi *et al.*, 2016b). Although studies have shown their superiority compared to the antimuscarinic agents (Khullar *et al.*, 2013), adverse effects such as hypertension,

nasopharyngitis and urinary tract infections (Nitti *et al.*, 2013) make their long-term use problematic.

Patients refractory to these two medications are treated either with botulinum toxin (botox) injection into the detrusor muscle, or percutaneous tibial nerve stimulation (PTNS). **Onabotulinumtoxin A** (Botox A) is a neurotoxic protein produced by the bacterium *Clostridium botulinum* (Montecucco and Molgó, 2005), which is injected into the bladder mucosa to inhibit muscle contraction, by suppressing the presynaptic release of acetylcholine from the motoneurons (Wooldridge, 2016). Botox has an average duration of effect of 6 to 9 months (Wooldridge, 2016), and so requires reinjection. The main adverse effects are urinary tract infections, increased post-void residual volume and urinary retention (Flynn *et al.*, 2009; Denys *et al.*, 2012; Chapple *et al.*, 2013; Nitti *et al.*, 2013, 2017). Instead, the **peripheral electrical stimulation of the tibial nerve** inhibits detrusor contraction via afferent action of the pudendum nerve (Berghmans *et al.*, 2000). It consists of placing a small needle electrode in the inner of both legs in relation to the internal malleolus, which gives way to a low voltage electrical pulse via the tibial nerve. The treatment consists of 30 minutes sessions for 12 weeks; the efficacy lasts up to 6 months (Marchal *et al.* 2011; Arrabal-Polo *et al.* 2012). Decreased OAB symptoms and improvement in the quality of life were demonstrated through questionnaires (Peters *et al.* 2013; Onal *et al.* 2012; Govier *et al.* 2001). Apart from local reactions on the site of the puncture, such as pain and bleeding (Peters *et al.* 2013; Govier *et al.* 2001), no side effects have been shown.

A more invasive treatment, **sacral neuromodulation** (SNM) is used in patients refractory to the previous one. It acts by activating the afferent sacral nerve fibres that inhibit parasympathetic motor neurons, and, thus, preventing detrusor contractions (Wooldridge, 2016). The treatment comprises two different phases. The first one consists of the implantation of a temporary or permanent electrode to which a set of programmed electrical impulses are delivered. If the patient responds well to this phase, he/she will undergo the second phase, which involves the implantation of the implantable generator (Truzzi *et al.*, 2016b). Some studies show long-term decrease of the number of incontinence episodes and voids per day, with little side effects such as local pain at the implantation site, electrode migration and infection (van Kerrebroeck *et al.*, 2007; Groen, Blok and Bosch, 2011). It is important, though, to educate the patients in terms of managing the remote control and being ready for electrode replacement.

In some cases, surgical intervention such as **bladder augmentation** or **urinary diversion** is considered the last chance for refractory overactive bladders. The first one consists of removing a small piece of intestine and placing it in the bladder wall, to enlarge it and, therefore, increase the volume of urine stored (Truzzi *et al.*, 2016b). In the second, the ureters are directly connected to the outside of the body, bypassing the bladder, and allowing urine to be stored in an ostomy bag worn on the abdomen (Daneshmand, 2017). The risks associated with surgery, such as infection, bleeding, pain, issues with the tube and urine leakage (Daneshmand, 2017), make surgery only the last procedure for the treatment of overactive bladder.

Hence, current treatments for OAB mainly aim to relax the bladder and, consequently, reduce the episodes of urgency; however, their side-effects and poor patients' adherence make these medications unsuitable for long-term treatment of the pathology.

1.1.4 Aetiology of OAB

As mentioned earlier, the treatments currently used in overactive bladder only aim to suppress the symptoms of this condition. This happens because the causes of the pathology are still largely unknown and not understood. It is thought OAB has a multifactorial nature, with a focus on possible roles of the central nervous system (CNS), the detrusor muscle and the urothelium/suburothelium in the pathogenesis. Hence, three main hypotheses have been hypothesized to explain the aetiology of OAB.

The first hypothesis, the so-called **neurogenic**, suggests that the stimulation of stretch-sensitive receptors is responsible for the sensation of bladder fullness, through the release of neurotransmitters such as acetylcholine, which in turn activates bladder contraction via the CNS (Miller and Hoffman, 2006). Damage to central inhibitory pathways or oversensitization of peripheral afferent terminals (De Groat, 1997), over secretion of neurotransmitters such as acetylcholine (Miller and Hoffman, 2006) may trigger voiding reflexes that cause bladder overactivity.

The second theory is the **myogenic**. The bladder volume can alter and enhance the spontaneous contractions (micromotions) of the bladder wall, leading to uncoordinated activity (Drake, Harvey and Gillespie, 2003). Moreover, the alteration of Ca^{2+} sensitivity of contractile proteins, such as myosin-filaments, can lead to increase of intracellular Ca^{2+} concentration and, consequently, enhance contractility, as demonstrated in some animal models generating increased spontaneous contractility (Chang *et al.*, 2006). The interaction between muscle and mucosa also plays an important role, as the mucosa can potentially generate spontaneous contractions (Sadananda, Chess-Williams and Burcher, 2008), especially in bladder pathologies such as OAB where the mucosa proliferates. Nevertheless, also structural changes in detrusor myocytes (Drake, Mills and Gillespie, 2001) may lead to uncontrolled detrusor contraction.

The **urotheliogenic** hypothesis implies that chemical and mechanical-induced release of neurotransmitters, such as adenosine triphosphate (ATP) and nitric oxide, from urothelial and suburothelial cells, activates bladder afferents; therefore, playing a role in bladder sensitization and potentially causing an alteration of detrusor excitability (De Groat, 2004). Spontaneous contractions of the mucosa itself can also trigger bladder contraction (Kushida and Fry, 2016).

Therefore, various factors, alone or in combination, can enhance CNS-mediated or spontaneous contractility of the detrusor muscle, but not sufficient to justify the onset of overactive bladder.

1.2 IGF-1 splice variants in OAB

1.2.1 Insulin-like growth factors

Insulin-like growth factors (IGFs) 1 and 2, or somatomedins, are protein hormones, mainly Growth-Hormone (GH)-dependent, involved in a broad range of tissue processes such as cell growth and survival, proliferation, differentiation and metabolism (Puche and Castilla-Cortázar, 2012; Bergman *et al.*, 2013). Their names come from the degree of homology between their N-terminal domain and the insulin B chain, but their nature is independent of insulin (Zapf *et al.* 1978). Both of them interact with various binding proteins, and act by binding to their own tyrosine kinase receptors IGF-1R (Leroith *et al.*, 1995) and IGF-2R (Humbel 1990), but also to the insulin receptor with lower affinity (Rinderknecht and Humbel, 1978; Bergman *et al.*, 2013). Although their biological functions are very similar, IGF-2 is primarily expressed in embryonic and fetal life in a variety of tissues, stimulating cell proliferation, differentiation, growth and survival (Engström *et al.*, 1998); whereas circulating IGF-1 levels rise in puberty and decline afterwards (Sara *et al.*, 1983).

IGF-2 was demonstrated to be subjected to parental imprinting, with the maternal allele silent in embryos (Lee *et al.*, 1993), and subsequently transcribed in the adult (Bergman *et al.*, 2013). The dysregulation of the imprinting mechanisms, with consequent overexpression of IGF-2, is the main cause of the Beckwith-Wiedemann syndrome (BWS), which causes conditions such as gigantism and hypoglycaemia at birth (Shuman and Weksberg, 2016). The affected children have also an increased probability to develop various kinds of tumours, such as hepatoblastoma, rhabdomyosarcoma and Wilms' tumour (Ward, 1997).

IGF-1 is mainly produced by the liver in a way that is GH-dependent (Daughaday *et al.*, 1972); however, in other tissues such as the uterus, it is regulated by specific local factors (Murphy and Friesen, 1988), suggesting the idea that it is an independent hormone. IGF-1 inhibits GH secretion with a negative feedback mechanism by suppressing its expression (Ghigo *et al.*, 1997) and stimulating somatostatin secretion (Bertherat, Bluet-Pajot and Epelbaum, 1995). Together with IGF-2, it stimulates fetal growth and differentiation (Leroith *et al.*, 1992), independently from the GH (Savage *et al.*, 1993; Laron, 2004), and postnatal bone growth, in synergy with the GH (Sjögren *et al.*, 1999). In the brain, local and systemic (Reinhardt and Bondy, 1994) IGF-1 has a neuroprotective (Carro *et al.*, 2002) and pro-proliferative role for oligodendrocytes and their precursors (Yao *et al.*, 1996), without the GH having an active part in this process. Although the liver is the main source of IGF-1, the amount of IGF-1R on the membrane of the hepatocytes is very low (Skrtic *et al.*, 1997), yet it is thought that IGF-1 plays a decisive role in liver regeneration by stimulating DNA synthesis (Desbois-Mouthon *et al.*, 2006) and hepatocytes proliferation (Pennisi *et al.*, 2004). IGF-1 also plays a crucial role in gametogenesis by promoting ovarian follicular growth (Silva, Figueiredo and van den Hurk, 2009) and testicular function (Saez, 1994), kidney (Martin *et al.*, 1991) and cardiovascular development (Sharma *et al.*, 2017), and immune modulation (Pete *et al.*, 1996; Delafontaine, Song and Li, 2004). In muscle there are different sources of IGF-1, being not only myocytes, but also satellite cells (Mauro 1961) and cells of the extracellular matrix, such as fibroblasts, adipocytes and vascular tissue (Ceafalan, Popescu and Hinescu, 2014), able to produce it. It

acts in a paracrine way, managing to stimulate growth even in the absence of the liver-secreted IGF-1 (Vassilakos and Barton, 2018). Fig. 1.2.1 summarizes IGF-1 main biological activities.

Fig. 1.2.1: IGF-1 range of actions in the human body. IGF-1 is involved in several cellular processes including tissue differentiation, maintenance of tissue mass and tissue repair.

Image adapted from: Puche JE, Castilla-Cortázar I. Human conditions of insulin-like growth factor-I (IGF-I) deficiency. *J Transl Med.* 2012;10:224. Published 2012 Nov 14. doi:10.1186/1479-5876-10-224

1.2.2 Alternative splicing and translational products

IGF-1 consists of six exons, of which exon 3 and exon 4 represent a constant region that will subsequently give rise to the mature IGF-1 protein (Barton, 2006) (Fig1.2.2). It is thought that one of the mechanisms through which circulating IGF-1 is regulated and exerts its function is through alternative splicing, which allows the production of different mRNAs, in a way that is dependent on the tissue, the developmental stage or external stimuli (Nilsen and Graveley, 2010).

The presence of two Promoters, P1 in exon 1 and P2 in exon 2 (Vassilakos and Barton, 2018), leads to two different transcript categories: class I (transcription starting in exon 1 and excluding exon 2) and class II (transcription starting in exon 2 and ligating to exon 3) (Barton, 2006). As shown in Fig. 1.2.2, due to various combinations of intron removal and exon ligation, human *IGF-1* has three transcript variants: the exclusion of exon 5, with consequent ligation of exon 4 to exon 6, gives rise to IGF-1Ea (Jansen *et al.*, 1983); alternatively, the transcription of poly-A signals at the end of exon 5 leads to the termination of the transcription, generating a variant found only in humans, IGF-1Eb (Wallis, 2009). The third variant, IGF-1Ec, contains the first 49 base pairs (bp) of exon 5 ligated to exon 6 (Chew *et al.*,

1995), causing a shift in the reading frame of exon 6 with the consequent introduction of a stop codon (Rotwein *et al.*, 1986).

IGF-1Ea represents the canonical and main variant found in liver (Lin and Oberbauer, 1998), but it is also produced in various tissues such as kidney, adrenal and skeletal muscle, and it is responsible for GH-dependent stimulation of normal growth and development (Chew *et al.*, 1995). As discussed further, together with IGF-1Ec, it is expressed in muscle with a predominant pro-differentiative function. IGF-1Eb was first discovered in the liver (Rotwein, 1986), but it is expressed in a variety of human tissues, such as skeletal muscle, prostate, endometrium and lens epithelial cells (Philippou *et al.*, 2009; Armakolas *et al.*, 2010; Milingos *et al.*, 2011; Moschos *et al.*, 2011). Specific roles of this splice variant are still mainly unknown. There is no evidence of IGF-1Eb analogues in other mammals (Wallis, 2009). IGF-1Ec was also originally found in liver, but is expressed only 10% compared to the Ea variant (Chew *et al.*, 1995). As discussed below, its main biological activities, such as stimulating satellite cells proliferation, have been studied in skeletal muscle. The human IGF-1Ec corresponds to the rat IGF-1Eb variant (Roberts *et al.*, 1987; Shimatsu and Rotwein, 1987).

The translation of the different IGF-1 transcripts produces various pre-pro-peptides, which are subsequently cleaved to release the mature IGF-1 peptide and undergo post-translational modifications. A cleavage site within the domain encoded by exon 3 sets free the N- terminal signal peptide (Rotwein, Folz and Gordon, 1987), whose function is to send IGF-1 out of the cell for secretion (Lingappa and Blobel, 1980). The structure of pro-IGF-1, the pre-pro-peptide without the signal peptide, consists of five domains: B C A D (Rinderknecht and Humbel, 1976), and a C-terminal E domain (Vassilakos, Philippou and Koutsilieris, 2017). Another cleavage site within the domain encoded by exon 4 (Duguay, Lai-Zhang and Steiner, 1995), sets free the E-domain, now called E-peptide, giving rise to the mature IGF-1 protein (domains B C A D) that is identical for all the transcript variants (Vassilakos, Philippou and Koutsilieris, 2017). As a consequence of the alternative splicing mechanism, three different E peptides exist in humans, which correspond to the three IGF-1 mRNA variants (Duguay, 1999). Figure 1.2.2 shows the splice variants of *IGF-1* and the translational products derived. The E peptide of the IGF-1Ec variant, Ec peptide, is also called Mechano-Growth Factor (MGF) because of its pro-proliferative action on skeletal muscle progenitor cells after injury/mechanical stretch, as further discussed.

Pro-IGF-1 can also remain as it is, without separation of the E peptide (Durzynska *et al.*, 2013; De Santi *et al.*, 2016). Pro-IGF-1Ea can undergo posttranslational modifications; thus, the Ea peptide contains an N-glycosylation site at Asn92, and both unglycosylated and glycosylated forms of pro-IGF1 forms have been detected (Durzynska *et al.*, 2013). Mature IGF-1 can also go through further modifications, i.e. the production of a truncated form of IGF-1 following cleavage of the first three amino-acids at the N-terminal (-3N:IGF-1) with subsequent production of a tripeptide glycyl-propyl-glutamate (GPE), which is found only in human brain and acts as a bioregulator of IGF-1 (Sara et al. 1989; Sara et al. 1993).

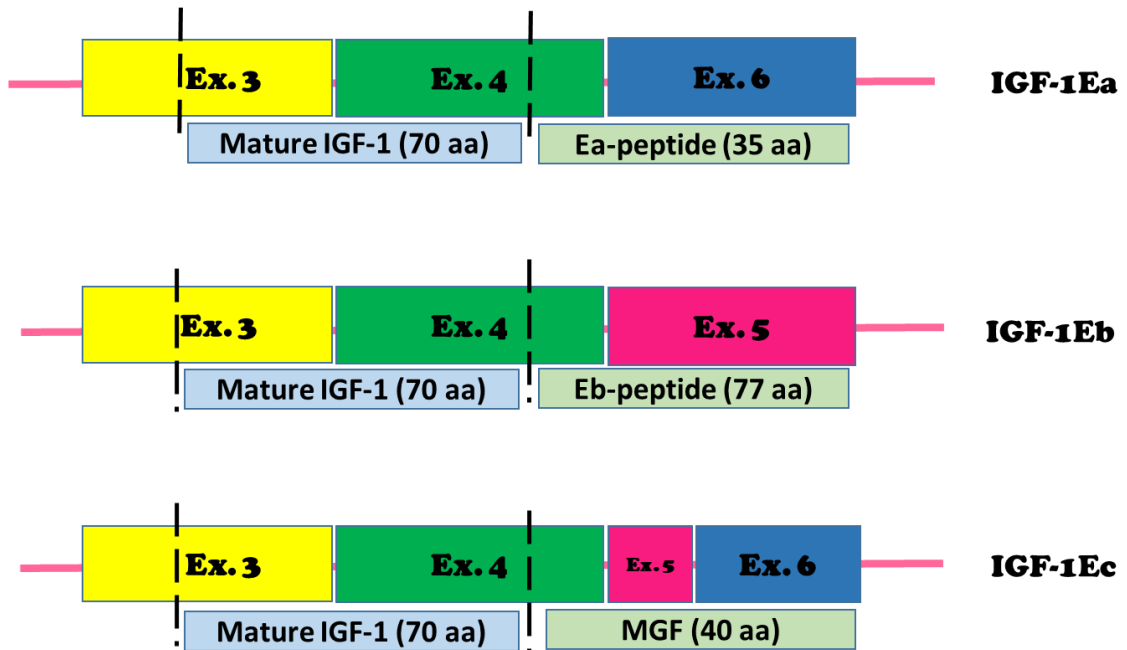


Fig. 1.2.2: Splice variants of the IGF-1 gene and translational products. All *IGF-1* splice variants contain exon 3 and exon 4, which will give rise to the mature IGF-1 peptide. Compared to IGF-1Ea, in IGF-1Ec an insertion of 49 bp (exon 5) causes a shift in the reading frame, resulting in a different E-peptide (MGF). The two cleavage sites within the prepropeptide set free an N-terminal signal peptide and a C-terminal E-peptide, unique to each variant.

1.2.3 MGF

1.2.3.1 Synthetic/overexpression studies

Note: the following terminology will be used from this point onwards in the thesis: we will call IGF-1Ec the transcript variant, MGF the 40-aa Ec peptide, MGF-24 the peptide corresponding to the last 24 amino acids of the 40-aa MGF, and pro-MGF the form consisting of MGF with mature IGF-1 attached.

As previously mentioned, IGF-1 plays an active role in skeletal muscle growth and regeneration; its actions are mainly to ascribe to its splice variants, based on the so-called “MGF hypothesis” (Yang et al. 1996). Most of the research showing a pro-proliferative role for MGF was performed through its overexpression or the application of a synthetic peptide corresponding to the last 24 amino acids of MGF (MGF-24). The first studies using mature IGF-1 and the native last 24-aa sequence of MGF (NH₂-YQPPSTNKNTKSQRRKGSTFEERK-COOH) were performed in skeletal muscle, using C2C12 mouse myoblasts, in which IGF-1Ec and IGF-1Ea mRNAs were both overexpressed and/or MGF and mature IGF-1 peptides administrated exogenously. These data show that in both IGF-1Ec-positive clones and MGF-24-treated cells, the rate of proliferation was higher compared to the non-transfected and non-treated controls, but not significantly higher than IGF-1Ea-transfected cells and mature IGF-1 treated cells (Yang and Goldspink, 2002; Philippou *et al.*, 2009). Moreover, MGF action seemed to inhibit myoblast terminal differentiation, in both IGF-1Ec-transfected cells and normal C2C12 cells treated with the synthetic peptide or with medium harvested from IGF-

1Ec-transfected cells (Yang and Goldspink, 2002). In fact, withdrawing MGF from the culture allowed cells to fuse and form myotubes, suggesting that its pro-proliferative action is not accompanied by stimulation of differentiation, which is instead performed by mature IGF-1, as shown by induction of myotube formation in IGF-1Ea-positive clones (Yang and Goldspink, 2002).

Later studies employed a slightly modified form of the MGF-24 peptide, in which the two-arginine amino acids were switched from the L to the D-form to increase the stability of the peptide (NH₂-YQPPSTNKNTKSQ(d)R(d)RKGSTFEEHK-COOH). This was also used in studies in brain, heart, tendons and bone marrow-derived mesenchymal stem cells.

In the brain, several studies demonstrated MGF biological activities, e.g. hippocampal neurogenesis in IGF-1Ec-overexpressing mice (compared to non-overexpressing) (Tang *et al.*, 2017), neuronal guidance and growth in MGF-24-injected brain-injured rats (compared to non-injected) (Liu *et al.*, 2018) and increased motor unit and motoneuron survival in MGF-24 and mature IGF-1-injected SOD1^{G93A} mice (compared to non-treated and vehicle-treated) (Riddoch-Contreras *et al.*, 2009). The modified peptide was also used in an *in vivo* study in a gerbil model of brain ischemia, where in MGF-24-injected animals the hippocampal neurons on the injected and contralateral sites had a higher rate of survival after the ischemic episode, compared to the mature IGF-1-injected (Dluzniewska, 2005), demonstrating for the first time the neuroprotective role played by MGF.

Other research groups, investigated MGF role in different tissues. Doroudian *et al.* (2014) fabricated a microrod delivery device loaded with MGF-24 to study its effects on cardiac damage. MGF increased the migration of human mesenchymal stem cells, assessed using a polycarbonate porous membrane insert, and protection from apoptosis, demonstrated by the TUNEL assay and Bcl-2 expression (Doroudian *et al.*, 2014). Zhang *et al.* (2016) demonstrated MGF actions in tendon repair: rats used as a model of Achilles tendon rupture were injected with different concentrations of the last 25 amino acids of the rat MGF peptide into the tendon injured sites, and mechanical tests of the tendons were performed to test MGF effects. The calculation of the Achilles functional index (AFI) showed significant improvement in the MGF-treated tendon compared to the sham tendon, and microscopic observation of the operated tendon demonstrated its healing (Zhang *et al.*, 2016). Sha *et al.* (2017) reproduced severe hypoxia with CoCl₂ to test MGF-24 effects on bone marrow. The proliferation of bone marrow derived mesenchymal stem cells was assessed through flow cytometry and EdU assay, and osteogenic differentiation through alkaline phosphatase and Alizarin Red S staining and RT-qPCR (Sha *et al.*, 2017).

As previously mentioned, it was shown that post-translational modifications of pro-IGF-1 consist of cleavage of the signal peptide and the E-peptide (Duguay *et al.*, 1997); however, there is no evidence of proteases being able to cleave within the Ec peptide at the exon 4/5 boundary to liberate the 24-amino acid peptide. Nevertheless, the so-called “MGF hypothesis” suggests that the pro-proliferative action has to be ascribed to the specific MGF peptide, and specifically to MGF-24, as reported above (Yang and Goldspink, 2002; Kandalla

et al., 2011), and not to pro-MGF neither to mature IGF-1 itself. The question that, therefore, many research groups have been trying to answer is whether such a small peptide, estimated to be around 3 kDa (Janssen *et al.*, 2016), actually exists and is stable within the cell.

1.2.3.2 Physiological detection of MGF

The important role played by MGF in tissue regeneration, demonstrated by the studies overexpressing IGF-1Ec or using *in vitro* and/or *in vivo* a synthetic form of the peptide, contributed to the interest on its physiological detection and actions. The first evidence showing IGF-1Ec gene expression in skeletal muscle were obtained using rabbits subjected to mechanical stretch (Yang *et al.* 1996) and mechanical combined with electrical stimulation (McKoy *et al.*, 1999). IGF-1Ea and IGF-1Ec mRNA transcripts were measured using *in situ* hybridisation, which demonstrated upregulation of the transcripts in the stimulated muscle compared to the control. In another study using mechanical and electrical-stimulated rats, IGF-1Ec transcript appeared the day after the operation compared to the sham-operated and normal control muscle, followed by the increase in IGF-1Ea mRNA transcript expression at a later time point (Hill, Wernig and Goldspink, 2003). These findings, together with the later association of IGF-1Ec upregulation with increased expression of satellite cells and myoblast proliferation markers (M-Cadherin and MyoD) in rat stretched muscle suggested the idea that IGF-1Ec and IGF-1Ea may have an active though different role in skeletal muscle regeneration following mechanical and/or electrical-induced damage, with MGF stimulating proliferation of satellite cells, and IGF-1Ea promoting their terminal differentiation (Hill and Goldspink, 2003).

The demonstration of IGF-1Ec gene expression triggered the interest in determining its circulating levels. To discriminate between MGF and the other IGF-1 isoforms, a lot of effort was put to raise antibodies specifically against MGF which recognize only MGF-related peptides, e.g. pro-MGF, MGF and, potentially, MGF-24. For this purpose, different techniques were performed. Kravchenko *et al.* (2006) were able to produce two different monoclonal antibodies to MGF using the cell fusion technique, and, therefore, producing two hybridoma clones. The antibodies were able to detect concentrations of MGF-24 synthetic protein down to 10 ng, but no detection was registered in 100 µg of murine skeletal muscle homogenate (Kravchenko *et al.*, 2006). Later, Philippou *et al.* (2008) immunized New-Zealand rabbits with the synthetic MGF-24 peptide, and the anti-serum was tested in both human skeletal muscle (down to 0.25 µg), and murine myocardium protein extract (down to 10 µg). The antibody was able to detect a 15.6 kDa band, as expected, in the human homogenate, and a 17.8 kDa band in murine myocardium, both corresponding to pro-MGF (Philippou *et al.*, 2008). No MGF or MGF-24 physiological forms were detected. The specificity of the anti-serum was confirmed by lack of MGF immunodetection using non-immune rabbit serum (Philippou *et al.*, 2008). In both studies, the synthetic MGF protein (around 3 kDa) was used as a positive control (Kravchenko *et al.*, 2006; Philippou *et al.*, 2008). More recently, another study (Du *et al.*, 2013) aimed to produce antibodies for the specific detection of circulating human pro-MGF in skeletal muscle. As a matter of fact, in the last decades, recombinant pro-MGF has

been circulating in amateur and/or elite sport as an anabolic drug, due to its reported induction of protein synthesis and cell proliferation. In 2005, it was included in the Prohibited List of the World Anti-Doping Agency (WADA) (Du *et al.*, 2013), making the development of unfailing methods for its detection an area of intense research focus. For this purpose, four polyclonal antibodies against four different regions of MGF, respectively (MGF, MGF-24, and two different sections of MGF) were obtained and analysed through western blotting, ELISA and reverse-phase protein microarrays (Du *et al.*, 2013). The antibodies were able to detect a 15 kDa band corresponding to the human pro-MGF (rhMGF), but could not identify it in C2C12 cells, demonstrating their specificity for hMGF (Du *et al.*, 2013). All of the research groups detected pro-MGF, as expected by the prediction of the molecular weight depending on the peptide sequence, which expects mature IGF-1 to be around 8 kDa, pro-IGF-1Ea of around 11.7 kDa, pro-MGF of around 12.4 kDa, and MGF-24 of about 3 kDa (Janssen *et al.*, 2016). Consistent with this consideration, another recent study measuring the endogenous forms of IGF-1 in murine skeletal muscle demonstrated that the pro-hormone forms are predominant (Durzynska *et al.*, 2013). In the same study, an antibody against the Ea variant used in western blot seemed to confirm the glycosylation of this isoform, detecting a 13 kDa band (attributed to pro-IGF-1) and a 20 kDa band (attributed to gly-pro-IGF-1) (Durzynska *et al.*, 2013). The veracity of the bands was confirmed by treatment with furin and/or glycosidase that revealed an increase in cleaved mature IGF-1 of 7 kDa, and a single 13 kDa pro-IGF-1Ea band (Durzynska *et al.*, 2013).

Thanks to these new-generation antibodies, it was possible to detect specifically and effectively physiological MGF, both by western blot and immunostaining. Immunostaining of human levator ani muscle from non-pregnant women and women after vaginal delivery revealed that MGF expression was higher in the delivery compared to the control group, as a confirmation for mRNA transcripts, which indicated that MGF expression is associated with muscle damage (Cortes *et al.*, 2005). Western blotting and immunolocalization of a gerbil hippocampi pre and post an ischemic episode, showed how MGF levels, not detectable in the preischemic hippocampi, increased following ischemic episode (Dluzniewska, 2005). MGF protein presence was also confirmed in human skeletal muscle and rat cardiac muscle by western blotting and immunostaining (Philippou *et al.*, 2008).

Although western blot is useful to detect and confirm the presence of a specific protein in a cell lysate or tissue homogenate, immunostaining techniques help to clarify in which compartment we can find the protein, whether nuclear, cytoplasm or extracellular. Immunostaining technique in the studies above mentioned revealed the presence of MGF in the cytoplasm and nuclear region of the levator ani muscle (Cortes *et al.*, 2005), and cytoplasm in pyramidal neurones (Dluzniewska, 2005), human skeletal muscle (Philippou *et al.*, 2008, 2009) and endometrium stromal cells (Milingos *et al.*, 2011). The specificity of the antibodies used was tested through neutralizing the antibody with MGF peptide, or with secondary antibody only control. MGF localization in the nucleus in addition to the cytoplasm seems to be confirmed by the presence of nuclear signals which lack in IGF-1Ea (Goldspink, 2005). However, MGF does not possess nucleolar localization signal, the amino acidic

sequence “R/K-R/K-X-R/K”, which is instead encoded by the C-terminal part of exon 5, and, therefore, found in IGF-1Eb (Tan, Cook and Chew, 2002).

To summarize, the data from the above studies show that IGF-1Ec expression in skeletal muscle is induced by mechanical and/or electrical stimulation, and it correlates with the proliferation of satellite cells. Moreover, the generation of specific antibodies to MGF seems to suggest that the main form circulating in skeletal muscle is pro-MGF, which is mainly located in the cytoplasm.

1.2.3.3 Mechanisms of action of MGF

A common interest, even of early studies on MGF, was to investigate whether MGF/pro-MGF would act via the IGF-1R or not. Various studies demonstrated that MGF actions are not affected by immunoneutralization of IGF-1 receptor (IGF-1R), suggesting that its biological functions may be independent of mature IGF-1 and mediated through an alternative route, even if a specific cell surface receptor has yet to be identified (Yang and Goldspink, 2002; Philippou *et al.*, 2009; Zhang *et al.*, 2009; Milingos *et al.*, 2011; Qin *et al.*, 2012). Unlike mature IGF-1, which activates both ERK 1/2 and Akt signalling pathways, MGF-24 seemed to activate only ERK 1/2 pathway in C2C12 myoblast-like (Philippou *et al.*, 2009) and Hc92 cardiomyocytes (Stavropoulou *et al.*, 2009), but not Akt. This preferred signalling pathway appeared to be turned on even in the presence of IGF-1R neutralizing antibodies, confirming MGF-independency of IGF-1R (Philippou *et al.*, 2009; Stavropoulou *et al.*, 2009). That may suggest that in skeletal muscle MGF stimulates proliferation through ERK pathway, whereas mature IGF-1 stimulates differentiation via Akt pathway.

It is yet not fully clear whether and how E-peptides affect IGF-1 actions and bioavailability, and whether there is a difference between IGF-1Ea and Ec. Pfeffer *et al.* (2008) showed that IGF-1Ea and IGF-1Eb (murine IGF-1Ec) transfected C2C12 murine cells revealed increased mature IGF-1 entry into neighbouring cells (Flag positive cells), compared to the IGF-1Stop (mature IGF-1 in the absence of either Ea-or Eb-peptides) and cleavage mutants expressing only proIGF-1Ea and proIGF-1Eb transfected cells, suggesting that E-peptides *a* and *b* enhance mature IGF-1 entrance in cells at the same level, and therefore potentiating its activity (Pfeffer *et al.*, 2009). It has also been demonstrated in mice that E-peptides bind more efficiently to the extracellular matrix, independently if they are attached to the mature IGF-1 or other constructs, showing that E-peptides may play an important role in modulating the bioavailability of IGF-1 (Hede *et al.*, 2012). Data from a recent study, though, contrasts with the findings above, showing that blockage of IGF-1R inhibited Ea and Eb synthetic peptides pro-proliferative and pro-differentiative actions in C2C12 cells (Brisson and Barton, 2012). Thus, these findings, together with the ones mentioned in the previous paragraph (page 12), seem to suggest that the prohormone is the main form of IGF-1 acting in skeletal muscle, with the E-peptides (such as MGF) being specific for its different functions, and modulating its bioavailability and cell entry (Hede *et al.*, 2012).

Another interesting aspect of IGF-1Ec/MGF way of action is the hypothesis of an age-related desensitivity to mechanical stress in muscles, firstly shown in mice (Brooks and Faulkner, 1994) and rats (Owino, Yang and Goldspink, 2001), demonstrating an increased inability of older animals to respond to mechanical overload, associated with IGF-1Ec mRNA lower expression (Owino, Yang and Goldspink, 2001). A similar study in young and old humans subjected to high resistance exercise confirmed that IGF-1Ec transcripts are decreased in old subjects compared to young (Hameed *et al.*, 2003), probably due to decreased proliferation ability of satellite cells (Chakravarthy, Davis and Booth, 2000). IGF-1Ea transcripts, however, did not show a significant change after exercise (Hameed *et al.*, 2003). Furthermore, also the action of MGF was tested in this scenario, in particular, its actions in human neonatal, young and old adult myoblasts (Kandalla *et al.*, 2011). The data showed that MGF stimulated proliferation of neonatal and, less significantly, young adult, but not old adult cells, consistent with the presence of an active pool of satellite cells in the first two categories, but not in the third. Unlike the previous findings, though, MGF actions on myoblast differentiation resulted similar to mature IGF-1, by inducing an increase in the myotube fusion index and in myosin heavy chain (MyHC) protein synthesis (Kandalla *et al.*, 2011). The authors suggested these different results could be due to a change in various factors such as the sequence of the peptide, dosage and duration of the treatment and culture conditions.

In the last couple of decades, MGF actions in skeletal muscle were extensively investigated *in vitro* and *in vivo* by numerous research groups. Very little is known about its activity in smooth muscle. The only study that demonstrated MGF role in smooth muscle was done in Montreal B2 phenotype fibrostenotic Crohn's disease (Li *et al.*, 2015), in which it is known that smooth muscle cell hyperplasia, one of the characteristics of the pathology, is due to increased TGF- β -mediated IGF-1 production. As a result, it was shown that TGF- β also promotes IGF-1Ec upregulation and peptide expression, with consequent hypertrophy of smooth muscle cells. Immunoneutralization of endogenous MGF protein in primary intestine muscle cells cultured with conditioned medium (with increased MGF production) inhibited muscle hypertrophy, demonstrating a role for MGF also in smooth muscle (Li *et al.*, 2015).

In conclusion, reviewing the studies from the various research groups reported, we propose that IGF-1 biological activities are mediated through its splice variants, with a mechanism that is tissue and age-dependent. In skeletal muscle pro-MGF and pro-IGF-1Ea are the predominant forms and stimulate proliferation and differentiation of progenitor cells, respectively; however, their mechanisms of action are not fully understood yet. Nevertheless, very little is known about IGF-1Ec/MGF expression and function in smooth muscle.

1.3 Hypothesis and aims of the project

Based on the evidence implicating MGF ability to promote muscle regeneration, we wished to investigate its functions in the bladder, as to date very little is known about its role in smooth muscle. Previous preliminary data from our research group detected IGF-1Ea and IGF-1Ec mRNAs in female human bladder biopsies from asymptomatic controls and different pathological groups. In the wake of these findings, the hypothesis that led this research is that MGF might be produced physiologically in the bladder in response to mechanical stretch during the filling phase to promote the proliferation of detrusor smooth muscle progenitor cells. On the contrary, in patients with overactive bladder (OAB), MGF response may be attenuated, leading to a reduction in *de novo* smooth muscle cell growth. This would result in increased extracellular matrix deposition, and, thereby, to detrusor muscle dysfunction. With the advent of MGF showing muscle and nerve regeneration properties in skeletal muscle, it opens the possibility for new diagnostic options and novel treatments which could potentially promote both muscle and neurological regeneration improving bladder function. The understanding of MGF activity in smooth muscle will also give an insight into its role in other smooth muscle-related pathologies.

Therefore, in this project we aimed to (i) detect and quantify IGF-1 splice variants, particularly IGF-1Ec/MGF, transcript and protein expression in healthy and overactive bladders; (ii) analyse the tissue composition of the biopsy samples, in terms of relative expression of each layer of the bladder; (iii) study the association between MGF expression, tissue composition and clinical parameters; (iv) investigate MGF effect on an *in vitro* culture of primary detrusor muscle cells.

2. MATERIALS AND METHODS

2.1 Processing of murine and human bladder biopsy samples using ThermoFisher PARIS Kit

The murine and human samples (the latter taken by Mr Eduardo Cortes at Kingston Hospital) were placed on absorbent paper and weighted. Afterwards, they were placed in RNase-free tubes with a stainless 5 mm bead and an amount of Cell Disruption buffer according to their weight and homogenised for 15 minutes at 20 Hz through a TissueLyser. Half of the homogenate was left on ice for 10 minutes and then centrifuged at full speed for two minutes at 4°C for protein extraction. The other half was used for RNA extraction. The procedure was conducted according to the manufacturer's protocol. The concentration (ng/μl) and quality of the RNA (A 260/280 and A260/230 ratios) were checked using BioDrop™ Spectrophotometer (ThermoFisher Scientific). Both RNA and protein samples from each biopsy were barcoded (following Kingston University Human Tissue Authority guidelines for storage of human tissue samples) and stored in a specific box at -80°C.

The characteristics (type, weight, date of collection and processing) and parameters (amount of cell disruption buffer, μl taken out for RNA extraction and μl for protein extraction, and amount of elution solution used) applied to the processing of each biopsy sample were recorded for further analysis.

2.2 Cell culture

The cell lines used for optimization purposes, PS-1 (pancreatic stellate cells) and AsPC-1 (pancreatic adenocarcinoma), were selected because used by our research group. These cell lines were cultured in Gibco X10 RPMI 1640 medium (1X) (Fisher Scientific) supplemented with 10% FBS and 10% pen/strep at 37°C/ PCO₂ 5% in an incubator. The cells were split every three to four days. The old medium was removed from the flask, the cells were washed with 5 ml DPBS, and incubated five minutes with 3 ml of 0.05% trypsin. The action of trypsin was blocked by adding 7 ml of new medium. From this final volume of 10 ml, 1 ml was taken and moved to a new flask with 19 ml of fresh medium.

Cell counting was performed if required. In this case, after trypsinizing the cells, the solution was centrifuged for 4 minutes at 1000 rpm. The media was discarded and replaced with 1 ml of fresh media. From this, 10 μl were added to 40 μl of 0.4% Trypan Blue solution; live cells were counted using a haemocytometer. The number of cells of five out of ten squares was counted and averaged. The final cell count was calculated using the following formula: averaged number of cells x 5 (dilution factor) x 10⁴.

2.3 Isolation of RNA from cell lines

After trypsinizing the cells, and blocked the action of trypsin by adding 7 ml of fresh media, the total volume of 10 ml was moved to a 25 ml tube and centrifuged at 1000 rpm for 4

minutes. The media was discarded, the pellet was disrupted and PBS added. The sample was centrifuged again 3 minutes at 1000 rpm, and the supernatant discarded.

To isolate total RNA, the RNeasy®MicroKit (50) (Qiagen) was used according to the manufacturer's recommendation.

The isolated RNA was quantified through spectrophotometric methods, using BioDrop™ Spectrophotometer (ThermoFisher Scientific), which gives a value of the sample concentration in ng/μl and an indication of the level of purity expressed as a relationship between the absorbance at 260 nm (A260) and A280, and between A260 and A230.

2.4 Reverse transcription of RNA into cDNA

To assess the level of expression of target genes, total mRNA (500 ng/reaction when working with cell lines, and 40 ng/reaction when working with murine and human samples) was reverse transcribed into cDNA. The synthesis of cDNA was performed using Thermo Scientific™ RevertAid™ First Strand cDNA Synthesis Kit. The reverse transcription was carried out using the 2X RT master mix consisting of Reaction buffer (5x), 10 mM dNTP, 100uM oligo(dT), RevertAid RT enzyme, and RNase-free H₂O up to a final volume of 20 μl. For the transcription of specific cDNA, the oligonucleotide 5' GAAACGCCCATC 3' (Hameed *et al.*, 2003) was used instead of the oligo(dT). Alongside, a "no reverse transcriptase control" (NRT, with water replacing the reverse transcriptase enzyme), "no template control" (NTC, with water instead of RNA) were used as negative controls.

The reaction was performed in Applied Biosystems Veriti 96 well thermal cycler, using the following thermal profile: 42° C for 60 ', 70° C for 5 '.

2.5 RT-PCR

RT-PCR was performed using DreamTaq Green PCR Master Mix (2X). DreamTaq PCR master mix (2x), forward and reverse primers, 10 ng of template cDNA and autoclaved water up to a final volume of 15 ul were added in a PCR microtube. As negative control for the RT-PCR, a "water only control" (W, with water instead of the product of the reverse transcription of RNA) was run.

RT-PCR amplification was performed in Applied Biosystems Veriti 96 well thermal cycler, using the following thermal profile: 95° C for 2 ', 35 cycles of 95° C for 30'', 55° C for 30'', 72° C for 30'', and 72° or 5 '.

2.6 Agarose gel electrophoresis

To prepare a 1x solution of 50x TAE buffer (1 L: 242 gr. Tris-Base, 57 ml of glacial acetic acid, 19.66 gr of 0.5M EDTA), 20 ml were dissolved in 980 ml of distilled water. 50-100 ml of 1x TAE buffer (depending on the dimension of the gel we wished to prepare) were boiled with 1-2 g. agarose to allow the preparation of a 2% gel. 5 (when using 50 ml of TAE buffer) or 10 (when using 100 ml of TAE buffer) μl of GelRed™ were added, and the solution poured

into the electrophoresis tray (previously sealed with autoclave tape, and the comb added) and let to solidify for around 30 minutes. The PCR products were loaded into the wells, together with 5 µl of GeneRuler 100 bp DNA ladder, and run for approximatively 1 hour and 30 minutes at 80/100 V. Images of the bands were taken using G:BOX (Syngene).

2.7 RT-qPCR

RT-qPCR was performed following the Minimum Information for publication of Quantitative real-time PCR Experiments (MIQE) guidelines (Bustin *et al.*, 2009), using SYBR green master mix (2X) (Fisher Scientific, 11873913). SYBR green master mix (2X), forward and reverse primer, template cDNA up to a final volume of 5 µl were added into a 96 well microplate. Alongside the reverse transcriptase sample, no reverse transcriptase, no template and water controls were run. Samples were tested for expression of desmin (DES), vimentin (VIM), uroplakin 2 (UPK2) and glyceraldehyde 3-phosphate dehydrogenase (GAPDH) (primer sequences in table 2.14). The stability of GAPDH was calculated by comparing the average Cq in pathological samples ($Cq=29.4 \pm 0.58$, $n=28$) compared to control ($Cq=28.1 \pm 0.61$, $n=12$). The difference between the two was not statistically significant ($p=0.18$), therefore, we assumed there was no difference. RT-qPCR amplification was performed in Techne Prime Pro 48 Real-time qPCR machine, using the following thermal profile: 95° C for 10'; 40 cycles of 95° C for 10", 55° C for 30" and 72° C for 15"; 95° C for 15", 55° C for 15" and 95° C for 15".

Based on the idea that lower Cq values indicate higher gene expression and vice versa, and that the total amplification cycles were 41, we applied the inverse formula $-(Cq-41)$ to have an idea of the relative composition of each biopsy.

2.8 BCA protein quantification

The total protein concentration of the lysates extracted from cell line and murine and human samples was assessed through the Bicinchoninic Acid (BCA) Protein assay. The Pierce™BCA Protein Assay Reagent A & B were used. The standards and the target samples were placed in triplicate in a 96-well plate, to which 200 µl of solution composed of two reagents with a ratio of 49:1 were added. The plate was then incubated for 30 min at 37°C/PCO₂ 5%, and then placed inside the BioTek Epoch 2 microplate spectrophotometer for measurement of the absorbance at 562 nm. With the readings of the individual standards and samples subtracted from the blank absorbance value, the tendency function was applied, which allowed the calculation of the concentration of the samples in µg/µl. From the values obtained it was possible to calculate the amount in µl for 30 µg of proteins to be used in western blotting analysis.

2.9 Western blot

2.9.1 SDS-PAGE

After the dosage of total proteins through the BCA assay, 30 µg of proteins were combined with sample buffer 5x (312mM Tris-Hcl pH 6.8, 10% SDS, 10% β-mercaptoethanol, 25% glycerol, 0.015% bromophenol blue) and heated at 95°C for 10 minutes.

The proteins were loaded onto a 4-20% precast polyacrylamide gradient gel in Running Buffer (0.025 m Tris-Base, 0.192 m glycine, 35 mM SDS, PH 8.3) and run at 120 V for about 1h30.

2.9.2 Transfer and blocking of the membrane

After the electrophoretic migration, a sandwich was prepared to allow the transfer of the proteins to a nitrocellulose membrane through electroblotting, conducted for 5 min in the BioRad Trans-Blot Turbo, using transfer buffer (for 1 L: 200 ml BioRad transfer buffer 5x, 200 ml 100% ethanol and 600 ml nanopure water). The membrane was then placed in a container containing ~10 ml of Red Panceau Solution, which allows understanding if the transfer was successful. After three washes in TBST (Tween-Tris-buffered Saline: 100mM Tris/HCl, 0.9% NaCl, 0.1% Tween-20) of about 5 minutes each, the membrane was placed into 10 ml of Li-Cor TBST blocking buffer solution and incubated for 1h in agitation. This way, all the non-specific sites were blocked. The gel, instead, was placed overnight in Coomassie buffer (for 500 ml: 1 gr Coomassie blue, 50 ml glacial acetic acid, 225 ml methanol, 225 ml dH₂O) and washed afterwards in destain buffer (for 1 L: 100 ml glacial acetic acid, 100 ml ethanol, 800 ml dH₂O) to check the amount of non-transferred proteins left on the gel.

2.9.3 Incubation in primary and secondary antibodies

After the blocking phase, the membrane was incubated in a solution made up of primary Ab (for MGF and IGF-1 raised in rabbit, for β-actin raised in mouse) diluted 1:1000 in 5 ml TBST and 5% BSA. The membrane was incubated overnight in agitation at 4°C. After treatment with the primary antibody three washes were performed in TBST for approximately 5/10 minutes each. Subsequently, the membrane was incubated for 1 h in slow agitation at RT with secondary antibodies labelled with NIR (near-infrared) fluorescent dyes diluted 1/15000 (Fig. 2.9.3).

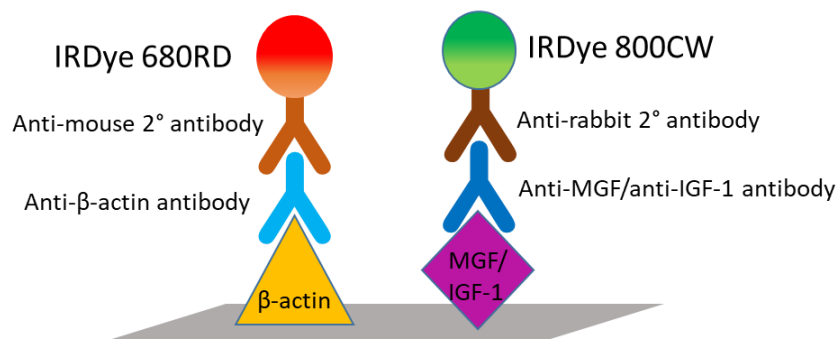


Fig. 2.9.3: Fluorescent detection of target proteins. In the western blot analysis, the Li-Cor IRDye 800CW and IRDye 680LT fluorescent secondary antibodies were used to detect MGF and IGF-1, and β -actin, respectively. In the fluorescent detection, the secondary antibodies are conjugated to fluorophores which emit a coloured light after being excited.

2.9.4 Membrane viewing and image analysis

After 3 washes of 5/10 min in TBST, the immunoblot was scanned through the NIR imager Li-Cor Odyssey CLx, where the fluorescent signal is directly proportional to the amount of target protein present. Quantification of the signal of the bands was made using Li-Cor Image Studio Lite V.5.2 software and normalized to the signal of β -actin chosen as loading control.

2.10 Immunohistochemistry

2.10.1 Fixation, preparation and embedding in paraffin of the tissue

The samples obtained from murine and human tissues were fixed in 10% neutral buffered formalin (NBF) for 24h, to fix tissue and therefore arrest biological degradation, and subsequently washed in several changes of PBS and then moved to 70% ethanol. The samples were put in a plastic box and processed through a Thermo Electron Corporation Shandon Citadel 1000 tissue processor according to the following program: 1h in 70% EtOH, 1h in 90% EtOH, 9h in 90% EtOH, 1h in 100% IMS (industrial methylated spirit), 1h in 100% industrial methylated spirit (IMS), 1h in 100% EtOH, empty, 1 h in histochoice, 1 h in histochoice, 1 h in histochoice, 2 h in histochoice, 1 h in paraffin, 2h in paraffin. The samples were then placed into a metallic box, covered in paraffin and let to cool through a Thermo Scientific HistoStar machine.

2.10.2 Slides preparation, antigen retrieval and permeabilization

5 μ m sections of the samples were cut using a Leica microtome, placed on poly-L-lysine coated slides and left to dry overnight. Slides were rehydrated by putting them in two different boxes of histochoice for 5 minutes each, two of 100% EtOH 5 minutes each, two of 70% EtOH 5 minutes each, and then washed in dH₂O 3 times for 2 minutes each. The

slides were washed 10 minutes in PBS (phosphate-buffered saline) and incubated 10 minutes in boiling 0.01 M citrate buffer (1.92 gr citric acid anhydrous, 1 L dH₂O, pH 6) for antigen retrieval, important to restore antigenicity following protein cross-linking of formalin fixation. The slides were then let to cool and washed with dH₂O. The tissue was permeabilized for 5 minutes with 0.1% Triton, to allow antibody access inside the cells to the target antigen.

2.10.3 Incubation in primary and secondary antibodies

Using a hydrophobic pen, circles were drawn around the sections and then blocked with diluted serum for 30 minutes at room temperature (RT) to prevent non-specific binding of the antibody. The sections were then covered in the primary antibody solution (1/50 or 1/100 primary antibody dilution in 5% BSA/PBS), alongside with a no-primary antibody control, overnight at 4°C. The following day the slides were washed for 2 and 5 minutes in PBS, and then secondary antibody (1/200 antibody dilution in PBS) was added for 1h at RT.

2.10.4 Development of the staining and counterstaining

After washes in PBS, the sections were incubated for 15 minutes in peroxidase blocking solution at RT, to block endogenous peroxidases that could result in non-specific background staining when using Horseradish Peroxidase (HRP) conjugated antibodies. After washes in PBS, the sections were incubated for 30 minutes in avidin-biotin complex (ABC) solution at RT. The ABC method for IHC detection is important to increase the staining intensity and sensitivity, thanks to the multiple binding opportunities between the tetravalent strept(avidin) and biotinylated antibodies (bound to the antigen) (Fig. 2.10.5). After washes in PBS, 3,3'-Diaminobenzidine (DAB) was added for the development of stain. In DAB staining, DAB is oxidized by hydrogen peroxide, with horseradish peroxidase (HRP) as catalyser, forming a brown precipitate. Slides were then washed in dH₂O three times 2 minutes each and counterstained in haematoxylin for 3 minutes to provide contrast making the stained structure easily visible using a microscope. After washes in running dH₂O, the slides were put in two boxes of 70% EtOH 5 minutes each and then two boxes of 100% EtOH 5 minutes each.

2.10.5 Mounting of slides and imaging

Sections were then mounted using one drop of mounting solution per section, covered with a coverslip and sealed with nail polish. Images of the sections were taken using a Nikon H550L microscopy with a 20X magnification.

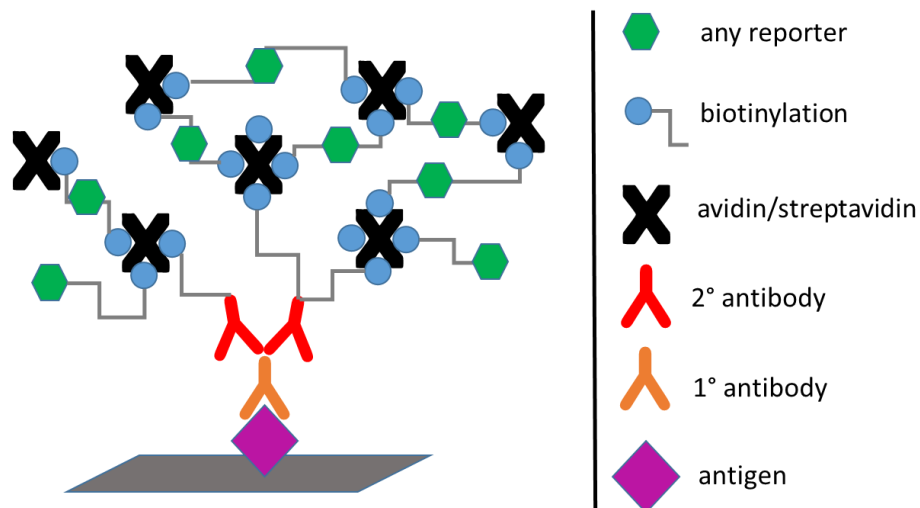


Fig. 2.10.5: The (sterpt)avidin-biotin complex (ABC) method for IHC detection. In this method, the intensity of the immunostaining is increased, taking advantage of the multiple binding sites of the (sterpt)avidin, which binds up to four molecules of biotin conjugated to the secondary antibody.

2.11 Establishment of primary cell culture

Mice were sacrificed by cervical dislocation at King's College London by Amanda Munasinghe, and heart, bladder and tight muscle removed. To preserve the sterility of the tissues, and limit the spread of any contamination, two different sets of surgical tools were used to dissect the mouse and to remove the organs; the working areas and tools were cleaned with 70% IMS and the disinfectant Distal™. The samples were stored in Advanced DMEM/F-12 supplemented with antibiotics and antifungal and transported on ice to the tissue culture facilities at Kingston University. After reviewing current protocols for the establishment of a primary culture from the bladder, we decide to follow and optimize the protocol by Pokrywczynska *et al.* (2016), method I (Pokrywczynska *et al.*, 2016). After four washes in DPBS supplemented with antibiotics and antifungal, the organs were minced using sterile scalpels and scissors and incubated at 37°C in digestion solution (1 ml Advanced DMEM/F-12 supplemented with antibiotics and antifungal, 2 mg/ml Collagenase D and Dispase II). After 1 hour the action of the digestive enzymes was blocked by adding an equal amount of the same medium, and the solution was passed through a 100 µm cell strainer to remove the undigested tissue. After that, the solution was centrifuged for 5 minutes at 1500 xg, the supernatant was discarded, and the pellet was resuspended in smooth muscle (SM) culture medium supplemented with 5% smooth muscle growth supplements (SMGS). The cells were seeded in a 96-well plate and incubated at 37°C/PCO₂ 5%. The medium was changed every day.

2.12 Treatment of primary cells with MGF protein

Murine primary cells, obtained from three murine bladders as specified above, were seeded in 96-well plates at a density of 0.01 x 10⁶/well and incubated with complete smooth muscle growth medium supplemented with/without 1/10/100 ng/ml MGF-24

synthetic peptide (NH₂-YQPPSTNKNTKSQ(d)R(d)RKGSTFEEHK-COOH) (Yang and Goldspink, 2002). As a separate experiment, cells were also incubated in smooth muscle medium without SMGS and smooth muscle medium without SMGS supplemented with 100 ng/ml MGF. The experiments were carried out for 48 and 72 hours.

2.13 Proliferation assay and immunocytochemistry

In the last 48 hours of treatment, the primary bladder cells were incubated with 10 μ M EdU at 37°C/PCO₂ 5%. After that, the medium was removed and cells were fixed in 4% paraformaldehyde (PFA) for 15 minutes at room temperature (RT). After three washes in PBS, the cells were permeabilised with 0.4% Triton X 100 in PBS for 10 minutes at RT to allow antibody entrance in the cells. The cells were then washed in PBS and blocked for 5 minutes in 0.05M glycine buffer (0.19 g glycine in 50 ml dH₂O) to reduce auto-fluorescence. Subsequent blockage in 5% horse serum for 30 minutes at RT reduced non-specific binding of the primary antibody. To confirm the muscular phenotype, cells were incubated in anti- α -smooth muscle actin/ anti-desmin/ anti-smooth muscle myosin heavy chain primary antibodies (1/100 dilution in 5% BSA/PBS) 1 hour at RT. As markers of smooth muscle cells we initially chose anti- α -smooth muscle actin (anti- α -SMA); however, its expression in myofibroblasts (Council and Hameed, 2009) led us to use desmin (DES) and anti-smooth muscle myosin heavy chain (SMMHC) (Nagai, Larson and Periasamy, 1988) instead. After two washes in PBS, the cells were incubated in secondary antibody (Alexafluor 1/200 dilution in PBS) for 1 hour at RT. After three washes in PBS, cells were counterstained for 4 minutes with DAPI to allow visualization of nuclei, and then washed in PBS. The cells were observed under the EVOS FLoid Cell Imaging Station Microscope. Quantification of total and proliferating cells was performed using the ImageJ software.

2.14 Bioinformatics

For the design of PCR primers, the sequence of the mRNAs of interest was obtained from NCBI Gene database, and copied into NCBI Primer Blast. The parameter values used were the default, except for the PCR product size, 100 to 1000 bps, and the primer specificity stringency: the minimum mismatches were increased to 4, with at least 3 mismatches within the last 5 bps at the 3' end. The optimum melting temperature of the primers was set to be 60°C. No preference was given for the exon junction span, if not specifically required by the single experiment. All the pairs of primers used have been designed by myself, except for humanEc and IGF-1Ea reverse primer for the nested reaction (Hameed *et al.*, 2003), IGF-1Eb reverse primer (designed by Dr Natasha Hill), full-length Ea/Ec (designed by Almas Mahmood) and QARS (Viloria *et al.*, 2016).

Clustal Omega website was used to check the alignment of multiple sequences. For the analysis of the sequencing data of PCR bands purified from agarose gel, FinchTv 1.4.0 was used for the analysis of the chromatogram.

The sequences of the primers used, together with the expected product length, are listed in the table 2.14, below.

A

Product name	Forward Primer Sequence	Nested Primer Sequence	Reverse Primer Sequence	Expected product length (bps)
Generic IGF-1 (NCBI ID: 3479)	CCTCGCATCTCTTCTACCTGG	REV: TCCACACACGAAGTGAAGAGC	CATACCCTGTGGGCTTG TTGA	F: 153 - N: 116
IGF-1Ea/Ec	CCTCGCATCTCTTCTACCTGG	Ea - REV: TCAAATGTACTTCTTCTGGGTC TTG Ec - FW: AGCCCCCATCTACCAACAA	CACCCATGCATTTGTGG CTC	F: 695 (Ea)/717 (Ec) - N: 330 (Ea)/424 (Ec)
IGF-1Eb	CCTCGCATCTCTTCTACCTGG	FW: CAGCCCCCATCTACCAACAA	TTGCTGTCTGCTCCTCTC TCA	F: 560 - N: 240
humanEc	CGAAGTCTCAGAGAAGGAAA GG	-	ACAGGTAAGTCGTGCA GAGC	150
New Ea/Ec	CAGACAGGCATCGTGGATGA	-	GCACTCCCTCTACTTGC GTT	176 (Ea) - 225 (Ec)
New IGF-1Ec	TCTACCAACAAGAACACGAAG TCT	-	TTTCATTGGGGGAAACG CCC	236
Full length Ea/Ec	CGGATCCTTAAGATGGAACAA AAATCATCTCAGAAGAGGAT CTGGGAAAAATCAGCAGTCTT CC	-	GAAACAAGAACTACAG GATGCACCACCACCAC CACCCTGAGAATTCGT CGAG	497 (Ea) - 549 (Ec)
QARS (NCBI ID: 5859)	TTCCGGTGTCTCTGCAATGG	-	CTGCTGAGCCTGAGTAG CG	142
HPRT1 (NCBI ID: 3251)	CCTGGCGTCGTGATTAGTGA	-	CGAGCAAGACGTTTCAG TCCT	137

B

Product name	Forward primer (5'→3')	Reverse primer (5'→3')	Expected product length (bps)	Flanking an intron?
GAPDH (NCBI ID: 2597)	CTCCTGTTCGACAGTCAGCC	CGCCCAATACGACCAATCC	112	Yes
UPK2 (NCBI ID: 7379)	GCAAGTAAGGAGGTCTGCCC	GGGGGAATTGTTATGGGGGT	283	No
DES (NCBI ID: 1674)	ACCATCGCGGCTAAGAACAT	TCACTGGCAAATCGGTCCTC	230	Yes
VIM (NCBI ID: 7431)	AAAAGTCCGCACATTCGAGC	CGCTGCTAGTCTCAGTGCT	140	No

Table 2.14: Lists of the primers used throughout the study. (A) Sequences and expected product size of the primers used in PCR. F (first reaction), N (nested reaction). (B) Sequences and expected product size of the primers used in RT-qPCR.

2.15 Statistics

Statistics were performed using MS Excel and IBM® SPSS® Statistics, the latter with advice from Dr. Rosemary McNiece (Kingston University, Department of Mathematics). Bivariate (Pearson) Correlation was used to determine the linkage between the variables of interest. Two-tailed Turkey's multiple comparison test (t-test) was automatically performed in SPSS, where needed. χ^2 test was performed in MS Excel. The nonparametric Mann-Whitney *U* test was used to compare means of groups not normally distributed. One-way analysis of variance (ANOVA) test, followed by the post hoc t-test, was used to compare the means of more than two samples. *p*-values ≤ 0.05 (*) and ≤ 0.01 (**) were considered statistically significant.

3. RESULTS

3.1 Validation and optimization of ThermoFisher PARIS Kit for RNA and protein extraction from murine samples

To ensure a good homogenization of the bladder biopsy samples, and therefore an optimal extraction of proteins and good quality RNA, murine samples (obtained from King's College London) were initially used to optimize some critical steps of the PARIS kit extraction procedure.

The size of the beads used for the homogenization phase played an important role. We started by using 50 mg of 150-212 microns glass beads and one or two 5 mm stainless steel beads per sample. The 150-212 μ m glass beads did not allow a visible disruption of the tissue; on the other hand, using two 5 mm stainless steel beads produced too much foam that would dissolve only after a few cycles of centrifugation and incubation on ice. Considering that the amount of homogenate to be used for RNA extraction should be ideally mixed with the 2x lysis/binding buffer straight after homogenization, the delay may cause a higher degradation of the RNA. To avoid that, one 5 mm stainless steel bead per sample was used.

Different speed levels and duration of the homogenization were also tested: 50 Hz for 3 minutes, 30 Hz for 6 minutes, 20 Hz for 10 minutes. 50 Hz and 30 Hz appeared to be too tough on the tissue, producing too much foam, creating a similar issue to the one mentioned above. 20 Hz, instead, turned out to be the best speed to have a visible homogenous homogenization, not requiring following centrifugation. The time of homogenization was increased to minimum 15 minutes, otherwise, the tissue did not homogenize properly. Eventually, 20 Hz for 15 minutes was then used as a standard combination for the homogenization of the samples.

Another crucial factor needing optimization was the amount of cell disruption buffer to be added to each sample, to ensure a proper homogenization, but at the same time avoiding an excessive dilution of the sample. The indication in the PARIS kit protocol for this purpose was to add 6-8 volumes of buffer per tissue mass, but that proved to be not enough to visibly homogenize the sample. Therefore, the amount of buffer was increased to 10-12 volumes per tissue mass and adopted throughout the study.

The validation and optimization of these elements of the PARIS kit protocol allowed us to routinely process the bladder biopsy samples as soon as they were collected from the hospital, even if the heterogeneity of the samples made the extraction of proteins and good quality RNA from the biopsies always quite challenging. The weight of the biopsies, together with the concentration of the RNA extracted and the RNA yield, are reported in table 3.2.

3.2 Optimization of protein and RNA yield extracted from biopsy samples

The main difference between the murine and the human samples was their volume and composition. The average volume of the former was around 15-20 mg, allowing us to obtain a good amount of homogenate to be used for RNA and protein extraction. The average volume of the human biopsies was 8 mg, with a range from 2 to 43.3 mg. Considering that the amount of homogenization buffer was proportional to the volume of tissue, the risk that the homogenate was not enough to extract both RNA and protein was not to be underestimated. Moreover, in some biopsies the fibrotic component was relatively high, leaving after the homogenization a sticky mass that could not further be disrupted, despite adding more homogenization buffer, increasing the duration of the homogenization, or passing the lysate through a syringe needle. In these cases, the amount of homogenate was even lower. These drawbacks drove us to change the ratio between the amounts of homogenate to take for RNA extraction and for protein extraction. In the beginning, the ratio used was 50:50, which was later adjusted to and kept at 25:75 for RNA and proteins, respectively. The larger protein lysates allowed us to test them through western blot even more than once, either to test the reproducibility of the technique or to run a second blot in the case the first immunoblot was unusable.

General guidelines on RNA extraction provided by ThermoFisher Scientific (ThermoFisher Scientific 2020, last accessed 31/01/2020) count the bladder as one of the tissues with the lowest RNA yield. Compared to the cell lines from which it is possible to extract large amounts of RNA and, therefore, working in downstream analysis with an optimal concentration of 500 ng/reaction, subsequently diluted 1/10, the yield obtained in the biopsy samples varied from mostly 200 ng to 8480 ng (table 3.2). The amount of RNA chosen to reverse transcribe into cDNA was 40 ng per reaction, allowing us to use the same concentration for all the samples.

Below- Table 3.2: Weight, concentration and yield of the RNA extracted from biopsy samples. In the table it is reported the weight (mg) of the biopsies, and the concentration (ng/μl), ratios of absorbance at 260/230 nm and 260/280 nm and yield (ng) of the RNA extracted from all the biopsy samples. The number in brackets indicates the piece of the biopsy, either 1 or 2. B14(N) indicates a piece of necrotic tissue obtained from the bladder of patient 14.

Biopsy	Weight (mg)	RNA conc. (ng/μl)	A260/230	A260/280	RNA yield (ng)
B1	-	3.2	0.016	4,000	320
B2	4.2	8	1.25	2	400
B3 (1)	5.5	4	-	1,667	400
B3 (2)	8.1	3.2	-	1,335	320
B4	7.7	21.6	1.28	2	1080
B5 (1)	3.5	6.4	0.1	3	320
B5 (2)	5.8	4.8	0.2	2	240
B6 (1)	4.4	18.4	0.121	2	920
B6 (2)	6.5	12.8	0.06	2	640
B7	4.9	8.8	0.164	2	440
B8	5.7	9.6	0.5	2	480
B9	3.2	1.6	0.18	2	80
B10	6.7	3.2	0.05	2	160
B11	9.5	15.2	0.5	2.1	760
B12	7.2	13.6	0.58	2.1	680
B13(1)	7.3	-	-	-	-
B13(2)	4.4	5.6	0.3	5.7	280
B14(1)	43.3	8	0.2	2	400
B14(N)	24	0	0	0	0
B14(2)	38.2	13.6	0.58	1.8	680
B15	4.7	8	-	5	400
B16	12.4	15.2	-	3	760
B17(1)	3.5	4.8	-	-	240
B17(2)	5.4	8	4	2	400
B18	11	13.6	1.8	0.8	680
B19	2.2	1.6	0.1	2	80
B20	7	6.4	0.5	1.6	320
B21	2	3.2	0.1	1.3	160
B22	7.6	8.8	1.8	2.2	440
B23A	35.3	169.6	0.6	2.1	8480
B23B	23.6	22.4	0.9	2.1	1120
B24	3.1	2.4	0.3	1.5	120
B25	6.3	13.6	0.2	2.1	680
B26	10	19.2	0.1	2	960
B27(1)	9.3	24	0.25	2	1200
B27(2)	6.7	19.2	0.5	2	960
B28(1)	7.2	11.2	0.37	1.75	560
B28(2)	11.8	7.2	0.5	1.5	360
B29(1)	14.4	21.6	0.3	2	1080
B29(2)	10.1	17.6	0.1	2	880
B30	8	8.8	0.5	2.2	440
B31	3.5	4.8	0.75	1.5	240
B32(1)	6.6	9.6	0.09	2.4	480
B32(2)	10.3	13.6	0.7	2.1	680
B33	8.5	11.2	0.5	2	560
B34	6.3	2.4	0.3	1.5	120
B35	6.5	7.2	0.15	2.2	360
B36	9.6	10.4	0.2	1.8	520
B37	6.5	7.2	0.05	2.2	360
B38	9.1	16.8	0.4	2.1	840
B39	3	4	0.07	1.6	200
B40	6	5.6	0.08	2.3	280
B41	7.5	8.8	0.07	2.2	440
B42	10.2	14.4	0.1	2	720
B43	6.7	8.8	0.019	2.75	440

3.3 Primer design strategy and optimisation in cell lines

To analyse IGF-1 splice variant gene expression in biopsy samples, nested PCR was initially performed to ensure sensitivity and specificity. Primers for the first and the nested reactions were designed to amplify generic IGF-1, IGF-1Ea, IGF-1Eb and IGF-1Ec (Fig. 3.3.1, A), following the IGF-1 gene structure and modifications after alternative splicing (Fig. 3.3.1, B). A forward primer in exon 3 was designed and used to amplify all the species in the first reaction. The reverse primers were designed according to the unique regions of each variant. For the amplification of generic IGF-1, a reverse primer at the boundary of exon 3/4 was used in the first reaction, and one in exon 3 in the nested reaction. IGF-1Ea and IGF-1Ec have both exon 6, therefore, the reverse primer of the first reaction was designed in exon 6 to amplify both of the variants simultaneously. What diversifies IGF-1Ea and IGF-1Ec is the presence of 49 bp in IGF-1Ec corresponding to the first part of exon 5, therefore, a reverse primer in the exon 4/6 boundary was chosen to detect IGF-Ea in the nested reaction, and a forward primer in exon 5 for IGF-1Ec. IGF-1Eb has exon 4 and stops at exon 5, therefore, a reverse primer in exon 5 was designed for its detection. Fig 3.3.1, A summarizes this strategy. See table 2.14, A for the sequences of the primers.

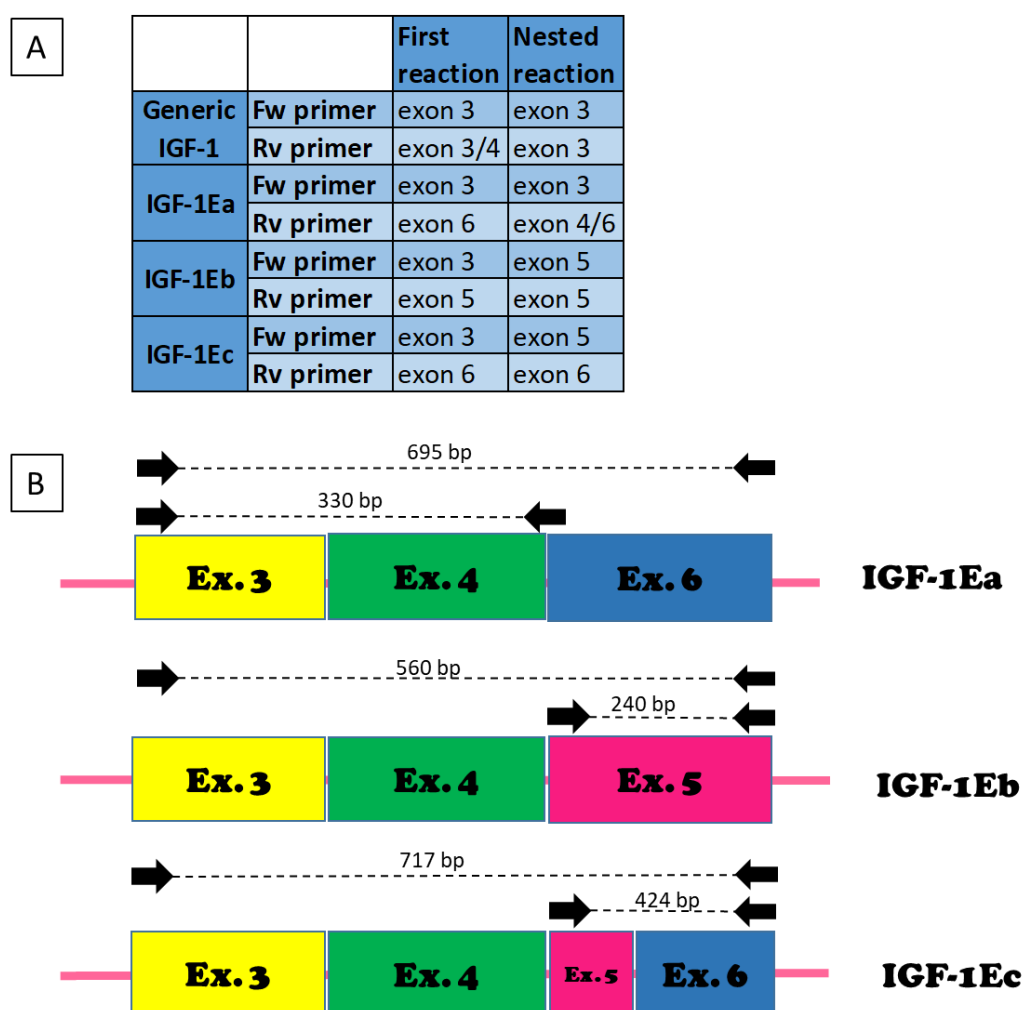


Fig. 3.3.1: Primer design for amplification of IGF-1 splice variants. (A) To perform nested PCR, two sets of primers were used for amplification of the target genes in the first and nested reactions. (B) IGF-1 splice variants mRNA structure and target regions of amplification of the first (dashed line on top) and nested (dashed line below) reactions.

Before using them in biopsy samples to detect IGF-1 splice variants, these primers were validated through RT-PCR in a cell line (PS-1) to confirm their expression. Fig 3.3.2 shows a representative nested PCR reactions using the primers described above. Primers for the detection of generic IGF-1 and IGF-1Ea amplified one single product of the expected size (116 bp and 330 bp, respectively). IGF-1Eb RT sample showed two additional single bands alongside with the expected of 240 bp. Detection of additional non-specific bands is consistent among different gels. Primers used for the detection of IGF-1Ec amplified various non-specific bands, with the strongest having a size different from the expected of 424 bp. A fainter band of the expected size can be seen, which would potentially represent IGF-1Ec. Hence, the goal was to sequence this band to confirm its identity. However, while detection of IGF-1Ea and IGF-1Eb was consistent in PS-1 cell lines, detection of IGF-1Ec was not robust, and it was not possible to confirm the identity of these bands by sequencing.

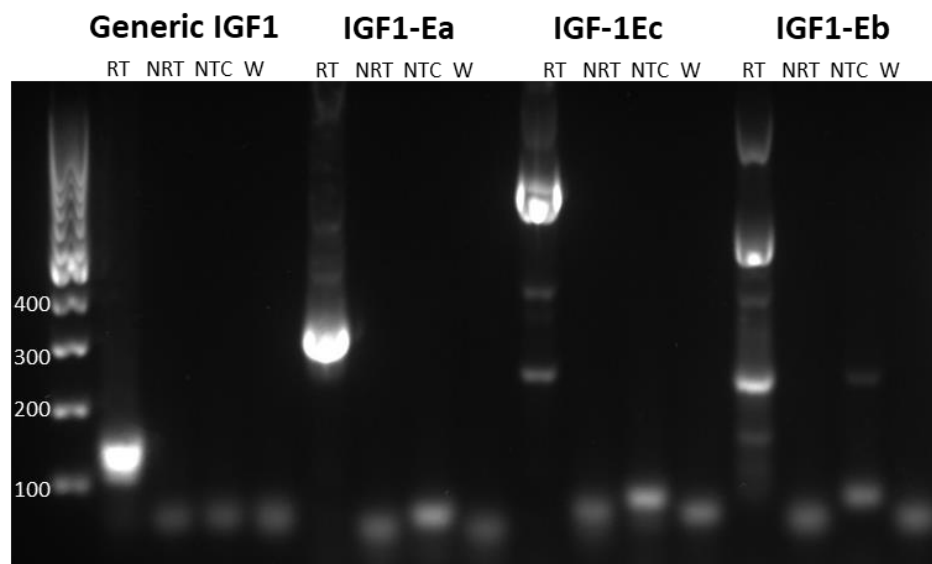


Figure 3.3.2: Detection of IGF-1 splice variants in PS-1 cell line. Although detection of generic IGF-1 (116 bp), IGF-1Ea (330 bp) and IGF-1Eb (240 bp) is reproducible, detection of IGF-1Ec (424 bp) is not.

RT: positive sample, NRT: no reverse transcriptase control, NTC: no template control, W: water control.

Primers (humanEc, see table 2.13, A) previously described for the detection of IGF-1Ec (Hameed *et al.*, 2003) were tested in PS-1. The fellow student Almas Mahmood detected and extracted the band amplified using these primers. Sequencing data seemed to confirm the nature of the band being IGF-1Ec, as it perfectly aligned with the IGF-1Ec sequence given in Clustal Omega, a web-based alignment tool (Fig. 3.3.3). The concern regarding the true identity of the band rose because the forward primer sat at the end of exon 5; therefore, the sequence obtained from the sequencing corresponds only to exon 6 (green sequence), and not exon 5, which is the feature of IGF-1Ec.

✓ Forward primer sequencing:

NNNNNNNNNNNANGNANTAGAGGGAGTGNAGGAACAAGAACTACAGGATGT
AGGAAGACCCCTCTGAGGAGTGAAGAGTGACATGCCACCGCAGGATCCTTTGCT
CTGCACGAGTTACTGTAAANNNNNNNNNNNNNNNNNNNNNNNNNNNNNNNN
NN
CNNNCNNTTTANN
NATTTNNNANTNN

✓ Reverse primer sequencing:

(after Reverse Complement)

NNTCGAAGTCTCAGAGAAGGAAAGGAAGTACATTGAAGAACGCAAGTAGAG
GGAGTGCAGGAAACAAGAACTACAGGATGTAGGAAGACCCCTCCNGAGGAGNN
AANN

CLUSTAL O(1.2.4) multiple sequence alignment

MGFfw	-----TAGA-GGGAGTGNAG	14
MGFrev	TCGAAGTCTCAGAGAAGGAAAGGAGTACATTTGAAGAACGCAAGTAGAGGAGTGCAGG	60

MGFfw	GAACAAGAACTACAGGATGTAGGAAGACCCCTCTGAGGAGTGAAGAGTGACATGCCACCG	74
MGFrev	AAACAAGAACTACAGGATGTAGGAAGACCCCTCCNGAGGAG-----	100

MGFfw	CAGGATCCTTTGCTCTGCACGAGTTACCTGTAA	107
MGFrev	-----	100

↓ aligns with IGF-1Ec
sequence

ATGGGAAAAATCAGCAGTCTTCCAAACCCAAATATTTAAGTGCTGCTTTTGTGATTCTTGAAGGTGAAGATGCACACCATGTCTCTCTACCTGGCGCTGTGCC
TGCTCACCTTCACCAGCTCTGCCACGGCTGGACCGGAGAGCGCTCTGCGGGGCTGAGCTGGTGGATGCTCTTCAGTTCGTGTGGAGACAGGGGCTTTTATTTCACAAAGCCAC
AGGGTATGGCTCCAGCAGTCGGAGGGCGCTCAGACAGGCATCGTGGATGAGTGTCTTCCGAGCTGTGATCTAAGGAGGCTGGAGATGTATTGCGCACCCCTCAAGCCTGCC
AAGTCAGCTCGCTCTCGTCCGTCGCCAGCGCCACCGACATGCCAAGACCCAGAAGTATCAGCCCCATCTACCAACAAGAACACGAAGTCTCAGAGAAGGAAAGGAAGTAC
ATTTGAAGAACGCAAGTAGAGggagtgacggaacaaagactacagqatgtggaagacccctcctgagqatgaaagatgacatgccaccgacagatcctttgctctgacagag
ttacotgttaaacctttggaacacctaaccataaagtttgataaacatttaaaagatggcgctttcccccaatgaaatacacaagtaaacattccaacattgtcttttag

sequenced

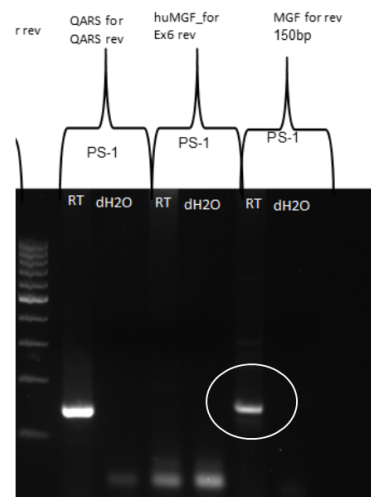


Figure 3.3.3: Sequencing of IGF-1Ec band in PS-1 cell lines. Sequencing of the IGF-1Ec 150 bp band detected in PS1 cell line using huIGF-1Ec primers (by Almas Mahmood) seemed to confirm the identity of IGF-1Ec. The forward primer, though, sat at the end of exon 5, allowing sequencing of exon 6 and not exon 5. The different colours in the IGF-1Ec sequence represent the different exons. The sequence underlined corresponds to the sequence sequenced. The data and the image of the gel were generated by Almas Mahmood.

Since IGF-1Ec is mainly expressed in muscle cells, it is possible that transcripts are not expressed above the level of detection. Therefore, the analysis was moved to bladder biopsy samples.

3.4 Inconsistent detection of IGF-1Ec transcripts in bladder biopsy samples

Nested PCR using the primers designed for the amplification of IGF-1 splice variants was tested on biopsy sample cDNA. As can be seen from Fig 3.4.1, amplification using generic IGF-1 primers, IGF-1Ea and IGF-1Eb was detected; IGF-1Ec, instead, was not amplified, consistently with the results in PS-1 cell line. The background is consistent with the further amplification of non-specific products made by the nested reaction.

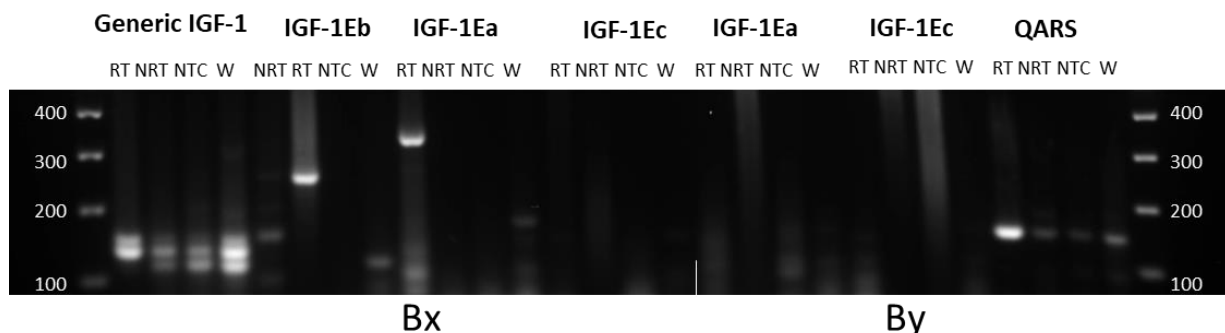


Figure 3.4.1: Nested PCR in biopsy samples. Amplification of generic IGF-1, IGF-1Eb and IGF-1Ea is consistent in biopsy samples (Bx and By); however, IGF-1Ec cannot be detected. QARS was amplified as positive control.

To ensure that the lack of detection of IGF-1Ec was not dependent on the primers, a new pair of primers expected to amplify both IGF-1Ea (176 bp) and IGF-1Ec (225 bp) was designed (new Ea/Ec, see table 2.13, A), as amplification of IGF-1Ea had already been detected in biopsy samples. The primers amplified a strong single band of the size expected for IGF-1Ea, which is consistent among different gels. Therefore, no detection of IGF-1Ec transcript was found in either PS-1 (Fig. 3.3.2) or biopsy samples (Fig. 3.4.2).

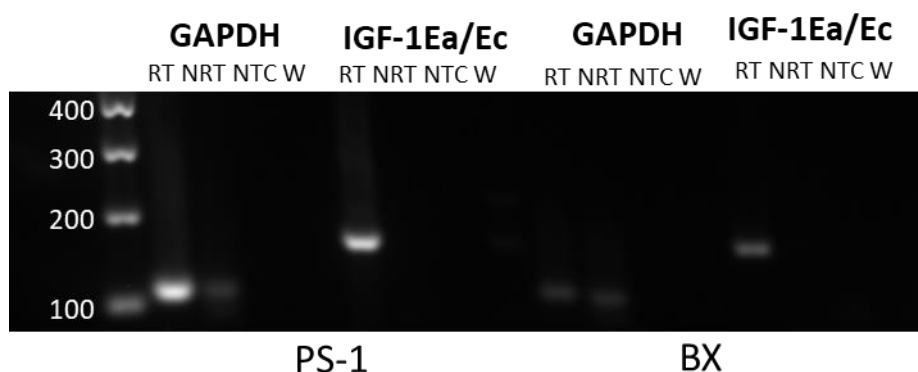


Figure 3.4.2: Use of newly designed primers to amplify both IGF-1Ea and IGF-1Ec in PS-1 cell line and biopsy sample. Newly designed primers expected to amplify both IGF-1Ea (176 bp) and IGF-1Ec (225 bp) were used in PS-1 and biopsy cDNAs, alongside with primers to amplify GAPDH (112 bp) as positive control. Although amplification of IGF-1Ea is consistent, there is no detection for IGF-1Ec.

Considering that the fellow MScR Almas Mahmood managed to amplify (and sequence) IGF-1Ec (see Fig. 3.3.3) using the primers humanEc, we decided to use these primers in biopsy samples. They amplified a 150 bp band, as expected; often two fainter additional single bands could be seen in the reverse transcriptase (RT) sample (Fig. 3.4.3). Detection, though, was not consistent, suggesting that the IGF-1Ec transcript is expressed just at or below the threshold of detection.

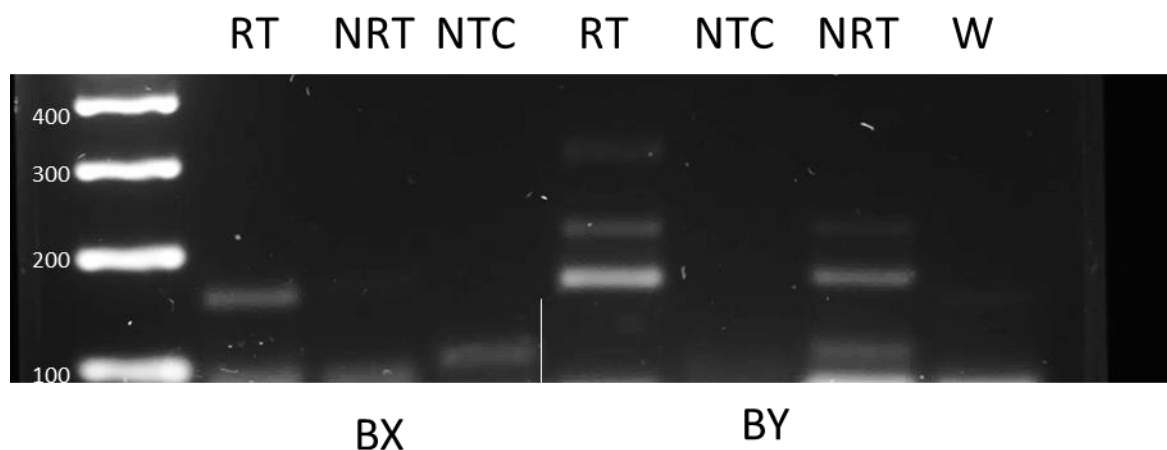


Figure 3.4.3: Detection of IGF-1Ec in biopsy samples using humanEc primers. Primers able to detect IGF-1Ec in PS-1 (fig. 3.3.3) were used in biopsy samples. They amplified an expected band of 150 bp and additional bands.

The issue concerning the identity of the band amplified in PS-1 using the humanEc primers (paragraph 3.3) led us to design a new pair of primers for the detection of IGF-1Ec, where the forward primer sat at the beginning of exon 5. Therefore, sequencing of the band would allow confirmation of IGF-1Ec because of the presence of exon 5 ligating to exon 6. However, the detection was not possible using these primers (Fig. 3.4.5).

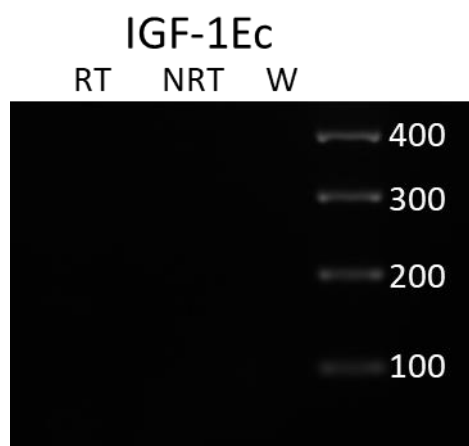


Figure 3.4.5: Use of new primers to amplify IGF-1Ec in biopsy samples. New primers expected to amplify IGF-1Ec (236 bp) were designed; however, no amplification was detected.

Another strategy trying to detect IGF-1Ec in bladder biopsies was using primers to allow amplification of full-length IGF-1Ec (549 bp) and IGF-1Ea (497 bp) transcript sequences (see table 2.13, A). The primers were designed by Almas Mahmood with the purpose of being used in her MScR project. The primers were tested both in PS-1 cell lines and in biopsy samples. As can be seen from Fig. 3.4.6, two single bands of a higher size than the expected were detected in PS-1 cell line. Neither of the two bands was detected in biopsy samples.

The presence of primer-dimers >100 bp in all the samples reflects the length of the primers themselves.

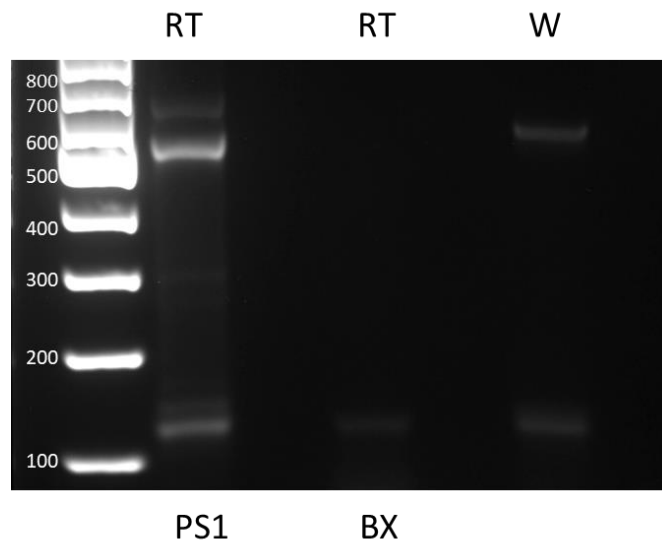


Figure 3.4.6: Use of primers to detect the full cDNA sequence of IGF-1Ea and IGF-1Ec in PS-1 cell line and biopsy sample. Primers designed to amplify IGF-1Ea (497 bp) and MGF (549 bp) in their full length were used in 10 ng of PS-1 cell line and biopsy cDNAs. No amplification was detected in the biopsy sample.

As a last opportunity to detect IGF-1Ec consistently, IGF-1Ec selective cDNA was used. This strategy was not considered at the beginning because gene-specific cDNA would not allow further analysis, such as detecting other genes as positive/negative controls. It was, therefore, decided to use half of the RNA extracted through the PARIS kit for the synthesis of selective cDNA, and the other half for oligo(dT) cDNA. An oligonucleotide previously described in literature (Hameed *et al.*, 2003) for this purpose was used instead of the oligo(dT) normally applied in the synthesis of cDNA. The cDNA was tested for the detection of IGF-1Ec using the “full-length” primers in PS-1 and biopsy samples. We observed the amplification of one single band, which was subsequently extracted and sequenced. However, the results of the sequencing demonstrated that the band corresponded, instead, to IGF-1Ea (Fig. 3.4.7, A). The cDNA was tested again for the detection of IGF-1Ec using the humanEc primers. *GAPDH* was chosen as negative control. Checking the transcript sequence of *GAPDH* we realized there was a sequence to which the oligonucleotide could potentially bind to. Amplification of a second “negative” control, *Hypoxanthine Phosphoribosyltransferase 1* (HPRT1), was also observed, confirming that the cDNA was not highly selective (Fig. 3.4.7, B). However, no amplification was observed with IGF-1Ec primers more than apparently non-specific bands not of the expected size.

MGF (Fig. 3.5.1). β -actin was chosen as loading control to allow normalization of the signal of the bands.

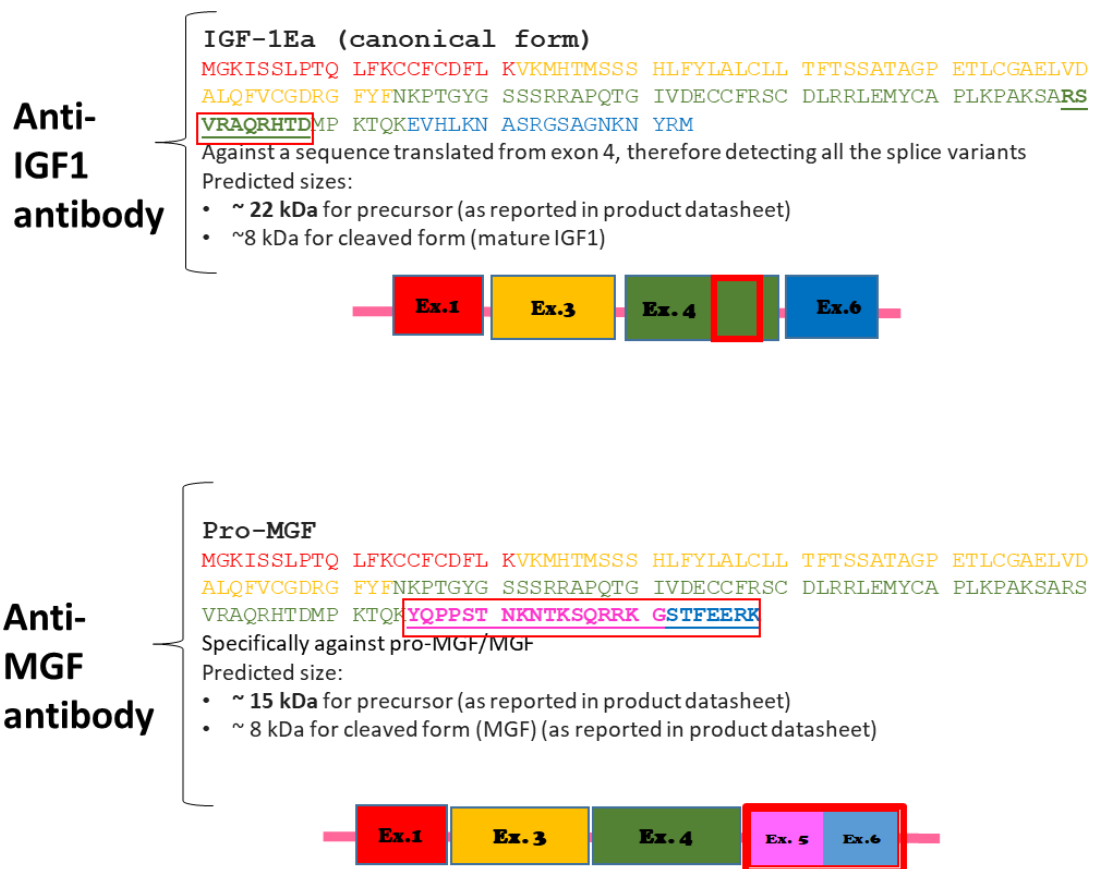


Figure 3.5.1: Epitopes of the antibodies used for the detection of mature IGF-1 and MGF. The epitope recognized by the anti-IGF1 antibody is a region common to all the three splice variants, therefore detecting all of them. The anti-MGF antibody, instead, is specific for MGF, as the epitope sits in the Ec peptide (MGF).

To be able to use both the anti-IGF-1 and the specific anti-MGF antibodies in the same immunoblot, we selected and purchased antibodies raised in different host species, to allow the use different fluorescent secondary antibodies and, therefore, detecting a green band for MGF and a red band for all the IGF-1 isoforms. Considering that the anti-IGF-1 antibody purchased was not working, the company (Abcam) replaced it with a different one, with the same host species of the anti-MGF. Moreover, the two predicted bands had a very close molecular weight (15 kDa MGF, 22 kDa IGF-1), leaving the stripping of the membrane the only option to use the two antibodies on the same immunoblot. Stripping procedures were tried, however, the result was incomplete (Fig. 3.5.2). Eventually, the detection of IGF-1 was not pursued, considering also the limited protein lysate extracted from each human biopsy sample often available for a single immunoblot.

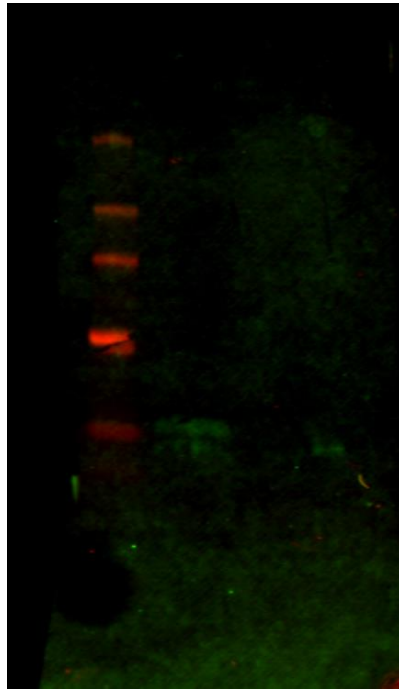


Figure 3.5.2: Stripping of the membrane. The stripping of the nitrocellulose membrane did not allow successful removal of the antibody.

To have a proper separation of proteins with a high range of molecular weight and clear detection of the bands of interest, avoiding background noise and non-specific binding of the antibodies, various elements of the western blotting protocol need to be optimized, depending on both the samples used and the proteins of interest. The optimization of the protocol was pursued in PS-1 and AsPC-1 lysates, alongside with murine tissues.

To test the optimal concentration of the anti-MGF primary Ab to be used in our samples, different dilutions were tested, including the recommended of 1/1000 (1 μ g/ml), 1/500 and 1/750. The best dilution to allow the detection of MGF, without non-specific bands, was 1/1000 (Fig. 3.5.3). The anti- β -actin Ab was also used at a concentration of 1 μ g/ml. The incubation time in primary antibody for the detection of MGF was increased from 1h-RT to overnight at 4°C.

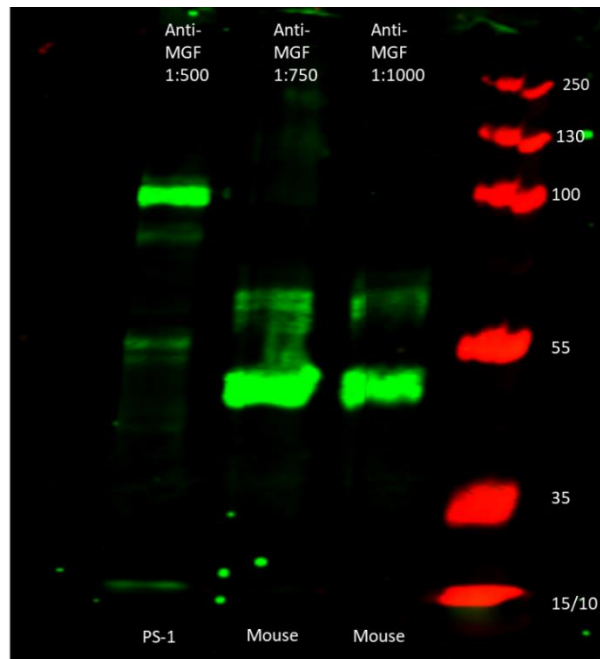


Figure 3.5.3: Titration of the anti-MGF antibody in western blot. Different dilutions of the anti-MGF antibody were tested both in PS-1 lysates and murine samples, in a 12% acrylamide gel. 1/1000 dilution of the Ab was chosen and used for the routine detection of MGF.

The concentration of the SDS-PAGE gel was also a critical factor to be optimized. Initially, 12 and 15% self-made acrylamide gels were adopted (Fig. 3.5.3), but eventually precast gradient gels 4-20% were used for optimal separation.

Other elements, such as the transfer conditions and the blocking buffers, had to be improved. Using the TransBlot (BioRad), different combinations of electrical potential (V) and duration of the transfer were tested. However, with the advent of TransBlot Turbo (BioRad) in our laboratory the manufacturer of the gels had to be changed (from FisherScientific to BioRad) as this machine was optimized for the use of items of the same brand; moreover, all the pre-made settings for the transfer were tested, leading us to eventually use the recommended of 5 minutes, 25V and 1.3 A. For blocking the membrane solutions made of TBST+5% BSA, TBST+5% milk were tested, but ultimately the Li-Cor pre-made blocking buffer in TBST was used because optimized for the use of the NIR imager Li-Cor Odyssey CLx.

The western blot protocol so-optimized allowed the detection of MGF and β -actin in both PS-1 and AsPc-1 lysates (Fig. 3.5.4) and murine samples (data not shown), leading us to continue with the analysis of human biopsy samples. It is interesting to notice that the form recognized by the anti-MGF Ab is the pro-MGF, consistent with the results of previous studies (Kravchenko *et al.*, 2006; Philippou *et al.*, 2008; Du *et al.*, 2013). No detection of MGF or MGF-24 was observed.

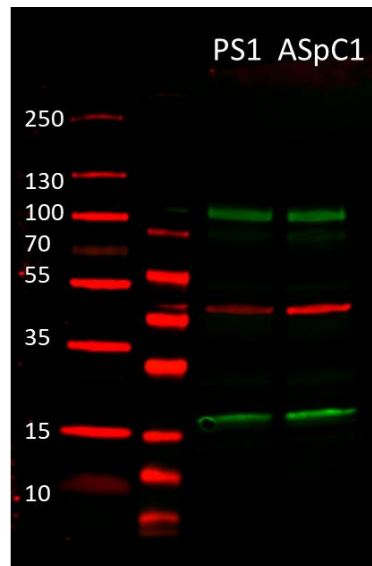


Figure 3.5.4: MGF protein detection in PS-1 and AsPC-1 cell lines. An anti-MGF antibody was used in PS-1 and AsPC-1 cell lysates to detect a ~15 kDa band (green). β -actin was used as a positive control (~42 kDa, red). The nature of the higher molecular weight bands is unknown.

3.6 Quantification of MGF protein in bladder biopsies

After optimizing the protocol for the detection of MGF, it was routinely used in human bladder samples (Fig. 3.6.1). Using the anti-MGF antibody we often observed two bands very close to each other, which could be due to degradation of the protein. In this case, both were considered in the quantification. Single higher molecular weight bands of about 50 kDa were seen quite consistently across the samples, in both cell lines (Fig. 3.5.4) and bladder biopsy samples (Fig. 3.6.1); however, we do not know the nature of such bands.

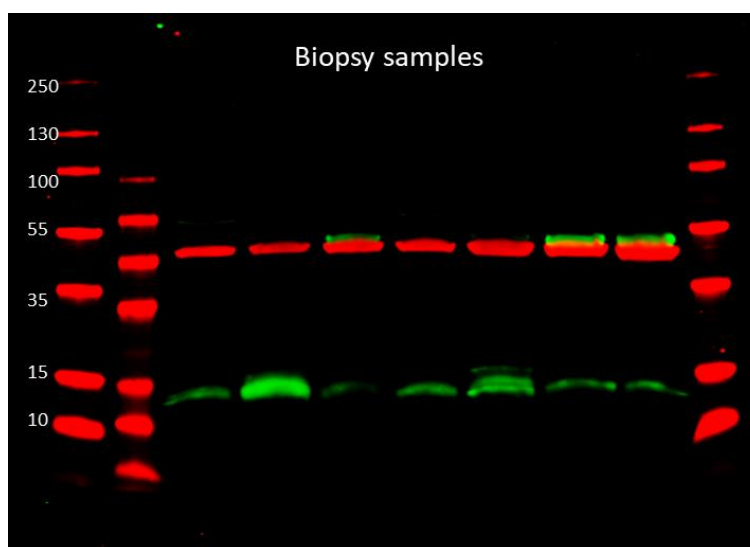


Figure 3.6.1: MGF protein detection by WB in bladder biopsy samples. A representative blot of MGF (~15 kDa, green band) detection in biopsy samples. β -actin was used as a positive control (~42 kDa, red). The identity of the higher molecular weight bands is unknown.

The quantification of the signal of the bands was carried out using the software Image Studio from Li-Cor, and normalized to the signal of β -actin. Normalization is an important step to minimize variations caused by experimental errors, such as loading mistakenly different amounts of sample in the gel.

The average expression of MGF in bladder biopsy samples is 0.52 ± 0.09 (SEM). As can be seen in Fig. 3.6.2, the expression of MGF was very different across the samples.

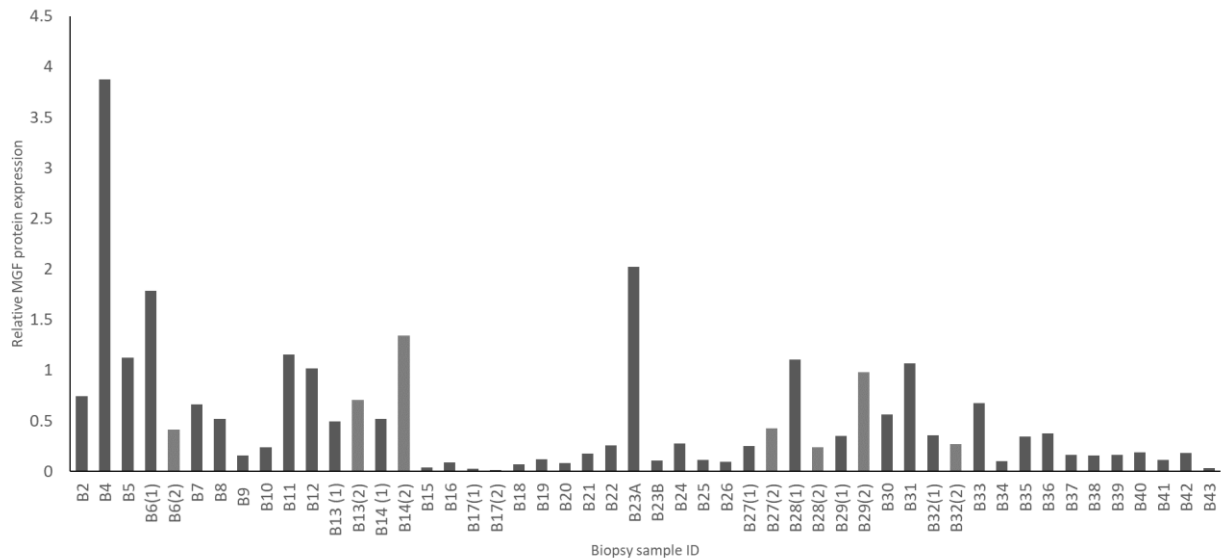


Figure 3.6.2: Average expression of MGF after normalization to β -actin. Expression of MGF protein in the biopsy samples was normalized to β -actin. The average expression is 0.52 ± 0.09 (SEM).

3.7 Optimization and validation of MGF detection by IHC in mouse samples and analysis of human biopsies.

The immunohistochemistry technique was performed to confirm MGF expression in the bladder and investigating the cell compartments expressing it. It was initially carried out in murine tissues to learn the procedure and optimize the concentration of anti-IGF-1 and anti-MGF primary antibodies (both antibodies recognise epitopes conserved across mouse and human species). From a starting concentration of 1mg/ml, dilutions of 1/50, 1/100, 1/200 and 1/400 were tried on murine heart, kidney and bladder tissue (Fig.3.7.1). The 1/200 and 1/400 dilutions allowed only a very faint detection of the proteins, therefore we decided to use 1/50 and 1/100 dilutions for the analysis of biopsy samples.

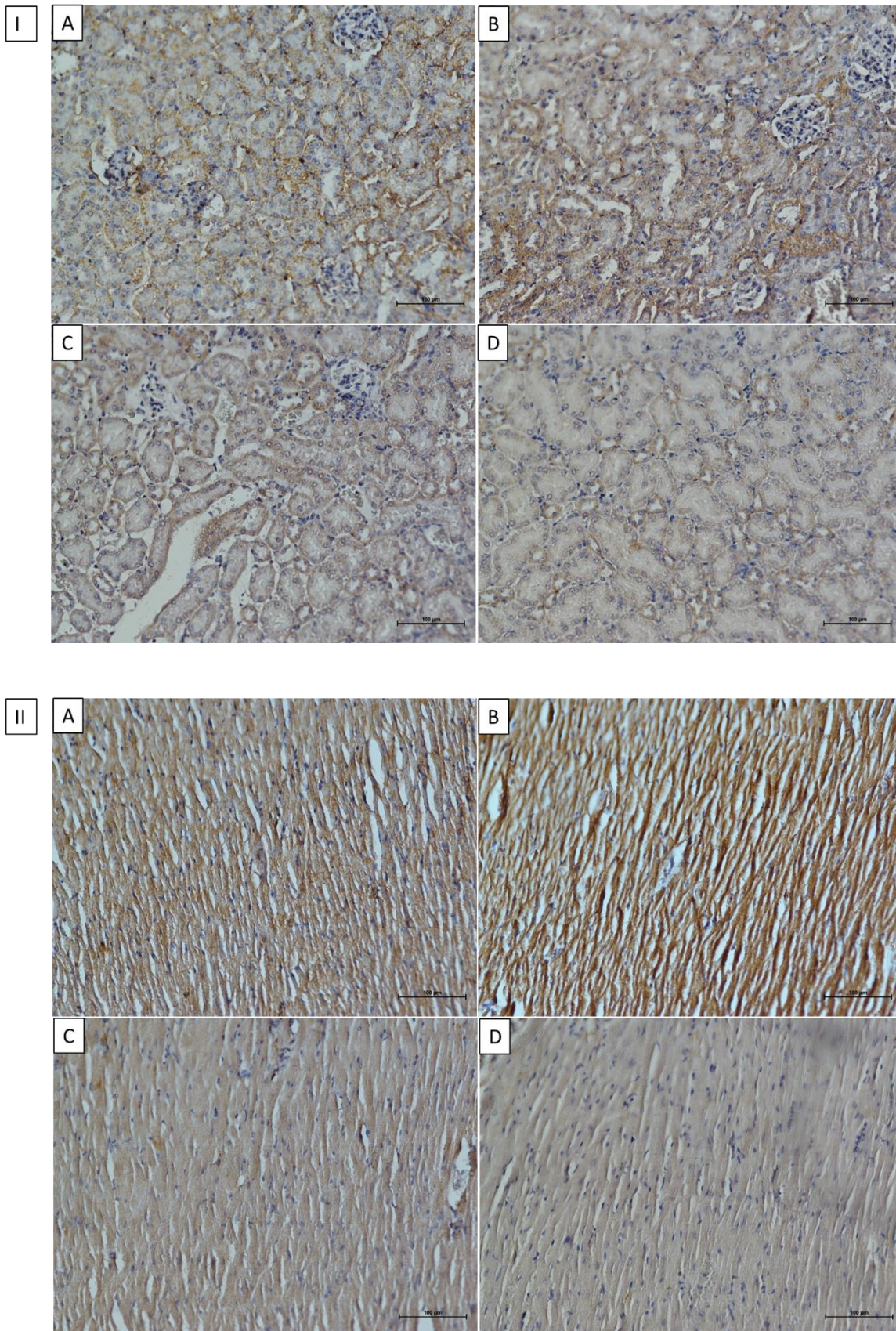


Figure 3.7.1: Titration of the anti-IGF-1 and anti-MGF antibodies in IHC. Various dilutions of the anti-MGF and anti-IGF-1 were tested in murine kidney (I) and heart (II), respectively. Section (5 µm) were stained as indicated below and counterstained with haematoxylin. In both pictures: (A) 1/50 dilution, (B) 1/100 dilution, (C) 1/200 dilution, (D) 1/400 dilution. All images taken with Nikon H550L microscope with 20X objective

As can be seen in Fig 3.7.2, the staining of IGF-1 in heart tissue (Fig. 3.7.2, A) was stronger than the one of MGF (Fig 3.7.2, B). Immunostaining in kidney (Fig. 3.7.2, C) showed a homogenous detection of MGF; in bladder tissue the staining is very strong (Fig. 3.7.2, D).

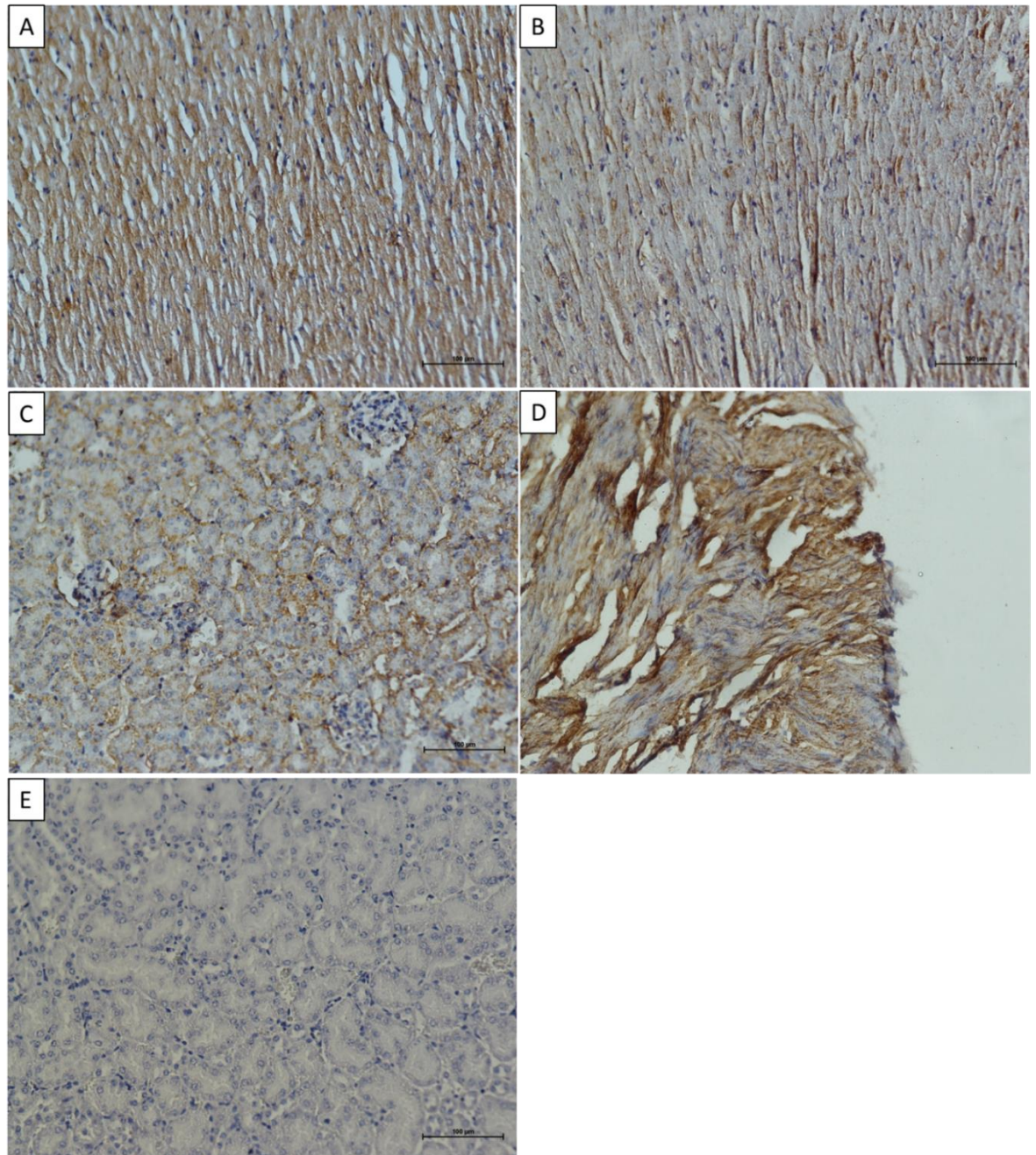


Figure 3.7.2: MGF protein detection by IHC in various murine tissues. Sections (5 µm) of murine tissue formalin-fixed and embedded in paraffin were stained as indicated below and counterstained with haematoxylin. (A) IGF-1 staining of heart tissue (1/50 dilution). (B) MGF staining of heart (1/50 dilution). (C) MGF staining of kidney (1/50 dilution). (D) MGF staining of bladder (1/50 dilution). (E) Secondary only control staining of kidney. All images taken with Nikon H550L microscope with 20X objective.

Immunostaining of bladder samples was realized following the optimized protocol. 1/50 and 1/100 dilutions of anti-MGF primary antibody allowed a widespread detection of the protein across the tissue (Fig. 3.7.3). The small size of the biopsies made extremely

challenging longitudinally sectioning of the sample for a satisfactory view of the tissue composition of the bladder. Therefore, our immunohistochemistry confirmed the presence of MGF in the bladder but did not clarify which cell compartment expresses it.

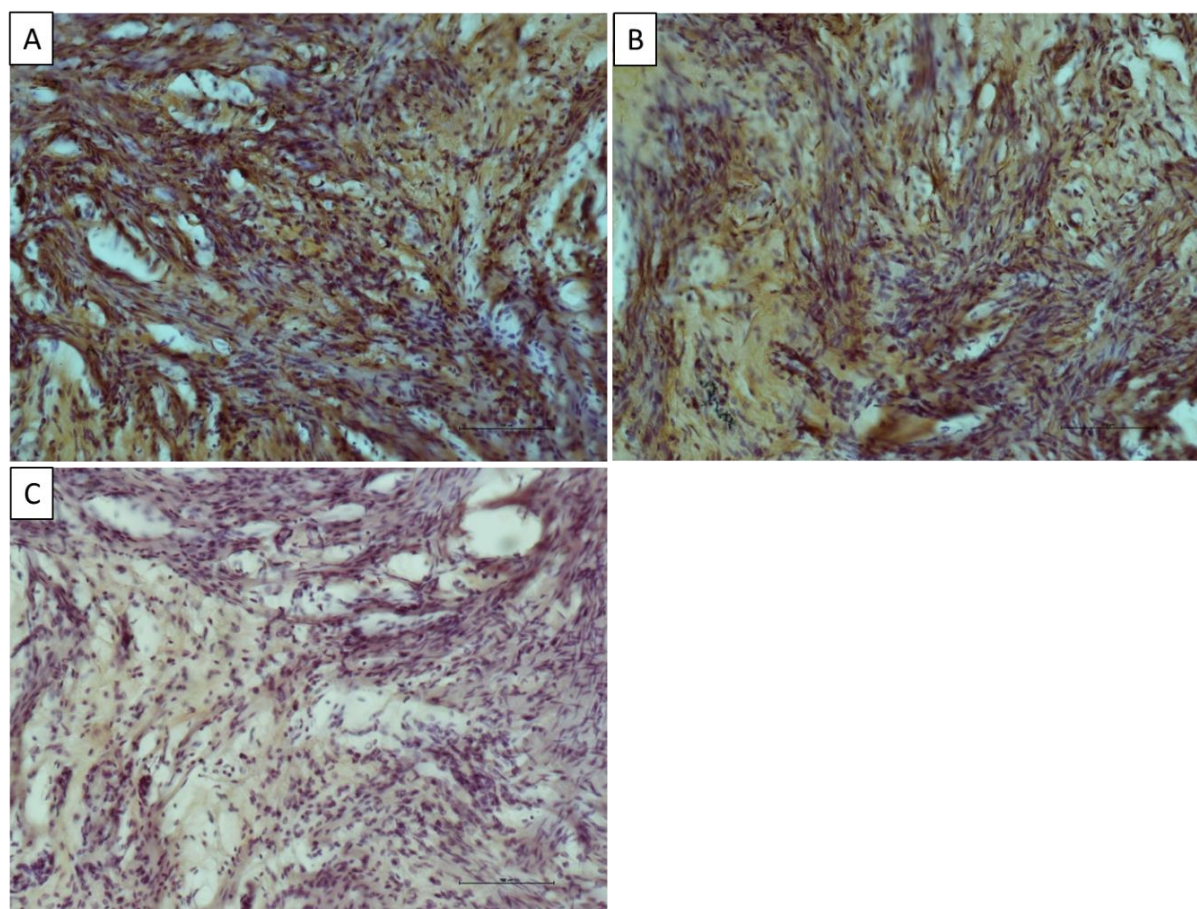


Figure 3.7.3: MGF protein detection by IHC in human bladder biopsies. Human bladder samples were formalin-fixed and embedded in paraffin. Sections (5 μm) were stained as indicated below and counterstained in haematoxylin. (A) MGF staining (1/50). (B) MGF staining (1/100). (C) Secondary antibody only control. All images were taken with Nikon H550L microscope with 20X objective.

3.8 Analysis of association between MGF expression and clinical symptoms

Having demonstrated and quantified (section 3.6, page 39) MGF protein expression in human bladder, the average expression was calculated separately in pathological and control samples. As shown in Fig. 3.8.1, contrary to what we expected, the expression of MGF was higher in OAB, with an overall expression of 0.27 ± 0.07 (SEM) in control samples ($n=12$), which increased to 0.48 ± 0.09 in the pathological ($n=28$), but not statistically significantly ($p=0.11$), assessed through Mann-Whitney U test.

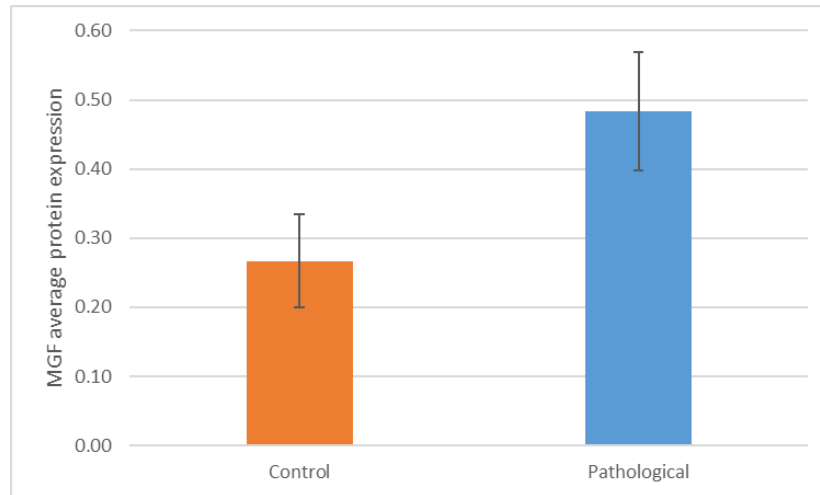


Figure 3.8.1: MGF protein expression in control and pathological. MGF protein was detected and quantified through western blot. Pathological samples (n=28) showed higher expression of MGF (0.48 ± 0.09) compared to control (n=12, 0.27 ± 0.07); however, the difference did not reach statistical significance (p=0.11).

Once assessed MGF expression in each biopsy samples, we found interesting to analyse whether it correlated with the maximum cystometric capacity (MCC). The MCC is a clinical parameter assessed during the urodynamic test and corresponds to the maximum volume of urine the bladder can store. Using Pearson's bivariate correlation in SPSS, we did not observe a statistically significant correlation between MGF expression and MCC (ml), when taking into account all the pathological samples which had the urodynamic test (n=23; correlation=0.15; p=0.49) (Fig. 3.8.2, A). However, when considering only DO+ patients, i.e. those patients who resulted positive for detrusor overactivity (DO+) at the urodynamic test (n=18) the correlation increased (correlation=0.36) yet not reaching statistical significance (p=0.15) (Fig. 3.8.2, B).

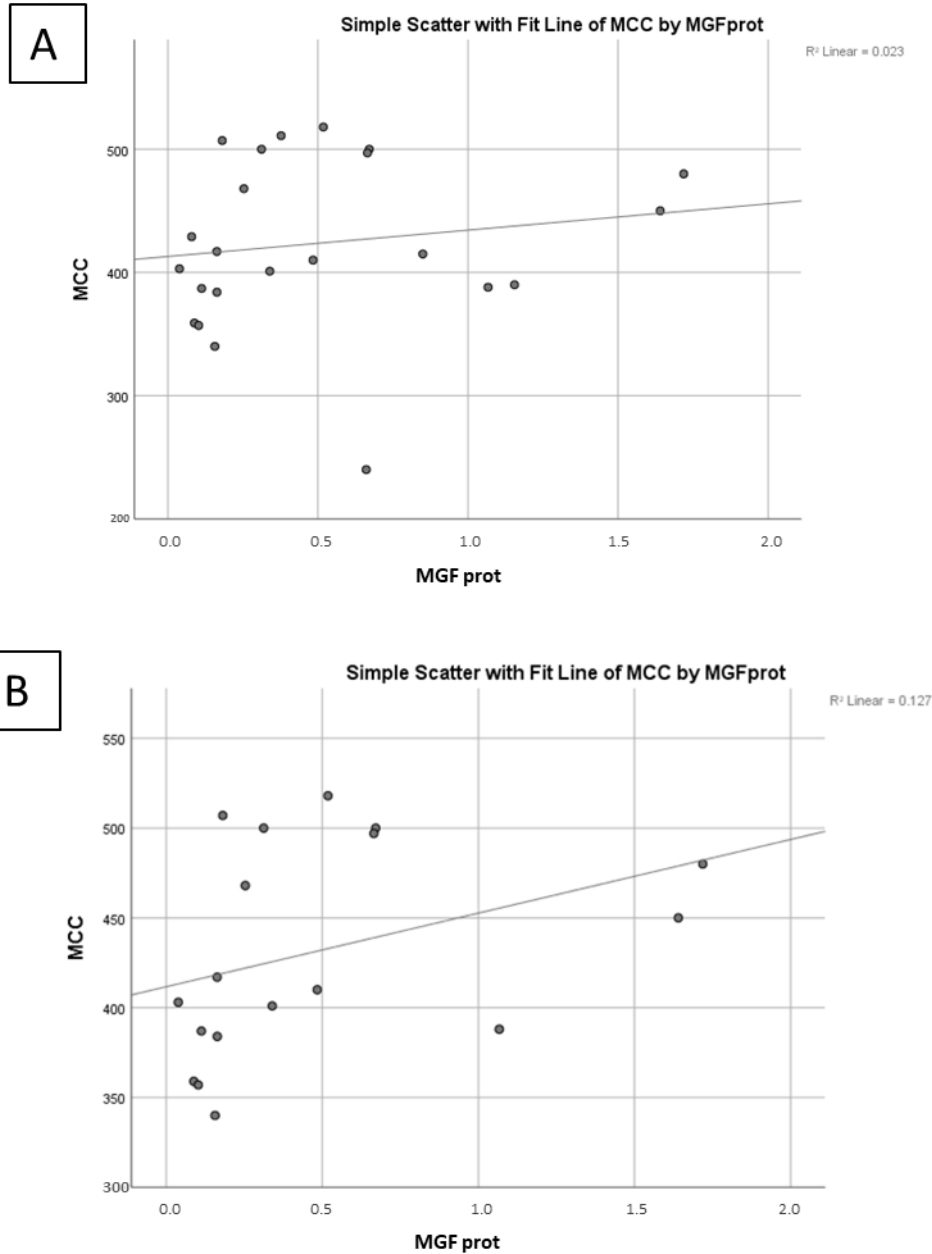


Figure 3.8.2: Correlation between MGF protein expression and MCC. We calculated the correlation between MGF protein expression and the maximum cystometric capacity (MCC) in (A) all pathological samples (n=23; correlation=0.15; p=0.49) and in (B) DO+ patients (n=18; correlation=0.36; p=0.15).

We also tested the association between MGF expression and self-completion questionnaire scores, which are the first step for the assessment of the pathology. If considering all the pathological samples for which we had a questionnaire score (n=22) there was not statistical correlation between MGF expression and either the B-SAQ scores (correlation=0.28, p=0.21) or the OAB-V8 (correlation=0.08, p=0.73) (Fig. 3.8.3, A and B). We observed a similar results when considering only DO+ patients (n=17. BSAQ: correlation=0.28, p=0.28; OAB-V8: correlation= 0.20, p=0.44) (Fig. 3.8.3, C and D).

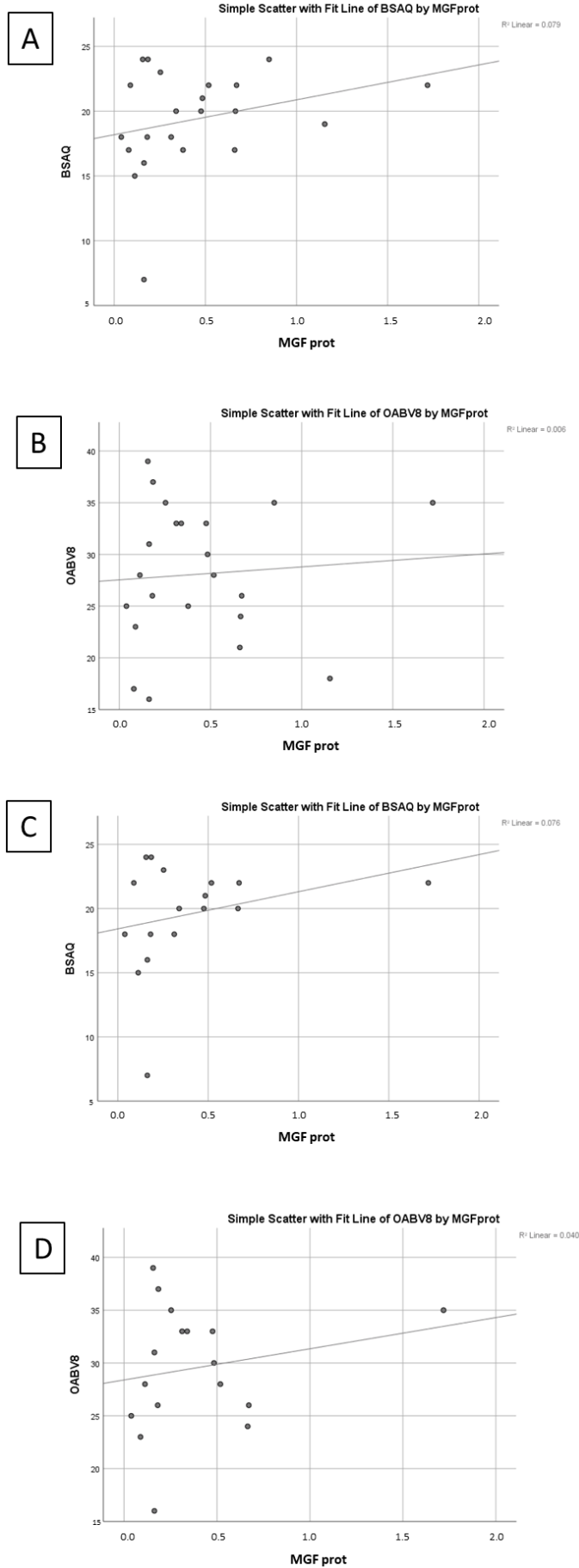


Figure 3.8.3: Correlation between MGF protein expression and self-completion questionnaires. We calculated the correlation between MGF protein expression and BSAQ/OAB-V8 scores in all pathological samples ($n=22$). (A) BSAQ: correlation=0.28, $p=0.21$; (B) OAB-V8: correlation=0.08, $p=0.73$) and in DO+ ($n=17$). (C) BSAQ: correlation=0.28, $p=0.28$; (D) OAB-V8: correlation= 0.20, $p=0.44$).

3.9 Composition analysis by RT-qPCR

3.9.1 Design and amplification efficiency of the primers

To assess the tissue composition of the biopsy samples in terms of the relative amount of each layer of the bladder (urothelium, stroma, smooth muscle), an RT-qPCR test was run. For this purpose, the cDNA obtained from reverse transcription of the RNA extracted from the biopsy samples was tested for markers of the above-mentioned layers of the bladder, alongside with a reference gene. After reviewing the current literature, primers to amplify markers for each layer were designed: UPK2 (*urolakin 2*) for the urothelium (Tian *et al.*, 2015), VIM (*vimentin*) for the stroma (Goodpaster *et al.*, 2008) and DES (*desmin*) for the detrusor muscle (Council and Hameed, 2009).

To choose as reference genes only those whose expression is not affected by OAB, we carefully review the current literature, leading us to design primers to amplify *Glyceraldehyde 3-phosphate Dehydrogenase (GAPDH)* (Jang, Han and Yuk, 2013).

When performing an RT-qPCR analysis, it is important to determine the efficiency of the amplification, which ideally should be 100%, indicating that the product is doubled during each cycle. Values of efficiency between 90 and 110% are usually considered valid (Rodríguez *et al.*, 2015). We tested the efficiency of the new designed-primers (GAPDH and VIM) using cDNA from PS-1 cell line before starting the composition analysis. Serial dilutions (1/10, 1/100 and 1/1000) of the cDNA were made and amplified in 40 cycles of reaction. The average Cq values were plotted into a logarithmic scale, and a linear regression curve was generated. After determining the slope (defined as the ratio of the vertical change between two points), the % efficiency was calculated through the following formula: $(10^{(-1/\text{slope})}-1) \times 100$ (Rodríguez *et al.*, 2015). The efficiency of all the primers was equal to 133.16% for GAPDH and 87.01% for VIM. Despite the primer efficiency being unequal to 100%, these primers were used to perform the experiment (Fig 3.9.1).

		GAPDH	VIM
Dilutions	Log10 dilution	Cq mean	
1/10	-1	17.63	28.10
1/100	-2	19.21	32.35
1/1000	-3	23.07	35.45

	slope	% efficiency
GAPDH	-2.72	133.16
VIM	-3.68	87.01

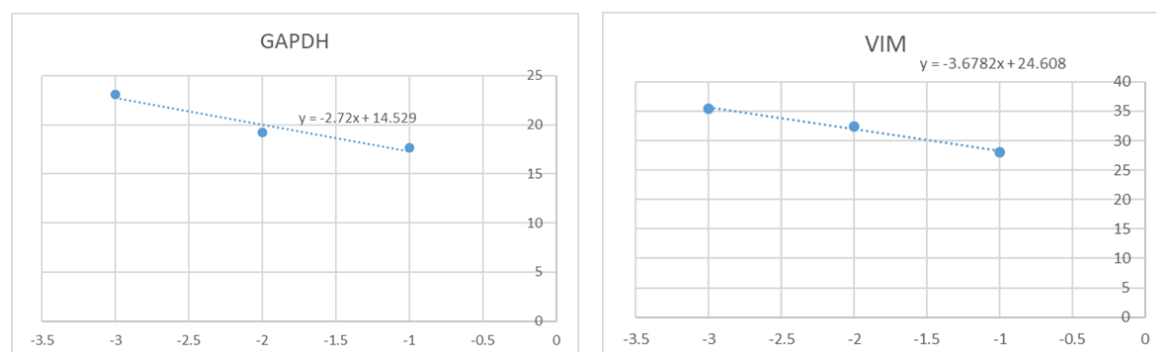


Figure 3.9.1: Primer efficiency test. The efficiency of the primers designed to amplify GAPDH, and VIM was tested in PS-1 cell line using the following formula: $(10^{(-1/\text{slope})}-1) \times 100$. Although the efficiency is not 100%, the primers were used to perform the composition analysis.

The amplification efficiency of the UPK2 and DES primers was tested on biopsy samples, as the cell line PS-1 does not express these genes, for they are specific for the urothelium and smooth muscle, respectively. Considering that the RNA extracted from the biopsies was more limited compared to cell lines, the dilutions of the cDNA had to be decreased to 1/1, 1/2, 1/4, 1/6, 1/16 and 1/32. No amplification of the products was detected, though. Hence, another set of dilution of the targets was tested: 1/10, 1/20, 1/40 and 1/80. Even in this case, the amplification appeared to be inaccurate and not consistent. Nevertheless, we decided to go on with the composition analysis using a 1/20 dilution. Therefore, the dilution of the cDNA that was chosen for the composition analysis was 40 ng/reaction of cDNA diluted 1/20.

3.9.2 Composition analysis

To have an idea of the tissue composition of the biopsies, we tested the biopsies for the amplification of *DES*, *VIM* and *UPK2*, using *GAPDH* as a reference. No reverse transcriptase, no template and water controls were run alongside to check the presence of genomic contamination. Fig. 3.9.2.1 shows a representative melt curve of a biopsy composition test. It shows a single peak for *DES* (blue). After analysis of uroplakin 2 and vimentin genomic sequences, we realized that *UPK2* and *VIM* primers were expected to amplify genomic DNA (gDNA) and *GAPDH* primers two splice variants of the expected size (112 bp) and other two products (240 and 352 bp, respectively). The amplified products were run on an agarose gel. Fig. 3.9.2.2 shows amplification of single products with all the primers. The presence of a band in the no reverse transcriptase (NRT) controls in *VIM* is consistent with the amplification of gDNA or additional variants. No amplification was detected using *UPK2* primers in NRT control. The composition analysis was nevertheless carried out.

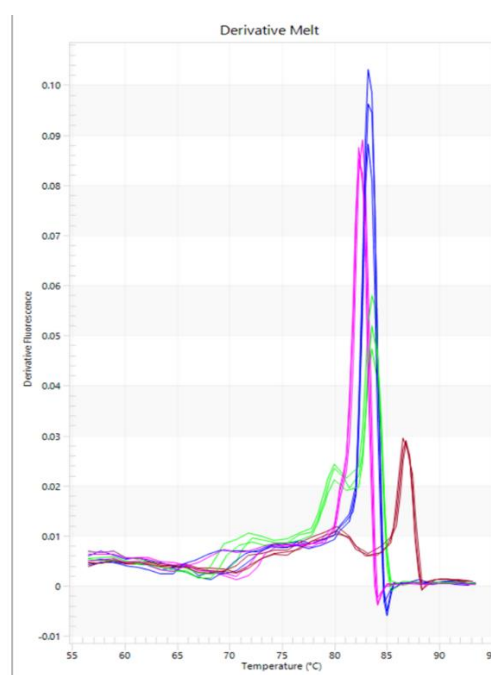


Figure 3.9.2.1: Representative derivative melt plot. In the image it is shown the melt curve of a representative composition analysis by RT-qPCR. The pink peak corresponds to *GAPDH*, the blue to *DES*, the green to *VIM*, the brown to *UPK2*.

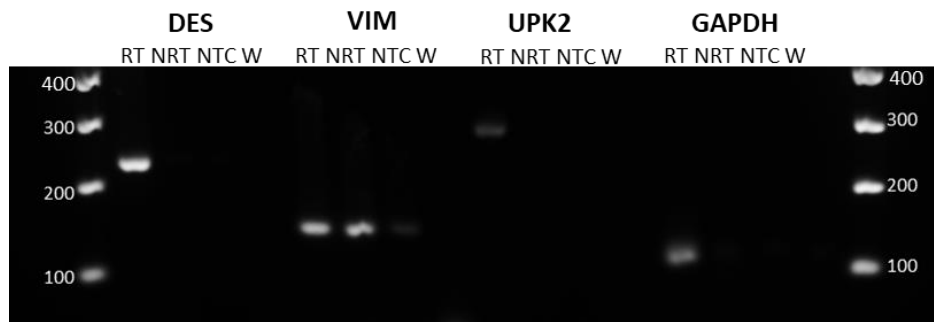


Figure 3.9.2.2: Amplification of composition markers. Running the products amplified through RT-qPCR revealed the detection of single products. The bands in the NRT using VIM primers is consistent with the amplification of genomic DNA.

Applying the formula $-(Cq-41)$ we had a representative idea of the relative gene expression in control and pathological samples. We can see that the smooth muscle was the predominant layer (10.65 in control and 12.43 in pathological, $SEM \pm 2.45$ and ± 1.41 , respectively), followed by stroma (10.42 and 9.95, $SEM \pm 0.68$ and ± 0.36 , respectively) and urothelium (8.28 and 6.23, $SEM \pm 0.89$ and ± 0.82 , respectively) (Fig. 3.9.2.3). The Mann-Whitney U test, performed as the variables in both groups were not normally distributed, showed that the change in the expression of muscle in pathological samples compared to controls is not statistically significant ($p=0.72$), same for stroma ($p=0.57$) and urothelium ($p=0.16$).

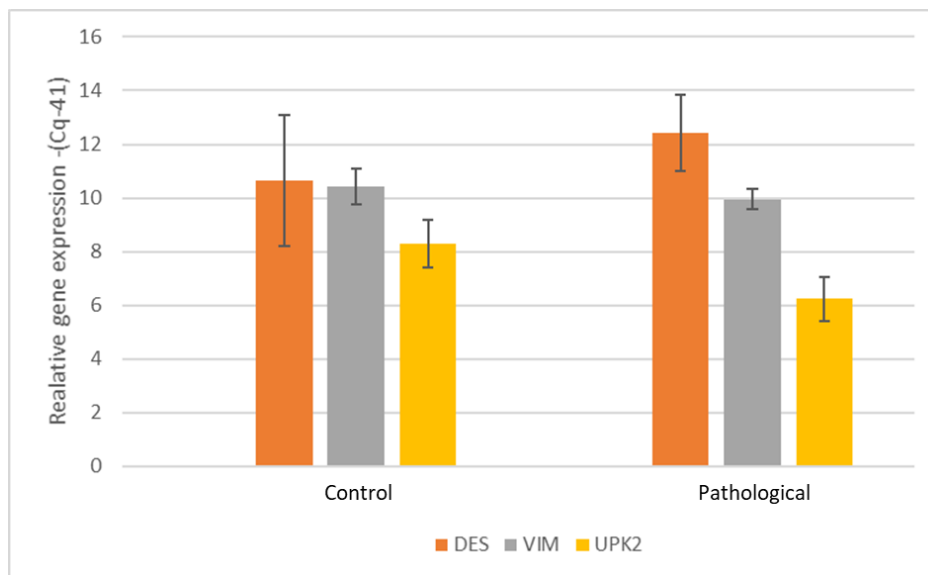


Figure 3.9.2.3: Average composition of human bladder biopsies. The relative composition of the biopsies was calculated by application of the formula $-(Cq-41)$. The average expression of the three layers of the bladder was calculated in pathological vs. control biopsies. Overall, there was not statistically significant difference in the expression of each layer in pathological compared to control samples ($p=0.72$, 0.57 and 0.16 , respectively).

However, looking at each biopsy individually there is great a difference in terms of expression of the different layers, and, in particular, in terms of presence/absence of one

or more layers. In fact, the RT-qPCR analysis showed different patterns of composition of the biopsy samples, allowing the categorization of the biopsies into four main groups: desmin positive/uroplakin 2 positive (DES+/UPK2+), desmin negative/uroplakin 2 negative (DES-/UPK2-), DES+/UPK2- and DES-/UPK2+ (Fig.3.9.2.4). Presence/absence of stroma (VIM) was not taken into account as all the samples (both pathological and control) did express it and overall expression did not change ($p=0.57$); moreover, we wanted to avoid interference of potential gDNA contamination with further statistical analyses.

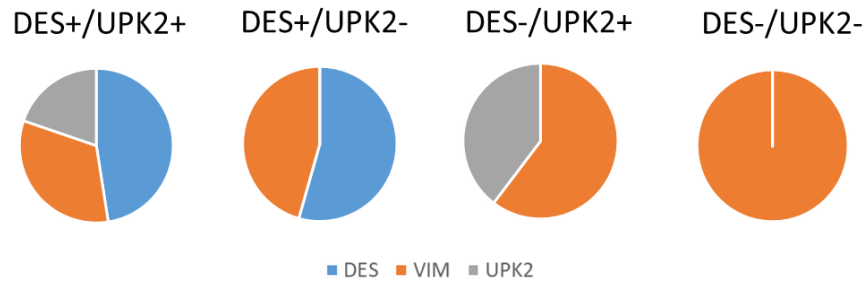


Figure 3.9.2.4: Categorization of human bladder biopsies. Following the composition test, it was possible to categorize the biopsies into four groups depending on presence/absence of smooth muscle (DES) and urothelium (UPK2+): DES+/UPK2+, DES+/UPK2-, DES-/UPK2+ and DES-/UPK2-. Presence of stroma (VIM) was not taken into account in the categorization as present in all the samples.

In both pathological and control samples the DES+ samples ($n=22$ and $n=8$) were more than DES- ($n=6$ and $n=4$). In order to investigate whether the expression of DES was dependent on pathological or physiological status, we performed the chi-squared test (χ^2 test). However, there was not statistically significant association between expression of DES and pathological/physiological condition ($p=0.43$) (Table 3.9, A).

All the control samples ($n=12$) expressed urothelium: 8 expressing also DES (DES+/UPK2+) and 4 not (DES-/UPK2+). Similarly, the majority of pathological samples ($n=17$) were DES+/UPK2+ (DES-/UPK2+: $n=4$). Again, the χ^2 test did not show any statistically significant connection between composition and presence/absence of OAB ($p=0.36$) (Table 3.9, B). As all the control samples expressed urothelium (UPK2+), we did not take into account UPK2- (DES+/UPK2-: $n=5$, DES-/UPK2-: $n=2$) pathological samples in the statistical analysis.

We can conclude that there was not statistically significant difference in the distribution of DES+/DES- and, more specifically, DES+/UPK2+ and DES+/UPK2- between pathological and control samples.

A		DES+ (n)	DES- (n)
	Pathological	22	6
	Control	8	4

B		UPK2+ (n)	
		DES+ (n)	DES- (n)
	Pathological	17	4
	Control	8	4

Table 3.9: Frequency of subgroups of biopsy in pathological and control samples. (A) DES+ samples are predominant in both pathological and control samples ($n=22$ and $n=8$, respectively); whereas 6 pathological and 4 control lacked smooth muscle (DES-). There is no statistically significant association between expression of DES and pathological/physiological condition ($p=0.43$). (B) We can further categorize the samples in DES+/UPK2+ and DES-/UPK2+ considering the concomitant presence of urothelium. There is no statistically significant association between this categorization and presence/absence of OAB ($p=0.36$). 49

3.10 Analysis of association between MGF expression and tissue composition

As previously mentioned (section 3.6, page 39), MGF protein expression is around two-fold higher in pathological samples compared to controls (though the difference is not statistically significant). Hence, we found interesting to examine how the average expression of MGF changed in the different categorization of the samples described in the previous section. As we can see in Fig. 3.10, MGF expression in both DES+/UPK2+ and DES-/UPK2+ is almost doubled in pathological (n=17 and n=4, respectively) compared to control (n=8 and n=4, respectively) samples. The Mann-Whitney U test showed no statistically significant difference in MGF expression in pathological DES-/UPK2+ samples compared to control (0.76 ± 0.36 and 0.34 ± 0.11 , respectively; $p=0.56$); however, almost reached statistical significance in DES+/UPK2+ samples (pathological: 0.49 ± 0.11 , control: 0.23 ± 0.09 ; $p=0.06$). Therefore, while overall higher expression of MGF protein is seen in pathological compared to control samples, this difference is more significant when considering only biopsies that contain muscle tissue (DES+). This suggests that while multiple cell types within the biopsies produce MGF, it is increased production of MGF by muscle cells that is associated with the pathology of OAB. However, specific experiments to test this hypothesis would need to be carried out.

In pathological samples, there is not statistically significant change in MGF expression in UPK2+ (n=21) and UPK- (n=7) samples (0.54 ± 0.11 and 0.28 ± 0.08 , respectively; $p=0.2$).

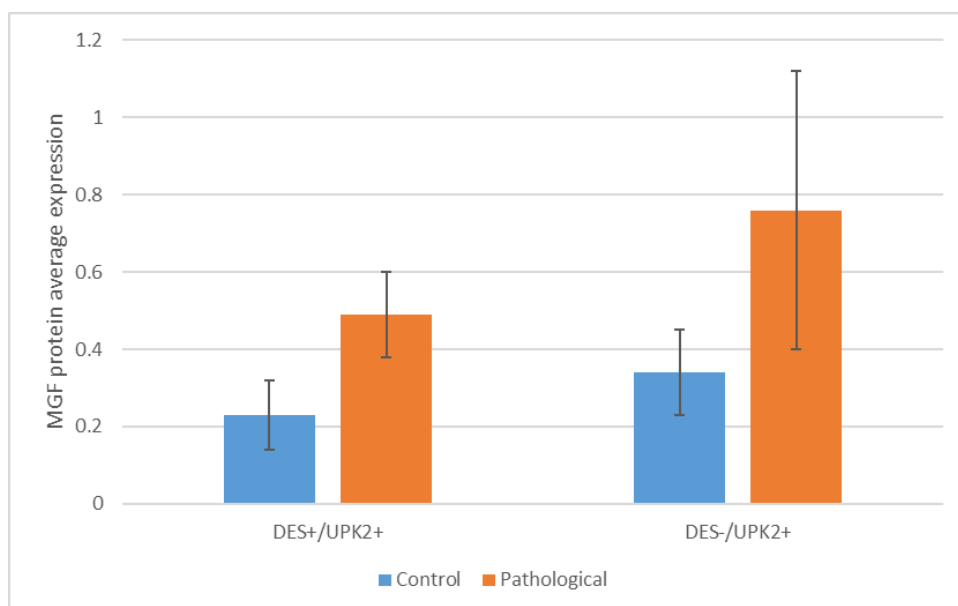


Figure 3.10: Average MGF protein expression after categorization of the samples. Mann-Whitney U test was used to assess statistical significance in the different MGF expression in DES+/UPK2+ and DES-/UPK2+ in control (n=8 and n=17, respectively) and pathological (n=4 and n=4, respectively) samples ($p=0.06$ and $p=0.56$, respectively).

3.11 Validation and optimization of primary smooth muscle cell culture from murine sample

Another aim of the project was to test MGF protein potential role in primary detrusor muscle cell proliferation. Primary cell culture is a technique as useful as challenging. To ensure the greatest outcome of cells and to prevent bacterial and fungal contamination, careful measures must be taken.

The digestion phase was a very delicate step of the primary cell culture procedure, considering that the aim was to maximize the outcome of living cells to be subsequently plated to start a primary culture. Two different methods were tested to achieve this goal. In the first, the tissues were incubated in Petri dishes or 24-well plates in the digestion solution for one to two hours in a cell culture incubator at 37°C/PCO₂ 5%. In the second, the samples were incubated in flat-surface tubes in a water bath at 37°C for two hours with periodic manual shaking. Since the second method coincided with the contamination of the culture, the first one was adopted as standard. Passing the digested suspension through a syringe needle, and then through a 100 µm cell strainer were also necessary points of the protocol, to allow the disruption of the undigested tissue left. It was critical to wash the bottom surface of the cell strainer with medium, otherwise most of the cells would remain stuck in there. These adjustments made possible to establish a primary culture of murine skeletal muscle, heart and bladder (Fig. 3.11.1).

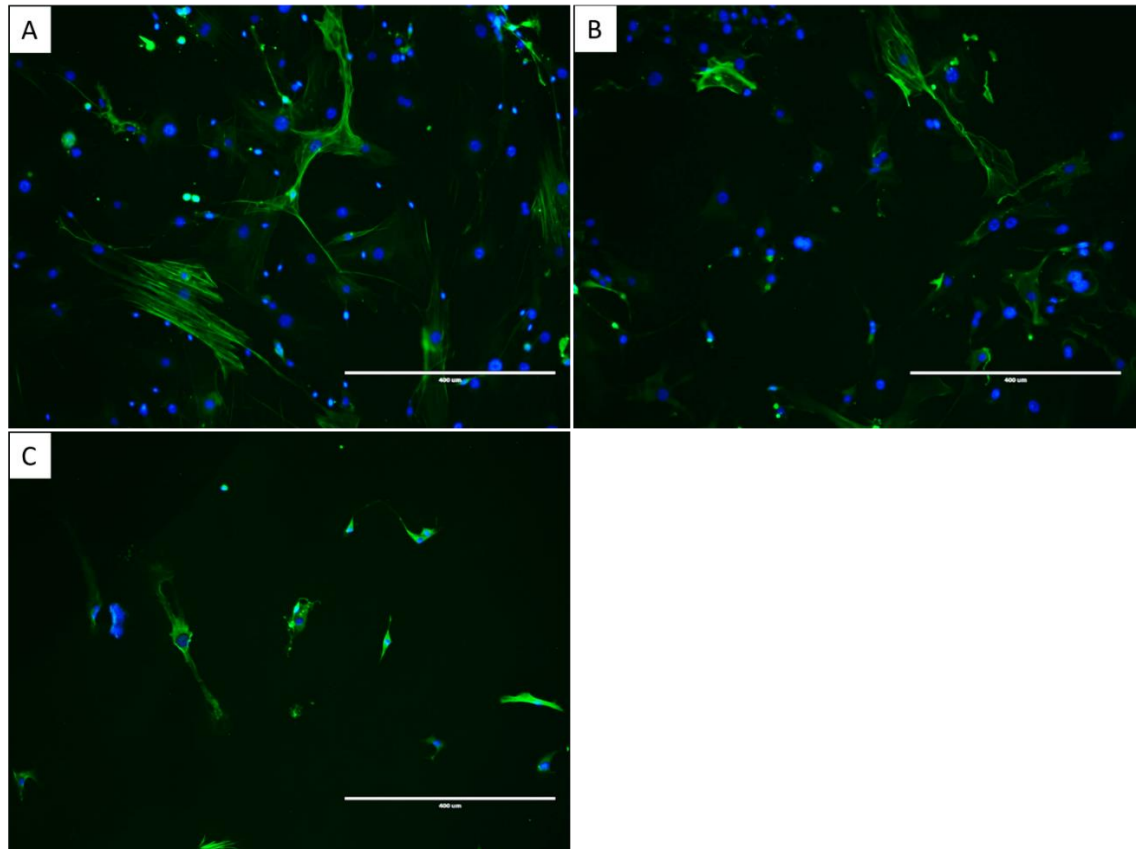


Figure 3.11.1: Establishment of murine primary tissue culture. A primary cell culture was established following digestion of murine (A) skeletal muscle, (B) heart and (C) bladder. Nuclei were stained with DAPI (blue). The phenotype was confirmed by immunostaining of α -smooth muscle actin (α -SMA) (green). All images taken with EVOS microscope, 10x objective.

To allow the attachment of the cells to the microplate, yet topping up of antibiotics and antifungal agents without unsettling the cells too much, only half of the media in each well was changed every day. After letting the cells to adjust to the culture conditions for a couple of days, the EdU-Click proliferation assay was performed and optimised for the detection of proliferating cells. Being primary cells very different from cell lines, we could not rely on the results obtained on PS-1 cell lines, in which 1h incubation with EdU was enough for the detection of about 90% proliferating cells (Fig. 3.11.2).

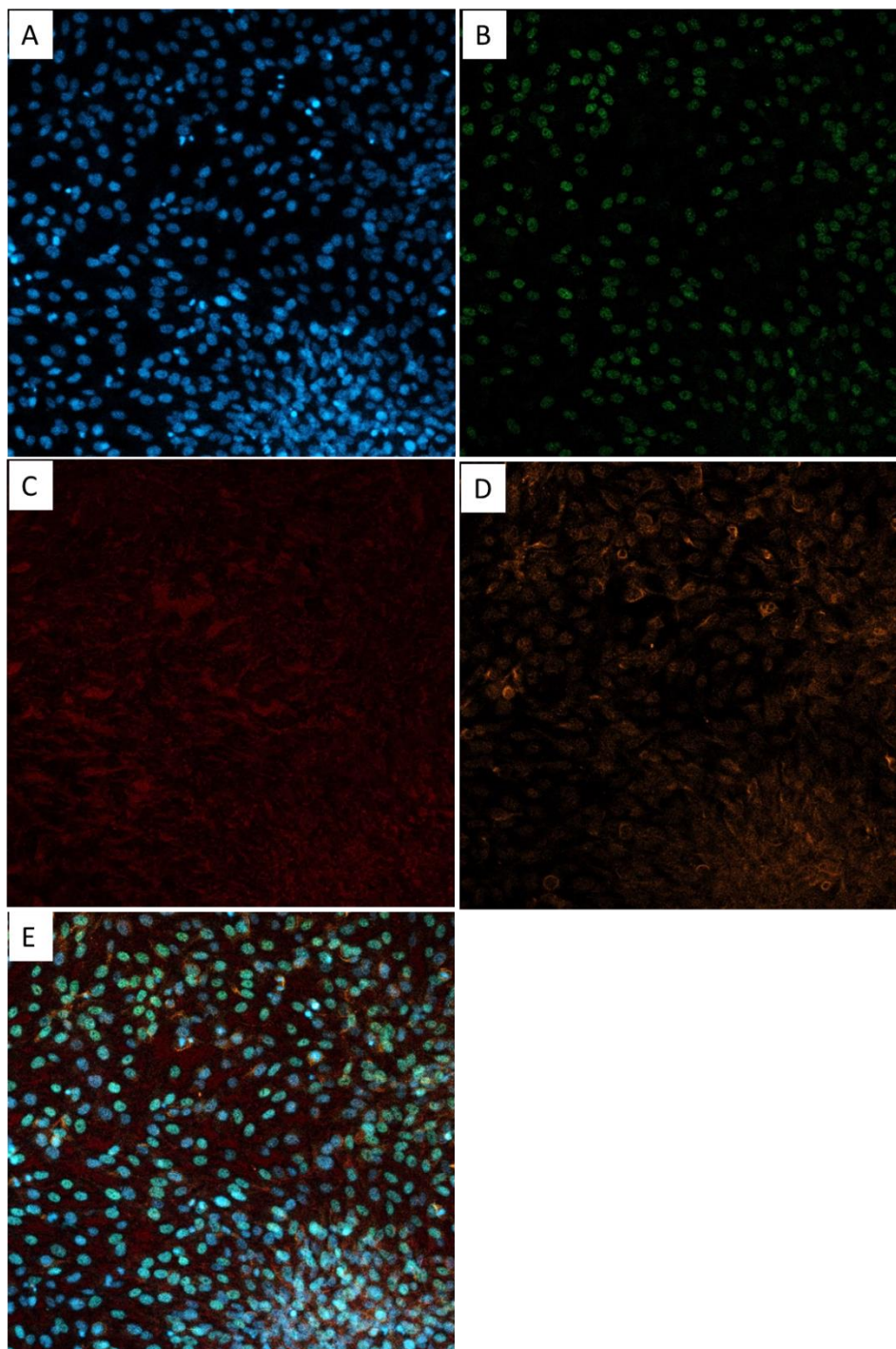


Figure 3.11.2: Validation of EdU-click proliferation assay on PS-1 cells. PS-1 cells were incubated 37C/5%PCO₂ with EdU for 1 hour, and further immunostained to confirm the phenotype. (A) DAPI staining of nuclei. (B) EdU staining of proliferating cells. (C) Desmin staining 1/200. (D) α-SMA staining 1/200. (E) Merge. All images taken with Confocal microscope, 4x objective.

To be able to identify proliferation in primary cultures, cells were firstly incubated with EdU for 24 hours, but no proliferation was detected (Fig. 3.11.3, I), and then for 48 hours consecutively (Fig. 3.11.3, II). Therefore, we selected this incubation time for the upcoming experiments. Moreover, the detection of the EdU staining was optimized both in terms of duration and point of the protocol to be performed, i.e. before or after immunodetection of other proteins. Thirty minutes and one hour incubation times were tested, resulting in no significant difference between the two; a stronger signal of EdU stained nuclei was obtained when the detection of EdU was performed before incubation with other primary antibodies, as suggested by the protocol.

Therefore, the optimization of the protocols for the establishment of a primary cell culture and the detection of proliferating cells allowed continuing with the following step of treatment of the primary bladder cells with MGF-24 synthetic peptide.

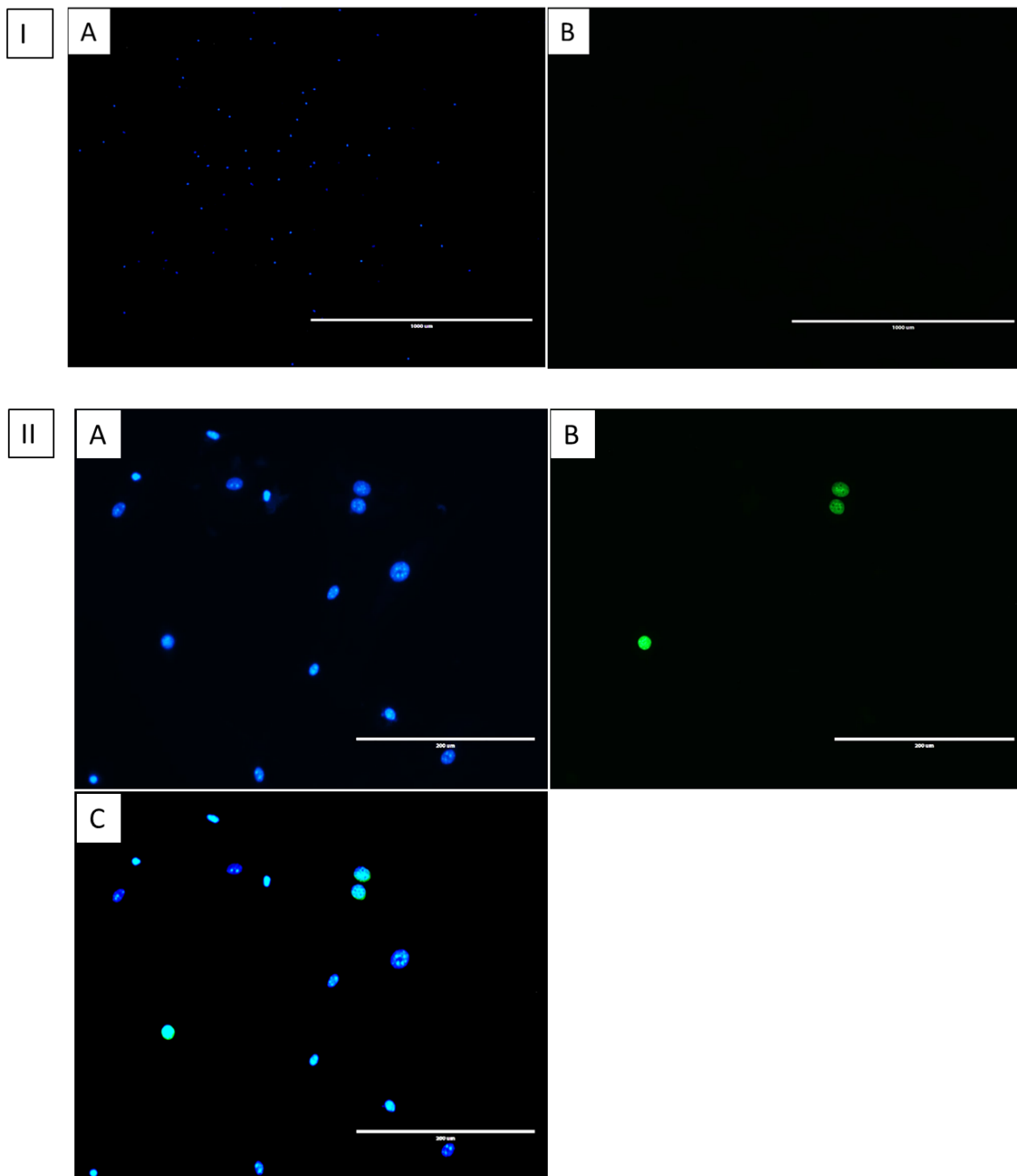


Figure 3.11.3: Proliferating bladder primary cells after 48h of incubation with EdU. Bladder primary cells were incubated 37C/5% PCO₂ in the presence of 10 μ M EdU for 24h (I) or 48h (II). (A) DAPI staining of the nuclei. (B) EdU⁺ nuclei. (C) Merge. No proliferation was detected after 24 hours (I). All images taken with EVOS microscope, 4x objective (I) and 20x (II) objective.

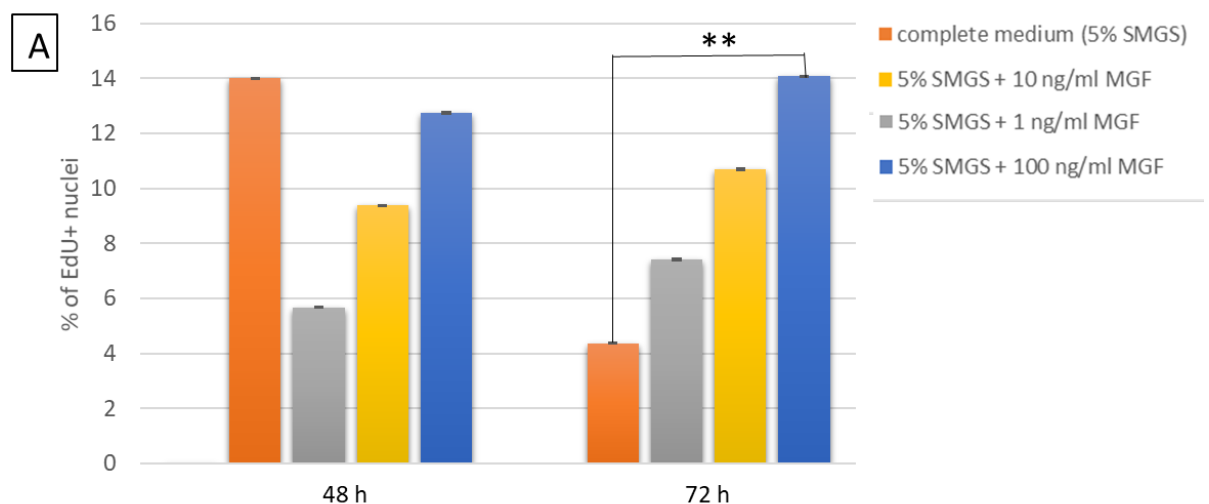
3.12 Effect of MGF on murine bladder primary cells *in vitro*

The preliminary treatment with MGF synthetic peptide was performed only in murine primary bladder cells, to ensure a more careful and quality experiment.

The analysis consisted in culturing different replicates of cells for 48/72 hours in smooth muscle (SM) complete medium (SM medium + 5% smooth muscle growth supplements, SMGS) supplemented with 1 (48h: n=10, 72h: n=11) /10 (48h: n=10, 72h: n=16) /100 (48h: n=11, 72h: n=15) ng/ml of synthetic MGF-24; as a control, cells were cultured in complete medium only (48h: n=5, 72h: n=11). As a separate experiment, we also cultured the cells in SM medium without any growth supplements (48h: n=3, 72h: n=7), and SM medium without growth supplements but supplemented with 100 ng/ml of MGF peptide (48h: n=5, 72h: n=10). In the last 48 hours of treatment, 10nm of EdU were added for the proliferation assay. Cells were immunostained for smooth muscle myosin heavy chain (SMMHC) to confirm the phenotype (Fig. 3.12.2, I to VI).

Fig. 3.12.1 shows the outcome of the experiment. After 48 and 72 hours (Fig.3.12.1, A), we can see an increasing trend in the increment of proliferation in the MGF-treated cells, with the highest outcome when applying 100 ng/ml of MGF. After 48 hours the % of EdU⁺ nuclei (proliferating cells) in the control (complete medium) is higher than in the treatments (14% \pm 0.03 in control, 5.7% \pm 0.02 with 1 ng/ml, 9.4% \pm 0.03 with 10 ng/ml, 12.7% \pm 0.04 with 100 ng/ml), but not statistically significantly (p=0.26). After 72 hours cell proliferation in the treatments is higher compared to the control (4.4% \pm 0.02 in control, 7.4% \pm 0.03 after 1 ng/ml, 10.7% \pm 0.03 after 10 ng/ml, 14.1% \pm 0.03 after 100 ng/ml). One-way ANOVA test showed a statistical significance of p=0.015 between the groups; the Turkey's multiple composition post-test confirmed a statistical significant increase in cell proliferation after 100 ng/ml of MGF treatment compared to control (p=0.008). Alongside, we cultured the primary cells in medium without any growth factors and in medium without growth factors supplemented with 100 ng/ml of MGF. There is not statistically significant difference in the proliferation rate in the two experimental conditions after 48 or 72 hours (48h: p=0.46; 72h: p=0.49) (Fig. 3.12.1, B).

Among the factors that may have influenced the outcome of the experiments, we can find the variability among the three murine bladders used and the number of replicates for each experimental condition. Further replicates of this experiment would be required to confirm these findings and deeper investigate MGF function in the bladder.



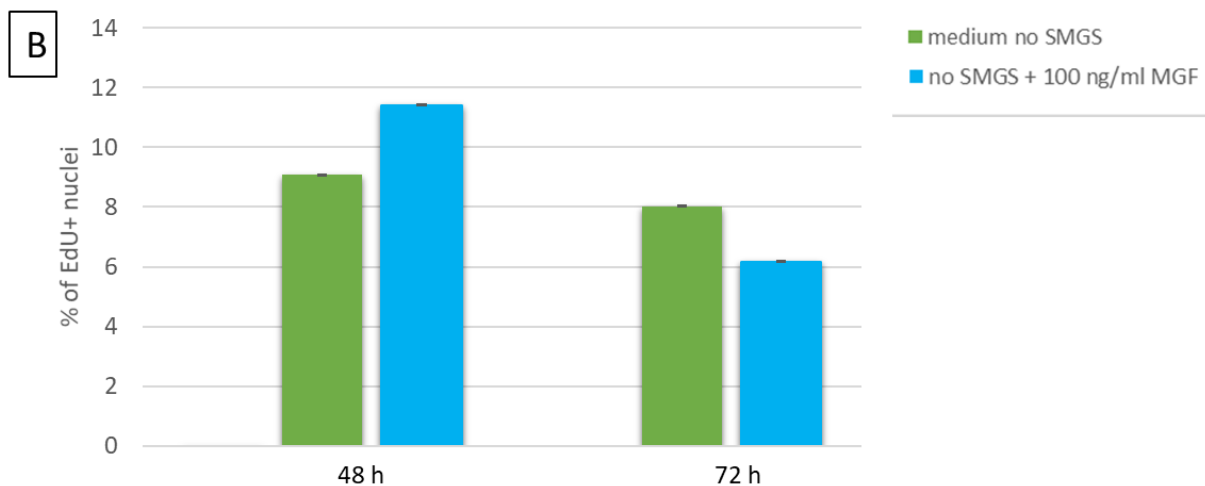
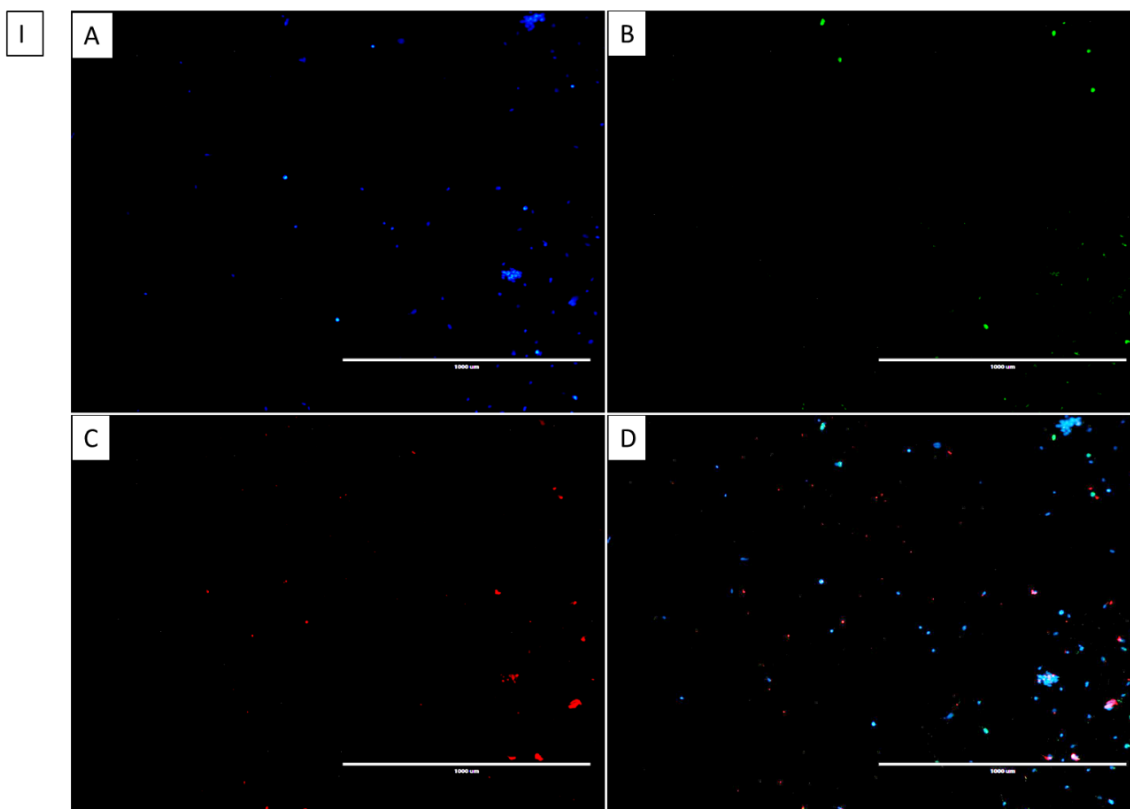
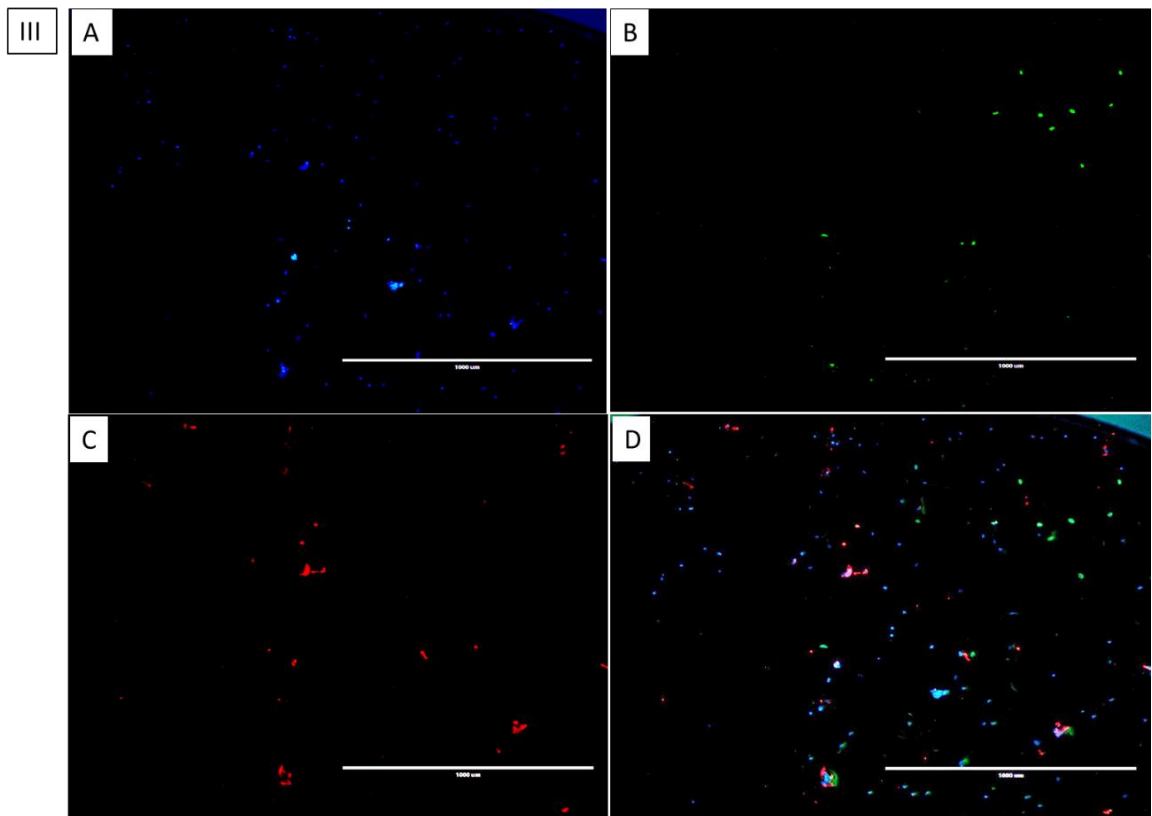
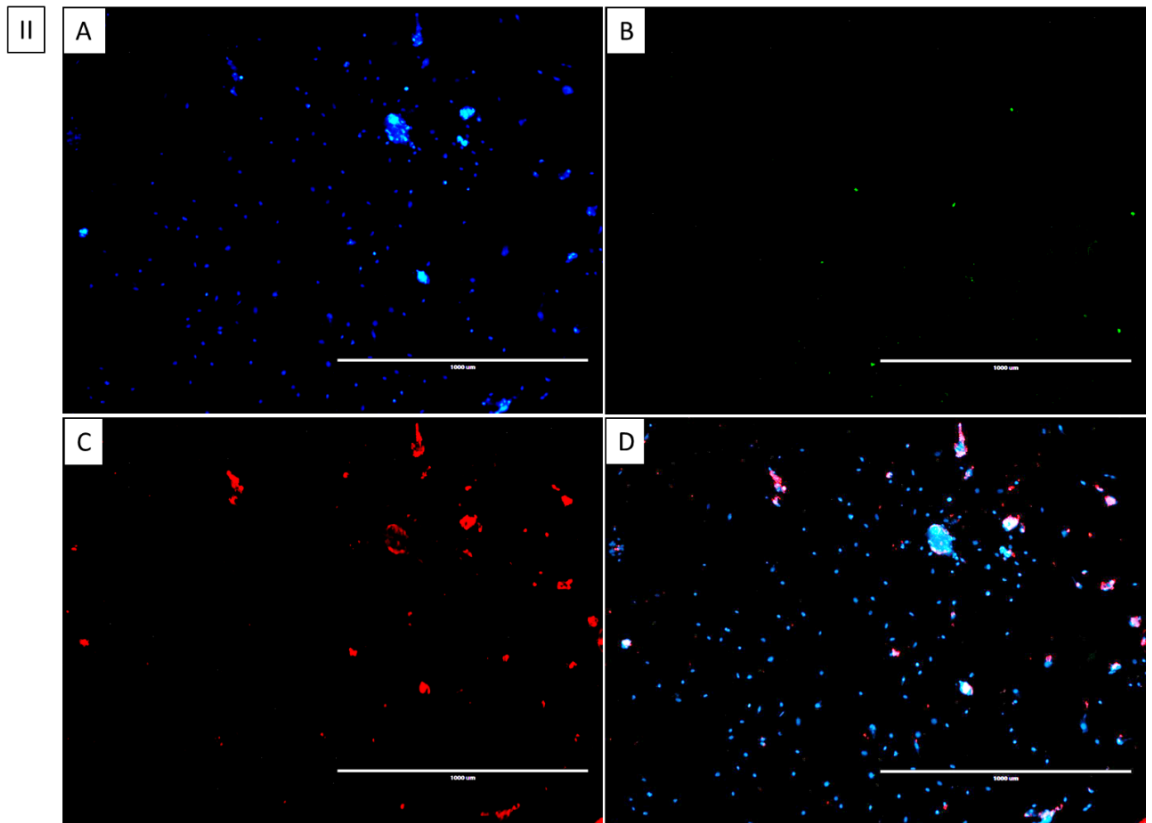
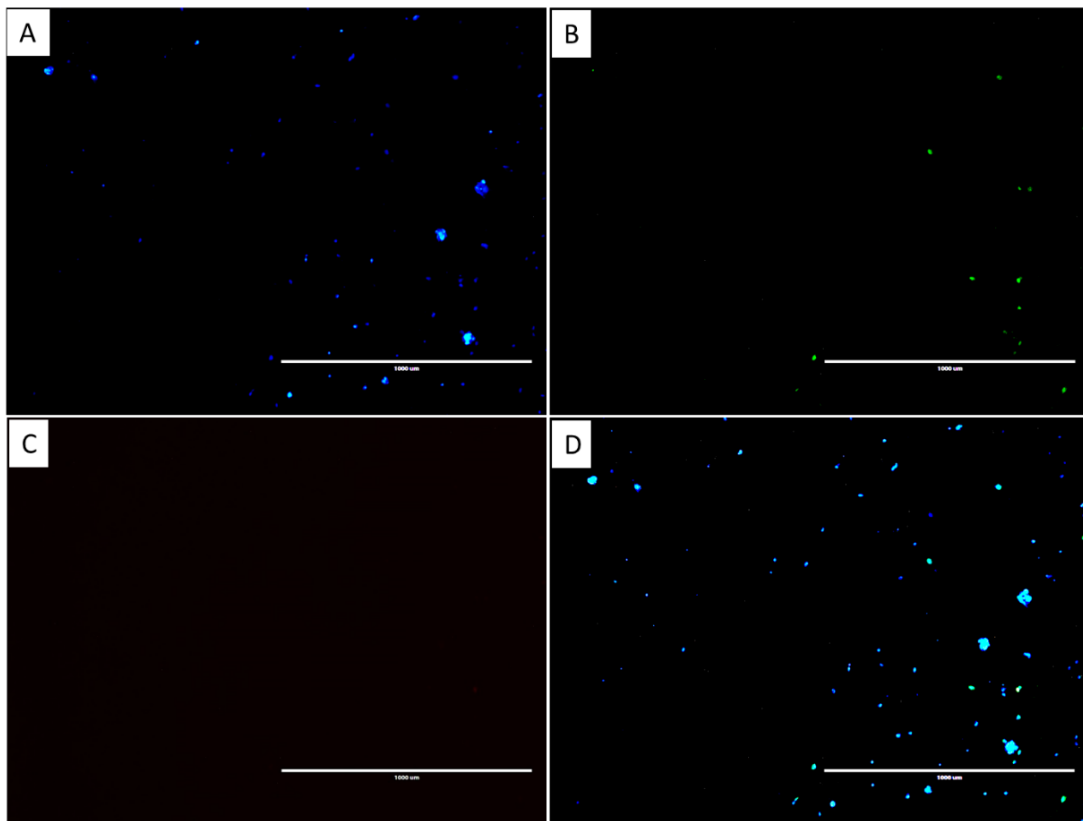


Figure 3.12.1: Treatment of primary bladder cells with MGF synthetic peptide. (A) Primary bladder cells were plated at a density of 0.01×10^6 and cultured in complete media supplemented (SM medium + 5% SMGS) with 1/10/100 ng/ml of MGF synthetic peptide for 48/72 hours. Complete medium without MGF was used as control. Results represent the mean of a culture analysed \pm SEM. (B) As a separate experiment, the cells were also cultured in medium without SMGS, and without growth factors + 100 ng/ml MGF. Results represent the mean of a culture analysed \pm SEM.

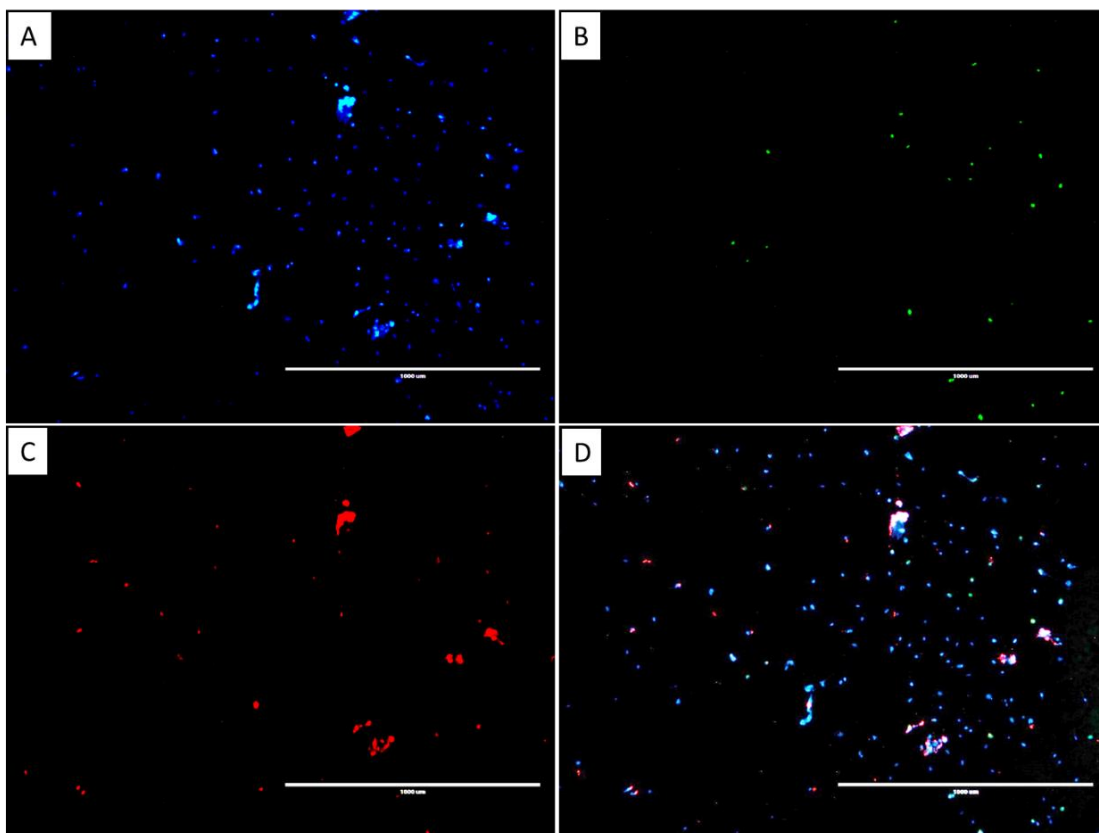




IV



V



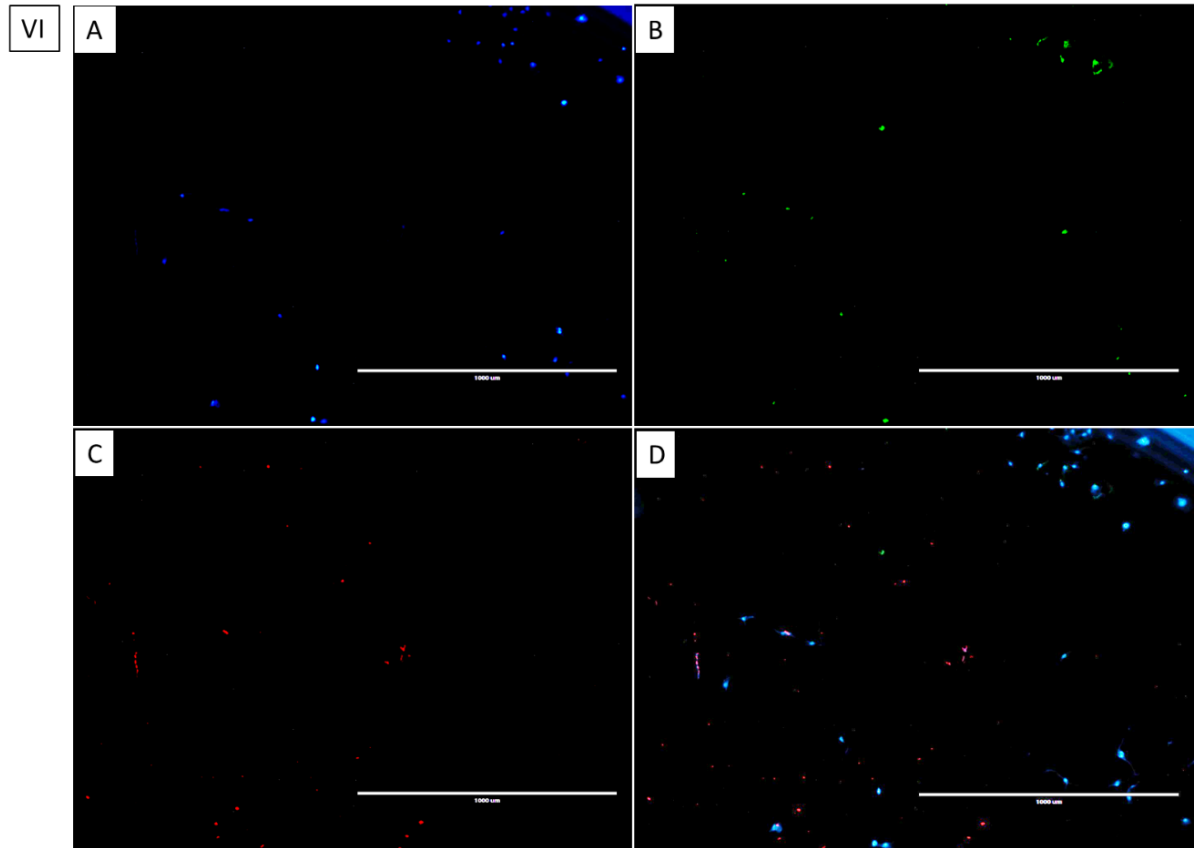


Figure 3.12.2: Treatment of primary bladder cells with 1 ng/ml of MGF synthetic peptide. Primary bladder cells were treated with 1 ng/ml (I), 10 ng/ml (II), 100 ng/ml (III) of MGF synthetic peptide for 72 hours at 37C/5%PCO₂. Cells cultured in SM medium only (IV) were chosen as control. As a separate experiment, cells were cultured in SM medium without growth factors (V), and in SM medium without growth factors supplemented with 100 ng/ml of MGF (VI). In all the pictures: (A) DAPI staining of the nuclei. (B) EdU staining of proliferating cells. (C) Immunostaining of smooth muscle myosin heavy chain (SMMHC). (C of IV is the secondary antibody only control). (D) Merge. All the images taken with EVOS microscope with 4x objective.

4. DISCUSSION

The goal of this study was to investigate MGF functions and possible applications in the overactive bladder pathology. Overactive bladder is a urological condition characterized by three main symptoms: urgency, frequency, nocturia, and sometimes incontinence. Although the aetiology of the pathology is not completely understood, it is presumed that the environmental-driven overactivity of the bladder smooth muscle, the detrusor, may be caused by changes in the physiological activity of the muscular and/or urothelial cells, and/or altered neurological signalling to the muscle. Treatments currently available aim either to relax the muscle and, therefore, reduce the contractions via neuromodulation, or to surgically improve urine storage. However, these approaches don't address the causes of the pathology and are often discontinued due to their side effects.

Insulin-like growth factor 1 (IGF-1) is involved in cell growth, proliferation and differentiation. Alternative splicing leads to the production of different products, among which IGF-1Ec/MGF. Previous studies have shown a determining role for MGF in a variety of body tissues, such as tendon (Zhang *et al.*, 2009), heart (Doroudian *et al.*, 2014), bone marrow (Sha *et al.*, 2017) and brain (Dluzniewska, 2005; Riddoch-Contreras *et al.*, 2009; Tang *et al.*, 2017; Liu *et al.*, 2018); however, the majority of studies have been performed in skeletal muscle, where MGF was shown to stimulate muscle cells proliferation by recruiting progenitor satellite cells. MGF function in smooth muscle, and especially in the bladder, has not been deeply studied yet. Our study aimed to investigate whether MGF is expressed and has an action in the bladder smooth muscle, and, therefore, whether it could possibly restore detrusor muscle function in the OAB syndrome by stimulating satellite cells proliferation.

Our data shows that MGF is expressed in the bladder and can be detected at the protein level, and the detection is consistent with the pro-form of the protein, pro-MGF (mature IGF-1 with MGF attached), as demonstrated by the detection of a 15 kDa band. It was not possible to detect a lower kDa band, 8 kDa, corresponding to the cleaved MGF peptide, consistent with previous findings of other research groups (Kravchenko *et al.*, 2006; Philippou *et al.*, 2008; Durzynska *et al.*, 2013). This may suggest that either the MGF peptide does not have a physiological function in the cleaved form, or its half-life is very short that it is rapidly degraded after cleavage. Moreover, through western blot it is difficult to detect very small proteins, due to the limitations of the technique itself. Immunohistochemistry staining methods also confirmed the presence of MGF throughout the bladder, even if the cell compartments producing it are not very clear. The detection of IGF-1Ec transcripts was more challenging, not allowing us to consistently confirm its expression in the bladder. Other research groups have successfully detected IGF-1Ec transcripts in rabbit (Yang *et al.*, 1997; McKoy *et al.*, 1999), rat (Hill and Goldspink, 2003) and human (Hameed *et al.*, 2003; Cortes *et al.*, 2005) skeletal muscle, starting either from total cDNA, or MGF-selective cDNA. RT-PCR detection is conditioned by a variety of factors, such as mRNA degradation, turnover, low stability and actions of miRNA. Proteins are more stable compared to mRNAs, as they tend to be stored and have a longer life (Yang *et al.* 2003; Cambridge *et al.* 2011).

MGF is physiologically expressed at a low level, and it is upregulated following injury/mechanical stretch, so it is fair to presume that its higher expression in skeletal muscle made its detection easier. Hence, when working with human bladder samples, the low expression of IGF-1Ec and the limited amount of cDNA were determining factors that hindered IGF-1Ec mRNA detection.

After confirming MGF expression in the bladder, we calculated the average expression in all pathological samples vs. controls. Contrary to our initial hypothesis, MGF is more expressed in pathological samples, but not statistically significantly ($p=0.11$), maybe reflecting a continuous attempt of muscle regeneration, which fails because of the potential muscle degenerative nature of OAB itself. A clear example of this condition, for example, is the Duchenne muscular dystrophy, in which mutations in the dystrophin gene cause progressive muscle weakness and degeneration (Blake *et al.*, 2002). In this pathology, the muscle attempt of regeneration is shown by the upregulation of several regeneration markers, such as TNF- α and bFGF, in human pathological samples compared to control ones, confirming the impairment of the regeneration (Abdel-Salam, Abdel-Meguid and Korraa, 2009). Moreover, we statistically analysed the correlation between MGF protein expression and clinical parameters, i.e. MCC and self-completion questionnaire scores. We did not observe any statistical correlation, although the correlation between MGF expression and MCC increased when considering only DO+ patients ($p=0.15$); that would stress the potential role played by MGF in muscle regeneration, as greater bladder volumes are more associated with higher expression of MGF. However, more biopsy samples would be needed to perform a more representative study on OAB and generate more statistically significant data.

In our study, we also assessed the composition of each biopsy in terms of the relative expression of markers of each layer of the bladder (muscle, connective tissue and urothelium). The smooth muscle was the predominant layer, followed by stroma and urothelium; however, there was not statistical difference in biopsy composition between pathological and control samples ($p=0.72$, 0.57 and 0.16). Looking at each biopsy individually, the composition pattern allowed their categorization into four subgroups depending on presence/absence of smooth muscle (DES) and urothelium (UPK2+): DES+/UPK2+, DES+/UPK2-, DES-/UPK2+ and DES-/UPK2-. The different MGF expression in DES+/UPK2+ between pathological and control samples almost reached statistical significance ($p=0.06$), contrary to DES-/UPK2+ samples ($p=0.56$). This may suggest that different layers express MGF, but only expression by the detrusor muscle is increased in OAB, stressing once again the potential attempt of regeneration to compensate for the muscular degeneration associated with the pathology. Again, we could speculate that working with a greater number of biopsy samples, and, therefore, having a more representative specimen of OAB, it would be possible to produce more significant data.

To assess MGF pro-proliferative action on muscle satellite cells, we established a primary culture of murine bladder cells and we treated them with MGF synthetic peptide in different experimental conditions. Other studies performing MGF treatment on C2C12

(Yang and Goldspink, 2002; Philippou *et al.*, 2009) and human skeletal muscle (Kandalla *et al.*, 2011) cells showed stimulation of proliferation using different concentrations of MGF synthetic peptide, but not always with a clear increasing trend. They used either serum-free medium, complete medium or medium without and then with FBS supplemented with the synthetic peptide. In our study, we performed two separate experiments: culture of primary murine bladder cells in complete smooth muscle medium supplemented with 1/10/100 ng/ml of MGF synthetic peptide for 48/72 hours at 37°C/PCO₂ 5%. After 72 hours, the % of proliferating cells treated with 100 ng/ml showed a statistically significant increase ($p=0.008$) compared to control. As a separate experiment, we did grow the cells in medium without growth factors and in medium without growth factors supplemented with 100 ng/ml of MGF, same experimental conditions. No statistically significant difference was observed in the proliferation rate in the two experimental conditions ($p=0.46$ and $p=0.49$). It should be considered that the replicates for each experiment were different, with the controls having the lowest number of replicates and, therefore, less reproducibility. Hence, various factors could have interfered with the outcome of the analysis, such as variability among the bladders and the replicates, and duration of the treatment.

Going forward it would be useful to expand the dataset of biopsy samples to study the expression of MGF and the tissue composition of different OAB subtypes, allowing a greater and more representative picture of the pathology. Our data so far suggests that MGF is more expressed in pathological bladders compared to physiological; therefore, an important step would be performing single-cell analysis, e.g. through flow-cytometry, to understand whether it is caused by increased production by a particular cell type, or by the expansion of cell types producing it. Moreover, to support the idea of the muscle degenerative nature of OAB, it would be essential to analyse the expression of other muscle regeneration markers in pathological biopsies compared to control.

To elaborate on the study of the effect of MGF on detrusor muscle survival, proliferation and function, not only it would be important to repeat the treatment of primary bladder cells with MGF-24, but it would also be helpful to study its effects within a 3D multicellular environment reproducing the interactions of the multiple cell types of the bladder.

Finally, the use of exon arrays could potentially allow to examine global changes in alternative splicing and, generally, gene expression of clinical subtypes of the pathology compared to controls and identify additional targets for OAB diagnosis and treatment.

5. CONCLUSIONS

The hypothesis of this project was that the IGF-1 splice variant IGF-1Ec/MGF, which was shown to be upregulated in skeletal muscle after injury/mechanical stretch and promoting muscle progenitor cells proliferation, could be expressed in normal bladders to allow muscle regeneration. We also hypothesised that in overactive bladders MGF expression might be decreased, impairing the muscle regeneration with subsequent deposition of fibrotic tissue causing dysfunctional contractility.

We demonstrated for the first time that MGF is expressed in the bladder by multiple cell layers and that its expression is higher in pathological samples compared to control; however, not reaching statistical significance. We analysed the tissue composition of the biopsies revealing different patterns; the change in MGF expression between pathological and control samples almost reached statistical significance in biopsies expressing marker for smooth muscle. Moreover, we did not observe statistically significant correlation between questionnaire scores and MGF expression; correlation with MCC was positive, but not statistically significant. These findings would suggest OAB has a muscular degenerative connotation, and increased MGF expression in the pathology may represent a continuous regeneration attempt by the detrusor muscle. However, it would be useful to amplify the dataset of biopsy samples to allow a greater study and, perhaps, the generation of statistically significant data.

The treatment of primary bladder cells with different concentration of MGF synthetic peptide did show an increasing trend in the proliferation rate in the treated cells; however, not always higher than the untreated control. More replicates of the experiment would be needed to clarify and confirm MGF proliferative action in bladder smooth muscle cells.

In conclusion, we could speculate that overactive bladder is a muscle degenerative condition with impaired degeneration. Treatment with MGF could potentially represent a new therapeutic avenue to promote muscle regeneration and restore of its contractility function, even if further research is required.

6. APPENDIX

6.1 Materials


Table 6.1: List of materials and reagents used throughout this study. All the materials and reagents used are listed with the name of their manufactures and catalogue numbers.

Name	Manufacturer	Catalogue number
4–20% Mini-PROTEAN® TGX™ Precast Protein Gels, 10-well, 30 µl	Bio Rad	4561093
4',6-diamidino-2-phenylindole, dilactate (DAPI, dilactate), 10mg	Fisher Scientific	11530306
Agarose (Low-EEO/Multi-Purpose/Molecular Biology Grade), Fisher BioReagents, 100g	Fisher Scientific	10766834
Anti-alpha smooth muscle Actin antibody	Abcam	ab7817
Anti-beta Actin antibody [mAbcam 8224] - Loading Control	Abcam	ab8224
Anti-desmin antibody	Abcam	ab15200
Anti-IGF1 antibody	Abcam	ab9572
Anti-Mechano Growth Factor (MGF) Antibody; rabbit polyclonal	Merck Millipore	07-2108
Anti-smooth muscle Myosin heavy chain 11 antibody	Abcam	ab53219
Biotinylated anti-rabbit IgG (H+L)	Vector Laboratories	BA-1100
Collagenase D from Clostridium histolyticum, pkg of 100 mg	Sigma-Aldrich	11088858001
Dispase II	Sigma-Aldrich	D4693-1G
DreamTaq Green PCR Master Mix (2X)	Fisher Scientific	11813933
EdU-Click 488	Sigma-Aldrich	BCK-EDU488
Fisher Bioreagents™ Bovine Serum Albumin Powder	Fisher Scientific	11413164
GelRed™ in water 10 000X	VWR	41003.
GeneRuler 100 bp DNA ladder	Fisher Scientific	10588170
Gibco™ Advanced DMEM/F-12, 500 ml	Fisher Scientific	11540446
Gibco™ DPBS without Calcium and Magnesium	Fisher Scientific	12559069
Gibco™ Fetal Bovine Serum, qualified, E.U.-approved	Fisher Scientific	11573397
Gibco™ Fungizone™ Fungizone Antimycotic, 50 ml	Fisher Scientific	11520496
Gibco™ Medium 231, 500 ml + Gibco™ Smooth Muscle Growth Supplement (SMGS), 25 ml	Fisher Scientific	10781934 10114733
Gibco™ Trypsin-EDTA (0.05%), Phenol red	Fisher Scientific	11590626

Gibco X10 RPMI 1640 medium (1X), liquid with L-glutamine	Fisher Scientific	12004997
Glass beads, acid-washed 150-212 µm	Sigma-Aldrich	G1145
Hematoxylin solution, gill n.2	Sigma-Aldrich	GHS232-1L
Hydrogen peroxide solution	Sigma-Aldrich	H1009-500ML
IgG (H+L) Highly Cross-Adsorbed Donkey anti-Rabbit, Alexa Fluor® 555	Fisher Scientific	10749004
ImmPACT™ DAB	Vector Laboratories	SK-4105
Invitrogen™ PARIS™ Kit	Fisher Scientific	10404794
IRDye® 680RD Donkey anti-Mouse IgG Secondary Antibody	Li-Cor	926-68072
IRDye® 800CW Donkey anti-Rabbit IgG Secondary Antibody	Li-Cor	926-32213
Maxima SYBR Green/ROX qPCR Master Mix (2X)	Fisher Scientific	11873913
Normal Horse Serum, 10ml	Sigma-Aldrich	H0146-10ML
Novex™ 4-20% Tris-Glycine Mini Gels, WedgeWell™ format, 12-well	Fisher Scientific	15466814
Novex™ SeeBlue™ Plus2 Pre-stained Protein Standard	Fisher Scientific	10174502
NuPAGE™ LDS Sample Buffer (4X) Invitrogen	Fisher Scientific	10718414
Odyssey® Blocking Buffer (TBS)	Li-Cor	P/N 927-50000
Penicillin-Streptomycin (10,000 U/mL)	Fisher Scientific	11548876
RNase-Free DNase Set	Qiagen	79254
RNeasy Mini Kit	Qiagen	74104
Stainless Steel Beads, 5 mm (200)	Qiagen	69989
Thermo Scientific™ PageRuler™ Plus Prestained 10-250kDa Protein Ladder	Fisher Scientific	11832124
Thermo Scientific™ Pierce™ BCA™ Protein Assay	Fisher Scientific	10678484
Thermo Scientific™ RevertAid™ First Strand cDNA Synthesis Kit	Fisher Scientific	15255146
Trans-Blot Turbo RTA Mini NC Kt 40 blots	Bio Rad	1704270
Triton® X-100	Fisher Scientific	BP151-100
VectaMount™	Vector Laboratories	H-5000
Vectastain® ABC kit	Vector Laboratories	PK-6100

6.2 Ethics

The project was originally granted approval on the 8th February 2010 by South East London Research Ethics Committee (REC) 5 (NHS), IRAS number 474470, A5-2: 10/H0805/51. It was finally approved on the 28th August 2018 by the Kingston University Science, Engineering and Computing (SEC) Faculty Research Ethics Committee (FREC) (1718.041.1).

Kingston Hospital 
NHS Foundation Trust

Urogynaecology unit
Women's Health Department
[\[Redacted\]](#)

CONSENT FORM

**Expression of IGF-1 splice variants and smooth muscle inflammatory markers in bladder detrusor muscle (MGF and IGF-1Ea).
REC Ref 10/H0805/51**

I can confirm that I have read the Patient Information Sheet (version 4, dated 15 August 2011) and I have had the opportunity to ask any questions or concerns I may have regarding my involvement in the above study.

I have been explained by the principal investigator Dr Eduard Cortes the procedure involving a bladder biopsy, and I understand that the risks associated with this are minimal. I understand that I will be given antibiotics once in theatre to reduce the risk of any infections.

I understand that the biopsy obtained as part of the above study, is not part of a diagnostic test and will not contribute to the management or treatment of my presenting condition.

I understand that the data obtained will be kept strictly confidential, in accordance with the terms of the Data Protection Act 1998

I have been provided with the necessary contact details, in case I had further questions during my involvement in the study.

I understand that my participation in the above research is voluntary and I can withdraw at any time without this compromising my overall care.

I agree for the sample obtained to be stored and used in future analysis including cell growth and protein studies, related to the above growth factors

Please initial each box

Participant's name

Signature

Date

Professional's name

Signature

Date

Consent Form - Version 2 -15/08/2011

Figure 6.2 Consent template for urogynaecology patients of Kingston Hospital. Before their involvement in the study, the patients were asked to sign a consent form to confirm their understanding of the procedures involving the biopsy samples and their rights related.

7. REFERENCES

- Abdel-Salam, E., Abdel-Meguid, I. and Korraa, S. S. (2009) 'Markers of degeneration and regeneration in Duchenne muscular dystrophy', *Acta Myologica*, 28(3), pp. 94–100.
- Armakolas, A. *et al.* (2010) 'Preferential expression of IGF-1Ec (MGF) transcript in cancerous tissues of human prostate: Evidence for a novel and autonomous growth factor activity of MGF E peptide in human prostate cancer cells', *Prostate*, 70(11), pp. 1233–1242. doi: 10.1002/pros.21158.
- Arrabal-Polo, M. A. *et al.* (2012) 'Clinical efficacy in the treatment of overactive bladder refractory to anticholinergics by posterior tibial nerve stimulation', *Korean Journal of Urology*, 53(7), pp. 483–486. doi: 10.4111/kju.2012.53.7.483.
- Barton, E. R. (2006) 'The ABCs of IGF-I isoforms: Impact on muscle hypertrophy and implications for repair', *Applied Physiology, Nutrition and Metabolism*, 31(6), pp. 791–797. doi: 10.1139/H06-054.
- Basra, R. *et al.* (2006) 'Design and Validation of a New Screening Instrument for Lower Urinary Tract Dysfunction: The Bladder Control Self-Assessment Questionnaire (B-SAQ)', *European Urology*, 52(1), pp. 230–237. doi: 10.1016/j.eururo.2006.11.015.
- Berghmans, L. C. M. *et al.* (2000) 'Conservative treatment of urge urinary incontinence in women: A systematic review of randomized clinical trials', *BJU International*, 85(3), pp. 254–263. doi: 10.1046/j.1464-410X.2000.00434.x.
- Bergman, D. *et al.* (2013) 'Insulin-like growth factor 2 in development and disease: A mini-review', *Gerontology*, 59(3), pp. 240–249. doi: 10.1159/000343995.
- Bertherat, J., Bluet-Pajot, M. T. and Epelbaum, J. (1995) 'Neuroendocrine regulation of growth hormone', *European Journal of Endocrinology*, 132(1), pp. 12–24.
- Blake, D. J. *et al.* (2002) 'Function and genetics of dystrophin and dystrophin-related proteins in muscle', *Physiological Reviews*. doi: 10.1152/physrev.00028.2001.
- Brisson, B. K. and Barton, E. R. (2012) 'Insulin-Like Growth Factor-I E-Peptide Activity Is Dependent on the IGF-I Receptor', *PLoS ONE*, 7(9). doi: 10.1371/journal.pone.0045588.
- Brocklehurst, J. C. (1993) 'Urinary incontinence in the community - Analysis of a MORI poll', *British Medical Journal*, 306(6881), pp. 832–834.
- Brooks, S. V. and Faulkner, J. A. (1994) 'Skeletal muscle weakness in old age: Underlying mechanisms', *Medicine and Science in Sports and Exercise*, 26(4), pp. 432–439.
- Bustin, S. A. *et al.* (2009) 'The MIQE guidelines: Minimum information for publication of quantitative real-time PCR experiments', *Clinical Chemistry*, 55(4), pp. 611–622. doi: 10.1373/clinchem.2008.112797.
- Marchal, C. *et al.* (2011) 'Percutaneous tibial nerve stimulation in treatment of overactive bladder: When should retreatment be started?', *Urology*, 78(5), pp. 1046–1050.
- Carro, E. *et al.* (2002) 'Serum insulin-like growth factor I regulates brain amyloid- β levels', *Nature Medicine*, 8(12), pp. 1390–1397. doi: 10.1038/nm1202-793.
- Caruso, D. J. *et al.* (2010) 'What is the predictive value of urodynamics to reproduce clinical findings of urinary frequency, urge urinary incontinence, and/or stress urinary incontinence?', *International Urogynecology Journal*, 21(10), pp. 1205–1209. doi: 10.1007/s00192-010-1180-7.

- Ceafalan, L. C., Popescu, B. O. and Hinescu, M. E. (2014) 'Cellular players in skeletal muscle regeneration', *BioMed Research International*. doi: 10.1155/2014/957014.
- Chakravarthy, M. V., Davis, B. S. and Booth, F. W. (2000) 'IGF-I restores satellite cell proliferative potential in immobilized old skeletal muscle', *Journal of Applied Physiology*, 89(4), pp. 1365–1379.
- Chang, S. *et al.* (2006) 'Increased basal phosphorylation of detrusor smooth muscle myosin in alloxan-induced diabetic rabbit is mediated by upregulation of Rho-kinase β and CPI-17', *American Journal of Physiology - Renal Physiology*, 290(3), pp. F650–F656. doi: 10.1152/ajprenal.00235.2005.
- Chapple, C. *et al.* (2013) 'OnabotulinumtoxinA 100 U significantly improves all idiopathic overactive bladder symptoms and quality of life in patients with overactive bladder and urinary incontinence: A randomised, double-blind, placebo-controlled trial', *European Urology*, 64(2), pp. 249–256. doi: 10.1016/j.eururo.2013.04.001.
- Chapple, C. R. (2012) ' β 3-Agonist therapy: A new advance in the management of overactive bladder?', *European Urology*, 62(5), pp. 841–842. doi: 10.1016/j.eururo.2012.08.006.
- Chew, S. L. *et al.* (1995) 'An alternatively spliced human insulin-like growth factor-I transcript with hepatic tissue expression that diverts away from the mitogenic IBE1 peptide', *Endocrinology*, 136(5), pp. 1939–1944. doi: 10.1210/endo.136.5.7720641.
- Cortes, E. *et al.* (2005) 'Insulin-like growth factor-1 gene splice variants as markers of muscle damage in levator ani muscle after the first vaginal delivery', *American Journal of Obstetrics and Gynecology*, 193(1), pp. 64–70. doi: 10.1016/j.ajog.2004.12.088.
- Council, L. and Hameed, O. (2009) 'Differential expression of immunohistochemical markers in bladder smooth muscle and myofibroblasts, and the potential utility of desmin, smoothelin, and vimentin in staging of bladder carcinoma', *Modern Pathology*, 22(5), pp. 639–650. doi: 10.1038/modpathol.2009.9.
- Coyne, K. S. *et al.* (2008) 'The impact of overactive bladder, incontinence and other lower urinary tract symptoms on quality of life, work productivity, sexuality and emotional well-being in men and women: Results from the EPIC study', *BJU International*, 101(11), pp. 1388–1395. doi: 10.1111/j.1464-410X.2008.07601.x.
- Coyne, K. S. *et al.* (2015) 'An overactive bladder symptom and health-related quality of life short-form: Validation of the OAB-q SF', *Neurourology and Urodynamics*, 34(3), pp. 255–263. doi: 10.1002/nau.22559.
- Daneshmand, S. (2017) 'Urinary diversion', *Urinary Diversion*, pp. 1–185. doi: 10.1007/978-3-319-52186-2.
- Daughaday, W. H. *et al.* (1972) 'Somatomedin: Proposed designation for sulphation factor [7]', *Nature*, 235(5333). doi: 10.1038/235107a0.
- Delafontaine, P., Song, Y. H. and Li, Y. (2004) 'Expression, Regulation, and Function of IGF-1, IGF-1R, and IGF-1 Binding Proteins in Blood Vessels', *Arteriosclerosis, Thrombosis, and Vascular Biology*, 24(3), pp. 435–444. doi: 10.1161/01.ATV.0000105902.89459.09.
- Denys, P. *et al.* (2012) 'Efficacy and safety of low doses of onabotulinumtoxinA for the treatment of refractory idiopathic overactive bladder: A multicentre, double-blind, randomised, placebo-controlled dose-ranging study', *European Urology*, 61(3), pp. 520–529. doi: 10.1016/j.eururo.2011.10.028.
- Desbois-Mouthon, C. *et al.* (2006) 'Hepatocyte proliferation during liver regeneration is

- impaired in mice with liver-specific IGF-1R knockout', *FASEB Journal*, 20(6), pp. 773–775. doi: 10.1096/fj.05-4704fje.
- Dluzniewska, J. (2005) 'A strong neuroprotective effect of the autonomous C-terminal peptide of IGF-1 Ec (MGF) in brain ischemia', *The FASEB Journal*, 19(13), pp. 1896–1898. doi: 10.1096/fj.05-3786fje.
- Doroudian, G. *et al.* (2014) 'Sustained delivery of MGF peptide from microrods attracts stem cells and reduces apoptosis of myocytes', *Biomedical Microdevices*, 16(5), pp. 705–715. doi: 10.1007/s10544-014-9875-z.
- Drake, M. J., Harvey, I. J. and Gillespie, J. I. (2003) 'Autonomous activity in the isolated guinea pig bladder', *Experimental Physiology*, 88(1), pp. 19–30. doi: 10.1113/eph8802473.
- Drake, M. J., Mills, I. W. and Gillespie, J. I. (2001) 'Model of peripheral autonomous modules and a myovesical plexus in normal and overactive bladder function', *Lancet*, 358(9279), pp. 401–403. doi: 10.1016/S0140-6736(01)05549-0.
- Du, H. *et al.* (2013) 'Generation and evaluation of antibodies against human MGF E-peptide by reverse phase protein microarray and reverse competitive ELISA', *Bioanalysis*. doi: 10.4155/bio.13.195.
- Duguay, S. J. *et al.* (1997) 'Processing of wild-type and mutant proinsulin-like growth factor-IA by subtilisin-related proprotein convertases', *Journal of Biological Chemistry*, 272(10), pp. 6663–6667. doi: 10.1074/jbc.272.10.6663.
- Duguay, S. J. (1999) 'Post-translational processing of insulin-like growth factors', *Hormone and Metabolic Research*, 31(2–3), pp. 43–49.
- Duguay, S. J., Lai-Zhang, J. and Steiner, D. F. (1995) 'Mutational analysis of the insulin-like growth factor I prohormone processing site', *Journal of Biological Chemistry*, 270(29), pp. 17566–17574. doi: 10.1074/jbc.270.29.17566.
- Durzynska, J. *et al.* (2013) 'The pro-forms of insulin-like growth factor i (igf-i) are predominant in skeletal muscle and alter igf-i receptor activation', *Endocrinology*, 154(3), pp. 1215–1224. doi: 10.1210/en.2012-1992.
- Engström, W. *et al.* (1998) 'Transcriptional regulation and biological significance of the insulin like growth factor II gene', *Cell Proliferation*, 31(5–6), pp. 173–189. doi: 10.1111/j.1365-2184.1998.tb01196.x.
- Govier, F.E. *et al.* (2001) 'Percutaneous afferent neuromodulation for the refractory overactive bladder: Results of a multicenter study', *Journal of Urology*, 165(4), pp. 1193–1198.
- Flynn, M. K. *et al.* (2009) 'Outcome of a Randomized, Double-Blind, Placebo Controlled Trial of Botulinum A Toxin for Refractory Overactive Bladder', *Journal of Urology*, 181(6), pp. 2608–2615. doi: 10.1016/j.juro.2009.01.117.
- Ghigo, M. C. *et al.* (1997) 'Effects of GH and IGF-I administration on GHRH and somatostatin mRNA levels: I. A study on ad libitum fed and starved adult male rats', *Journal of Endocrinological Investigation*, 20(3), pp. 144–150. doi: 10.1007/BF03346893.
- Goldspink, G. (2005) 'Mechanical signals, IGF-I gene splicing, and muscle adaptation', *Physiology*. doi: 10.1152/physiol.00004.2005.
- Goodpaster, T. *et al.* (2008) 'An immunohistochemical method for identifying fibroblasts in formalin-fixed, paraffin-embedded tissue', *Journal of Histochemistry and Cytochemistry*,

56(4), pp. 347–358. doi: 10.1369/jhc.7A7287.2007.

De Groat, W. C. (1997) 'A neurologic basis for the overactive bladder', *Urology*, 50(6A Suppl), pp. 36–52.

De Groat, W. C. (2004) 'The urothelium in overactive bladder: Passive bystander or active participant?', *Urology*, 64(6 Suppl 1), pp. 7–11. doi: 10.1016/j.urology.2004.08.063.

Groen, J., Blok, B. F. M. and Bosch, J. L. H. R. (2011) 'Sacral neuromodulation as treatment for refractory idiopathic urge urinary incontinence: 5-year results of a longitudinal study in 60 women', *Journal of Urology*, 186(3), pp. 954–959. doi: 10.1016/j.juro.2011.04.059.

Hameed, M. *et al.* (2003) 'Expression of IGF-I splice variants in young and old human skeletal muscle after high resistance exercise', *Journal of Physiology*, 547(Pt 1), pp. 247–254. doi: 10.1113/jphysiol.2002.032136.

Haylen, B. T. *et al.* (2010) 'An international urogynecological association (IUGA)/international continence society (ICS) joint report on the terminology for female pelvic floor dysfunction', *Neurourology and Urodynamics*, 29(1), pp. 4–20. doi: 10.1002/nau.20798.

Hede, M. S. *et al.* (2012) 'E-Peptides Control Bioavailability of IGF-1', *PLoS ONE*, 7(12). doi: 10.1371/journal.pone.0051152.

Hegde, S. S. (2006) 'Muscarinic receptors in the bladder: From basic research to therapeutics', *British Journal of Pharmacology*, 147(Suppl 2), pp. S80–S87. doi: 10.1038/sj.bjp.0706560.

Hill, M. and Goldspink, G. (2003) 'Expression and splicing of the insulin-like growth factor gene in rodent muscle is associated with muscle satellite (stem) cell activation following local tissue damage', *Journal of Physiology*, 549(Pt 2), pp. 409–418. doi: 10.1113/jphysiol.2002.035832.

Hill, M., Wernig, A. and Goldspink, G. (2003) 'Muscle satellite (stem) cell activation during local tissue injury and repair', *Journal of Anatomy*, 203(1), pp. 89–99. doi: 10.1046/j.1469-7580.2003.00195.x.

Humbel, R. E. (1990) 'Insulin-like growth factors I and II', *European Journal of Biochemistry*, 190(3), pp. 445–462. doi: 10.1111/j.1432-1033.1990.tb15595.x.

Jang, H., Han, D. S. and Yuk, S. M. (2013) 'Changes of neuregulin-1(NRG-1) expression in a rat model of overactive bladder induced by partial urethral obstruction: Is NRG-1 a new biomarker of overactive bladder?', *BMC Urology*. doi: 10.1186/1471-2490-13-54.

Jansen, M. *et al.* (1983) 'Sequence of cDNA encoding human insulin-like growth factor I precursor', *Nature*, 306(5943), pp. 609–611. doi: 10.1038/306609a0.

Janssen, J. A. M. J. L. *et al.* (2016) 'Potency of full-length MGF to induce maximal activation of the IGF-I R is similar to recombinant human IGF-I at high equimolar concentrations', *PLoS ONE*, 11(3). doi: 10.1371/journal.pone.0150453.

Kandalla, P. K. *et al.* (2011) 'Mechano Growth Factor E peptide (MGF-E), derived from an isoform of IGF-1, activates human muscle progenitor cells and induces an increase in their fusion potential at different ages', *Mechanisms of Ageing and Development*, 132(4), pp. 154–162. doi: 10.1016/j.mad.2011.02.007.

van Kerrebroeck, P. E. V. *et al.* (2007) 'Results of Sacral Neuromodulation Therapy for Urinary Voiding Dysfunction: Outcomes of a Prospective, Worldwide Clinical Study', *Journal*

of *Urology*, 178(5), pp. 2029–2034. doi: 10.1016/j.juro.2007.07.032.

Khullar, V. *et al.* (2013) 'Efficacy and tolerability of mirabegron, a β_3 -adrenoceptor agonist, in patients with overactive bladder: Results from a randomised European-Australian phase 3 trial', *European Urology*, 63(2), pp. 283–295. doi: 10.1016/j.eururo.2012.10.016.

Kravchenko, I. V. *et al.* (2006) 'Monoclonal antibodies to mechano-growth factor', *Hybridoma*, 25(5), pp. 300–305. doi: 10.1089/hyb.2006.25.300.

Kushida, N. and Fry, C. H. (2016) 'On the origin of spontaneous activity in the bladder', *BJU International*, 117(6), pp. 982–992. doi: 10.1111/bju.13240.

Laron, Z. (2004) 'Laron Syndrome (Primary Growth Hormone Resistance or Insensitivity): The Personal Experience 1958-2003', *Journal of Clinical Endocrinology and Metabolism*, 89(3), pp. 1031–1044. doi: 10.1210/jc.2003-031033.

Lee, J. E. *et al.* (1993) 'Parental imprinting of an IGF-2 transgene', *Molecular Reproduction and Development*, 35(4), pp. 382–390. doi: 10.1002/mrd.1080350411.

Leroith, D. *et al.* (1992) 'Insulin-like growth factors', *NeuroSignals*, 1, pp. 173–181. doi: 10.1159/000109323.

Leroith, D. *et al.* (1995) 'Molecular and cellular aspects of the insulin-like growth factor I receptor', *Endocrine Reviews*, 16(2), pp. 143–163. doi: 10.1210/edrv-16-2-143.

Li, C. *et al.* (2015) 'Increased IGF-IEc expression and mechano-growth factor production in intestinal muscle of fibrostenotic Crohn's disease and smooth muscle hypertrophy', *American Journal of Physiology - Gastrointestinal and Liver Physiology*, 309(11), pp. G888–G899. doi: 10.1152/ajpgi.00414.2014.

Lin, W. W. and Oberbauer, A. M. (1998) 'Alternative splicing of insulin-like growth factor I mRNA is developmentally regulated in the rat and mouse with preferential exon 2 usage in the mouse', *Growth Hormone and IGF Research*. doi: 10.1016/S1096-6374(98)80115-9.

Lingappa, V. R. and Blobel, G. (1980) 'Early events in the biosynthesis of secretory and membrane proteins: the signal hypothesis.', *Recent Progress in Hormone Research*, 36, pp. 451–475.

Liu, M. *et al.* (2018) 'Potential effect of mechano growth factor E-domain peptide on axonal guidance growth in primary cultured cortical neurons of rats', *Journal of Tissue Engineering and Regenerative Medicine*, 12(1), pp. 70–79. doi: 10.1002/term.2364.

Lucas, M. G. *et al.* (2013) 'Guidelines on urinary incontinence', in *European Association Guidelines*.

Martin, A. A. *et al.* (1991) 'IGF-I and its variant, des-(1-3)IGF-I, enhance growth in rats with reduced renal mass', *American Journal of Physiology - Renal Fluid and Electrolyte Physiology*, 261(4 Pt 2), pp. F626–F633.

Mauro, A. (1961) 'Satellite cell of skeletal muscle fibers.', *The Journal of biophysical and biochemical cytology*, 9(2), pp. 493–495.

Mcghan, W. F. (2001) 'Cost Effectiveness and Quality of Life Considerations in the Treatment of Patients with Overactive Bladder', 7(2 Suppl), pp. S62–S75.

McKoy, G. *et al.* (1999) 'Expression of insulin growth factor-1 splice variants and structural genes in rabbit skeletal muscle induced by stretch and stimulation', *Journal of Physiology*, 516(Pt 2), pp. 583–592. doi: 10.1111/j.1469-7793.1999.0583v.x.

- Milingos, D. S. *et al.* (2011) 'Insulinlike growth factor-1Ec (MGF) expression in eutopic and ectopic endometrium: Characterization of the MGF E-peptide actions in vitro', *Molecular Medicine*, 17(1–2), pp. 21–28. doi: 10.2119/molmed.2010.00043.
- Miller, J. and Hoffman, E. (2006) 'The causes and consequences of overactive bladder', *Journal of Women's Health*, 15(3), pp. 251–260. doi: 10.1089/jwh.2006.15.251.
- Montecucco, C. and Molgó, J. (2005) 'Botulinal neurotoxins: Revival of an old killer', *Current Opinion in Pharmacology*, 5(3), pp. 274–279. doi: 10.1016/j.coph.2004.12.006.
- Moschos, M. M. *et al.* (2011) 'Expression of the insulin-like growth factor 1 (IGF-1) and type I IGF receptor mRNAs in human HLE-B3 lens epithelial cells', *In Vivo*, 25(2), pp. 179–184.
- Murphy, L. J. and Friesen, H. G. (1988) 'Differential effects of estrogen and growth hormone on uterine and hepatic insulin-like growth factor i gene expression in the ovariectomized hypophysectomized rat', *Endocrinology*, 122(1), pp. 325–332. doi: 10.1210/endo-122-1-325.
- Nagai, R., Larson, D. M. and Periasamy, M. (1988) 'Characterization of a mammalian smooth muscle myosin heavy chain cDNA clone and its expression in various smooth muscle types', *Proceedings of the National Academy of Sciences of the United States of America*, 85(4), pp. 1047–1051. doi: 10.1073/pnas.85.4.1047.
- Nilsen, T. W. and Graveley, B. R. (2010) 'Expansion of the eukaryotic proteome by alternative splicing', *Nature*, 463(7280), pp. 457–463. doi: 10.1038/nature08909.
- Nitti, V. W. *et al.* (2013) 'Mirabegron for the treatment of overactive bladder: A prespecified pooled efficacy analysis and pooled safety analysis of three randomised, double-blind, placebo-controlled, phase III studies', *International Journal of Clinical Practice*, 67(7), pp. 619–632. doi: 10.1111/ijcp.12194.
- Nitti, V. W. *et al.* (2017) 'OnabotulinumtoxinA for the Treatment of Patients with Overactive Bladder and Urinary Incontinence: Results of a Phase 3, Randomized, Placebo Controlled Trial', *Journal of Urology*, 197(2S), pp. S216–S223. doi: 10.1016/j.juro.2016.10.109.
- Onal, M., Ugurlucan, F. G. and Yalcin, O. (2012) 'The effects of posterior tibial nerve stimulation on refractory overactive bladder syndrome and bladder circulation', *Archives of Gynecology and Obstetrics*, 286(6), pp. 1453–1457. doi: 10.1007/s00404-012-2464-6.
- Owino, V., Yang, S. Y. and Goldspink, G. (2001) 'Age-related loss of skeletal muscle function and the inability to express the autocrine form of insulin-like growth factor-1 (MGF) in response to mechanical overload', *FEBS Letters*, 505(2), pp. 259–263. doi: 10.1016/S0014-5793(01)02825-3.
- Pennisi, P. A. *et al.* (2004) 'Role of Growth Hormone (GH) in liver regeneration', *Endocrinology*, 145(10), pp. 4748–4755. doi: 10.1210/en.2004-0655.
- Pete, G. *et al.* (1996) 'Insulin-like growth factor-I decreases mean blood pressure and selectively increases regional blood flow in normal rats', *Proceedings of the Society for Experimental Biology and Medicine*, 213(2), pp. 187–192.
- Peters, K. M. *et al.* (2013) 'Sustained therapeutic effects of percutaneous tibial nerve stimulation: 24-month results of the STEP study', *Neurourology and Urodynamics*, 32(1), pp. 24–29. doi: 10.1002/nau.22266.
- Peterson, A. C. *et al.* (2018) 'Evaluating the 8-item overactive bladder questionnaire (OAB-v8) using item response theory', *Neurourology and Urodynamics*, 37(3), pp. 1095–1100. doi: 10.1002/nau.23420.

- Pfeffer, L. A. *et al.* (2009) 'The insulin-like growth factor (IGF)-I E-peptides modulate cell entry of the mature IGF-I protein', *Molecular Biology of the Cell*, 20(17), pp. 3810–3817. doi: 10.1091/mbc.E08-12-1202.
- Philippou, A. *et al.* (2008) 'Characterization of a rabbit antihuman Mechano Growth Factor (MGF) polyclonal antibody against the last 24 amino acids of the E domain', *In Vivo*, 22(1), pp. 27–35.
- Philippou, A. *et al.* (2009) 'Expression of IGF-1 isoforms after exercise-induced muscle damage in humans: Characterization of the MGF E peptide actions in vitro', *In Vivo*.
- Pokrywczynska, M. *et al.* (2016) 'Isolation, expansion and characterization of porcine urinary bladder smooth muscle cells for tissue engineering', *Biological Procedures Online*, 18. doi: 10.1186/s12575-016-0047-9.
- Puche, J. E. and Castilla-Cortázar, I. (2012) 'Human conditions of insulin-like growth factor-I (IGF-I) deficiency', *Journal of Translational Medicine*. doi: 10.1186/1479-5876-10-224.
- Qin, L. L. *et al.* (2012) 'Mechano growth factor (MGF) promotes proliferation and inhibits differentiation of porcine satellite cells (PSCs) by down-regulation of key myogenic transcriptional factors', *Molecular and Cellular Biochemistry*, 370(1–2), pp. 221–230. doi: 10.1007/s11010-012-1413-9.
- Reinhardt, R. R. and Bondy, C. A. (1994) 'Insulin-like growth factors cross the blood-brain barrier', *Endocrinology*, 135(5), pp. 1753–1761. doi: 10.1210/endo.135.5.7525251.
- Reviewed by Melinda Ratini (2018) *WebMD Medical Reference, Diagnosing Overactive Bladder*.
- Riddoch-Contreras, J. *et al.* (2009) 'Mechano-growth factor, an IGF-I splice variant, rescues motoneurons and improves muscle function in SOD1G93A mice', *Experimental Neurology*, 215(2), pp. 281–289. doi: 10.1016/j.expneurol.2008.10.014.
- Rinderknecht, E. and Humbel, R. E. (1976) 'Amino terminal sequences of two polypeptides from human serum with nonsuppressible insulin like and cell growth promoting activities: evidence for structural homology with insulin B chain', *Proceedings of the National Academy of Sciences of the United States of America*, 73(12), pp. 4379–4381. doi: 10.1073/pnas.73.12.4379.
- Rinderknecht, E. and Humbel, R. E. (1978) 'The amino acid sequence of human insulin-like growth factor I and its structural homology with proinsulin', *Journal of Biological Chemistry*, 253(8), pp. 2769–2776.
- Roberts, C. T. *et al.* (1987) 'Molecular cloning of rat insulin-like growth factor I complementary deoxyribonucleic acids: Differential messenger ribonucleic acid processing and regulation by growth hormone in extrahepatic tissues', *Molecular Endocrinology*. doi: 10.1210/mend-1-3-243.
- Robinson, D. and Cardozo, L. (2012) 'Antimuscarinic drugs to treat overactive bladder', *BMJ (Online)*, 344. doi: 10.1136/bmj.e2130.
- Rodríguez, A. *et al.* (2015) 'Design of primers and probes for quantitative real-time PCR methods', *Methods in Molecular Biology*, 1275, pp. 31–56. doi: 10.1007/978-1-4939-2365-6_3.
- Rotwein, P. *et al.* (1986) 'Organization and sequence of the human insulin-like growth factor I gene. Alternative RNA processing produces two insulin-like growth factor I precursor peptides', *Journal of Biological Chemistry*, 261(11), pp. 4828–4832.

- Rotwein, P. (1986) 'Two insulin-like growth factor I messenger RNAs are expressed in human liver', *Proceedings of the National Academy of Sciences of the United States of America*. doi: 10.1073/pnas.83.1.77.
- Rotwein, P., Folz, R. J. and Gordon, J. I. (1987) 'Biosynthesis of human insulin-like growth factor I (IGF-I). The primary translation product of IGF-I mRNA contains an unusual 48-amino acid signal peptide', *Journal of Biological Chemistry*, 262(24), pp. 11807–11812.
- Rovner, E. S. *et al.* (2002) 'Evaluation and treatment of the overactive bladder.', *Revista do Hospital das Clínicas*, 57(1), pp. 39–48. doi: 10.1590/S0041-87812002000100007.
- Sadananda, P., Chess-Williams, R. and Burcher, E. (2008) 'Contractile properties of the pig bladder mucosa in response to neurokinin A: A role for myofibroblasts?', *British Journal of Pharmacology*, 153(7), pp. 1465–1473. doi: 10.1038/bjp.2008.29.
- Saez, J. M. (1994) 'Leydig Cells: Endocrine, Paracrine, and Autocrine Regulation', *Endocrine Reviews*, 15(5), pp. 574–626. doi: 10.1210/edrv-15-5-574.
- Saks, E. K. and Arya, L. A. (2009) 'Pharmacologic Management of Urinary Incontinence, Voiding Dysfunction, and Overactive Bladder', *Obstetrics and Gynecology Clinics of North America*, 36(3), pp. 493–507. doi: 10.1016/j.ogc.2009.08.001.
- De Santi, M. *et al.* (2016) 'Human IGF1 pro-forms induce breast cancer cell proliferation via the IGF1 receptor', *Cellular Oncology*, 39(2), pp. 149–159. doi: 10.1007/s13402-015-0263-3.
- Sara, V. R. *et al.* (1983) 'Ontogenesis of somatomedin and insulin receptors in the human fetus', *Journal of Clinical Investigation*, 71(5), pp. 1084–1094. doi: 10.1172/JCI110858.
- Sara, V. R. *et al.* (1989) 'Identification of Gly-Pro-Glu (GPE), the aminoterminal tripeptide of insulin-like growth factor 1 which is truncated in brain, as a novel neuroactive peptide', *Biochemical and Biophysical Research Communications*, 165(2), pp. 766–771. doi: 10.1016/S0006-291X(89)80032-4.
- Sara, V. R. *et al.* (1993) 'The Biological Role of Truncated Insulin-like Growth Factor-1 and the Tripeptide GPE in the Central Nervous System', *Annals of the New York Academy of Sciences*, 692, pp. 183–191. doi: 10.1111/j.1749-6632.1993.tb26216.x.
- Savage, M. O. *et al.* (1993) 'Clinical features and endocrine status in patients with growth hormone insensitivity (Laron syndrome)', *Journal of Clinical Endocrinology and Metabolism*, 77(6), pp. 1465–1471. doi: 10.1210/jcem.77.6.7505286.
- Sha, Y. *et al.* (2017) 'MGF E peptide pretreatment improves the proliferation and osteogenic differentiation of BMSCs via MEK-ERK1/2 and PI3K-Akt pathway under severe hypoxia', *Life Sciences*, 189, pp. 52–62. doi: 10.1016/j.lfs.2017.09.017.
- Sharma, M. D. *et al.* (2017) 'Cardiovascular Disease in Acromegaly', *Methodist DeBakey cardiovascular journal*, 13(2), pp. 64–67. doi: 10.14797/mdcj-13-2-64.
- Shimatsu, A. and Rotwein, P. (1987) 'Mosaic evolution of the insulin-like growth factors', *The Journal of Biological Chemistry*.
- Shuman, C. and Weksberg, R. (2016) 'Beckwith-Wiedemann Syndrome', *GeneReviews*. doi: 10.1016/B978-0-12-374984-0.00146-7.
- Silva, J. R. V., Figueiredo, J. R. and van den Hurk, R. (2009) 'Involvement of growth hormone (GH) and insulin-like growth factor (IGF) system in ovarian folliculogenesis', *Theriogenology*, 71(8), pp. 1193–1208. doi: 10.1016/j.theriogenology.2008.12.015.

- Sjögren, K. *et al.* (1999) 'Liver-derived insulin-like growth factor I (IGF-I) is the principal source of IGF-I in blood but is not required for postnatal body growth in mice', *Proceedings of the National Academy of Sciences of the United States of America*, 96(12), pp. 7099–7092. doi: 10.1073/pnas.96.12.7088.
- Skrtic, S. *et al.* (1997) 'Insulin-like growth factors stimulate expression of hepatocyte growth factor but not transforming growth factor β 1 in cultured hepatic stellate cells', *Endocrinology*, 138(11), pp. 4683–4689. doi: 10.1210/endo.138.11.5540.
- Stavropoulou, A. *et al.* (2009) 'IGF-1 expression in infarcted myocardium and MGF E peptide actions in rat cardiomyocytes in vitro', *Molecular Medicine*, 15(5–6), pp. 127–135. doi: 10.2119/molmed.2009.00012.
- Stewart, W. F. *et al.* (2003) 'Prevalence and burden of overactive bladder in the United States', *World Journal of Urology*, 20(6), pp. 327–336. doi: 10.1007/s00345-002-0301-4.
- Tan, D. S. W., Cook, A. and Chew, S. L. (2002) 'Nucleolar localization of an isoform of the IGF-I precursor', *BMC Cell Biology*, 3, p. 17. doi: 10.1186/1471-2121-3-17.
- Tang, J. J. *et al.* (2017) 'Mechano growth factor, a splice variant of IGF-1, promotes neurogenesis in the aging mouse brain', *Molecular Brain*, 10(1), p. 23. doi: 10.1186/s13041-017-0304-0.
- ThermoFisher Scientific (2020) 'RNA content can vary widely between tissues, cell-types, physiological state, etc.' Available at: <https://www.thermofisher.com/uk/en/home/references/ambion-tech-support/rna-isolation/general-articles/rna-yields-from-tissues-and-cells.html>.
- Tian, W. *et al.* (2015) 'Utility of uroplakin II expression as a marker of urothelial carcinoma', *Human Pathology*, 46(1), pp. 58–64. doi: 10.1016/j.humpath.2014.09.007.
- Truzzi, J. C. *et al.* (2016a) 'Overactive bladder - 18 years - Part I', *International Braz J Urol*, 42(2), pp. 188–198. doi: 10.1590/S1677-5538.IBJU.2015.0365.
- Truzzi, J. C. *et al.* (2016b) 'Overactive bladder - 18 years - Part II', *International Braz J Urol*, 42(2), pp. 199–214. doi: 10.1590/S1677-5538.IBJU.2015.0367.
- Urology Care Foundation (2019) *Overactive Bladder: Introduction*.
- Vassilakos, G. and Barton, E. R. (2018) 'Insulin-Like Growth Factor I Regulation and Its Actions in Skeletal Muscle', *Comprehensive Physiology*, 9(1), pp. 413–438. doi: 10.1002/cphy.c180010.
- Vassilakos, G., Philippou, A. and Koutsilieris, M. (2017) 'Identification of the IGF-1 processing product human Ec/rodent Eb peptide in various tissues: Evidence for its differential regulation after exercise-induced muscle damage in humans', *Growth Hormone and IGF Research*. Elsevier Ltd, 32, pp. 22–28. doi: 10.1016/j.ghir.2016.11.001.
- Viloria, K. *et al.* (2016) 'A holistic approach to dissecting SPARC family protein complexity reveals FSTL-1 as an inhibitor of pancreatic cancer cell growth', *Scientific Reports*, 6. doi: 10.1038/srep37839.
- Wallis, M. (2009) 'New insulin-like growth factor (IGF)-precursor sequences from mammalian genomes: the molecular evolution of IGFs and associated peptides in primates', *Growth Hormone and IGF Research*. Elsevier Ltd, 19(1), pp. 12–23. doi: 10.1016/j.ghir.2008.05.001.
- Ward, A. (1997) 'Beck-Wiedemann syndrome and Wilms' tumour', *Molecular Human*

Reproduction, 3(2), pp. 157–168. doi: 10.1093/molehr/3.2.157.

Wooldridge, L. S. (2016) 'Overactive bladder', *The Nurse Practitioner in Urology*. Elsevier Inc, 43(1), pp. 251–268. doi: 10.1007/978-3-319-28743-0_14.

Yang, E. *et al.* (2003) 'Decay rates of human mRNAs: Correlation with functional characteristics and sequence attributes', *Genome Research*, 13(8), pp. 1863–1872. doi: 10.1101/gr.1272403.

Yang, S. *et al.* (1996) 'Cloning and characterization of an IGF-1 isoform expressed in skeletal muscle subjected to stretch', *Journal of Muscle Research and Cell Motility*, 17(4), pp. 487–495. doi: 10.1007/BF00123364.

Yang, S. Y. and Goldspink, G. (2002) 'Different roles of the IGF-I Ec peptide (MGF) and mature IGF-I in myoblast proliferation and differentiation', *FEBS Letters*. doi: 10.1016/S0014-5793(02)02918-6.

Yao, D. L. *et al.* (1996) 'Insulin-like growth factor-I given subcutaneously reduces clinical deficits, decreases lesion severity and upregulates synthesis of myelin proteins in experimental autoimmune encephalomyelitis', *Life Sciences*, 58(16), pp. 1301–1306. doi: 10.1016/0024-3205(96)00095-1.

Zapf, J., Schoenle, E. and Froesch, E. R. (1978) 'Insulin-Like Growth Factors I and II: Some Biological Actions and Receptor Binding Characteristics of Two Purified Constituents of Nonsuppressible Insulin-Like Activity of Human Serum', *European Journal of Biochemistry*, 87(2), pp. 285–296. doi: 10.1111/j.1432-1033.1978.tb12377.x.

Zhang, B. *et al.* (2016) 'Mechano-growth factor E peptide promotes healing of rat injured tendon', *Biotechnology Letters*, 38(10), pp. 1817–1825. doi: 10.1007/s10529-016-2162-8.

Zhang, B. B. *et al.* (2009) 'Expression and subcellular localization of mechano-growth factor in osteoblasts under mechanical stretch', *Science in China, Series C: Life Sciences*. doi: 10.1007/s11427-009-0122-4.